# Disentangled polyethylene with sharp molar mass distribution : implications for sintering

*Citation for published version (APA):*
Talebi, S. (2008). *Disentangled polyethylene with sharp molar mass distribution : implications for sintering*. [Phd Thesis 1 (Research TU/e / Graduation TU/e), Chemical Engineering and Chemistry]. Technische Universiteit Eindhoven. https://doi.org/10.6100/IR639413

*DOI:*
10.6100/IR639413

*Document status and date:*
Published: 01/01/2008

*Document Version:*
Publisher's PDF, also known as Version of Record (includes final page, issue and volume numbers)

*Please check the document version of this publication:*

• A submitted manuscript is the version of the article upon submission and before peer-review. There can be important differences between the submitted version and the official published version of record. People interested in the research are advised to contact the author for the final version of the publication, or visit the DOI to the publisher's website.
• The final author version and the galley proof are versions of the publication after peer review.
• The final published version features the final layout of the paper including the volume, issue and page numbers.

Link to publication

*General rights*
Copyright and moral rights for the publications made accessible in the public portal are retained by the authors and/or other copyright owners and it is a condition of accessing publications that users recognise and abide by the legal requirements associated with these rights.

- Users may download and print one copy of any publication from the public portal for the purpose of private study or research.
- You may not further distribute the material or use it for any profit-making activity or commercial gain
- You may freely distribute the URL identifying the publication in the public portal.

If the publication is distributed under the terms of Article 25fa of the Dutch Copyright Act, indicated by the "Taverne" license above, please follow below link for the End User Agreement:

www.tue.nl/taverne

*Take down policy*
If you believe that this document breaches copyright please contact us at:

openaccess@tue.nl

providing details and we will investigate your claim.

Download date: 04. Oct. 2023

# Disentangled Polyethylene with Sharp Molar Mass Distribution; Implications for Sintering

PROEFSCHRIFT

ter verkrijging van de graad van doctor aan de
Technische Universiteit Eindhoven, op gezag van de
Rector Magnificus, prof.dr.ir. C.J. van Duijn, voor een
commissie aangewezen door het College voor
Promoties in het openbaar te verdedigen
op woensdag 3 december 2008 om 16.00 uur

door

Saeid Talebi

geboren te Ardebil, Iran

Dit proefschrift is goedgekeurd door de promotoren:

prof.dr. S. Rastogi
en
prof.dr. P.J. Lemstra

Copromotor:
dr. R. Duchateau

A catalogue record is available from the Eindhoven University of Technology Library

ISBN: 978-90-386-1477-9

Copyright © 2008 by S. Talebi

Printed at the Universiteitsdrukkerij, Eindhoven University of Technology, Eindhoven.

Cover-design by S. Talebi and Oranje Vormgevers

The research described in this thesis was performed in the Faculty of Chemistry & Chemical Engineering group (SKT) Eindhoven University of Technology, The Netherlands. The work was partially financially supported by the Ministry of Science, Research and Technology, I.R. Iran under scholarship no. 811106.

*Dedicated to,*
*Shabnam and Aysan*

# Table of Contents

Summary 1

Chapter 1 General introduction

1.1 Polymers and entanglements 6
1.2 Solution (gel) spinning 7
1.3 Solvent-free processing routes for UHMWPE 9
1.4 Crossing from the disentangled solid state to the entangled melt state 11
1.5 Scope of thesis 12
1.6 References 14

Chapter 2 Synthesis of disentangled polyethylene

2.1 Introduction 17
2.2 Materials and methods 19
2.3 Homogeneous versus heterogeneous polymerization 20
2.4 Living or controlled polymerization 20
2.5 Effect of polymerization parameters 21
  2.5.1 Polymerization time 21
  2.5.2 Polymerization temperature ($T_p$) 22
  2.5.3 Type of solvent 24
  2.5.4 Co-catalyst to catalyst ratio 25
2.6 Conclusions 27
2.7 References 28

Chapter 3 Molar mass and molecular weight distribution determination from melt rheometry

3.1 Introduction 31
3.2 Basic Definitions 31
3.3 Experimental techniques 34
3.4 Methods of determining MWD from melt rheology 35
3.5 Rheological measurements 38
3.6 Molar mass data obtained from melt rheometry and GPC 42
3.7 Creating a master curve from time-MW superposition 46
3.8 Conclusions 49
3.9 References 50

## Chapter 4 Rheological aspects of disentangled polymer melts

4.1 Introduction 54
4.2 Experimental techniques 57
4.3 Following entanglements formation in disentangled polymers 57
    4.3.1 Modulus build-up 58
    4.3.2 Dependence on the build-up of modulus on molar mass 61
4.4 Effect of frequency and strain on modulus build-up 63
    4.4.1 Frequency effect 64
    4.4.2 Strain effect 67
4.5 Annealing experiment 69
4.6 Conclusions 71
4.7 References 73

## Chapter 5 Melting of disentangled crystals and its implications on crystallization

5.1 Introduction 75
5.2 High melting temperature in nascent polymers 75
5.3 Heating rate dependence in melting of polymers 77
5.4 Annealing experiment below the melting point 79
    5.4.1 Influence of annealing time at a constant annealing temperature 80
    5.4.2 Influence of annealing temperature at a constant annealing time 80
    5.4.3 Influence of molar mass at a constant annealing time and temperature 81
5.5 WAXS/SAXS studies on the disentangled polyethylenes 83
5.6 Influence of annealing on the onset of crystallization 85
    5.6.1 Annealing in the melt state 85
    5.6.2 Annealing in the vicinity of the melting point 88
5.7 Conclusions 89
5.8 References 90

## Chapter 6 Technology Assessment

6.1 Outlook for homogenous polymerization 93
6.2 Outlook for disentangled UHMWPE 94
6.3 References 97

Appendix 1 Reproducibility of GPC measurements for different molar masses 99

Appendix 2 Following entanglement formation on the initially disentangled polymer using high resolution SAXS 103

Appendix 3 Reproducibility of modulus build up for initially disentangled polymer 107

Acknowledgment 111

Curriculum Vitae 113

# Summary

## Disentangled Polyethylene with Sharp Molar Mass Distribution; Implications for Sintering

Synthetic polymers, often referred to as plastics, have surpassed steel two decades ago in production volume. At present, over 200 million tones of plastics are produced annually. There are various reasons for the almost exponential growth of plastics since World War II such as cheap production routes (based on oil) , ease of processing complexly shaped parts e.g. via injection-molding and a large range of properties ranging from soft rubbers to fibers stronger than steel. Synthetic polymers are long chain molecules and the majority is processed via the molten state, the so-called thermoplastics. The properties of polymeric products are not solely determined by the chemistry and chemical structure of the polymer molecules but equally well by the processing step, notably the orientation of the long chain molecules. A prime example in this respect is the simplest polymer: polyethylene which is used to make flexible containers but is also the base material for the super-strong Dyneema® fiber of DSM.

Thermoplastic polymers, viz. synthetic polymers which are processed via the molten state (melt) possess a high melt-viscosity which is strongly increasing with increasing molar mass. In fact, the so-called zero-shear viscosity, $\eta_o$, scales with $Mw^{3.4}$, viz upon doubling the molar mass, the melt-viscosity increases more than 10 times! Properties such as toughness and strength also increase with increasing molar mass and hence polymer processing in practice is a balance between ease (speed) of processing, which requires a low(er) molar mass and properties of the end-product where a high(er) molar mass is required. The reason for the strong dependence of the melt-viscosity on molar mass is related to existence of intermolecular topological interactions which is referred to as entanglements, the long chains are inter-hooked like in cooked spaghetti. The number of entanglements per molecule is dependent on the chemical structure and is expressed in the so-called $\langle M_e \rangle$, the average molecular weight in between two neighboring entanglements. If we accept the current models of polymer rheology that chain entanglements play a dominant role in the melt-viscosity of polymer melts then the question arises whether the entanglement density can be changed in favor of a low(er) melt-viscosity and hence easier processability?

An effective way to remove chain entanglements is via dissolution. In solutions the chains are relatively separated from each other and in the case of dilute solutions, below the so-called overlap concentration, the chains are completely separated physically and hence all entanglements have been removed. Upon removal of the solvent, the chains re-entangle again but for crystallizable polymers the chain disentanglement can be made permanent in the solid state. A well-studied system in this respect is ultra-high molecular weight polyethylene, UHMW-PE, which is considered to be an intractable polymer, viz. can not be processed via the melt in view of an excessively high melt-viscosity related to its molar mass, well above $10^6$ g/mol. UHMW-PE can be dissolved in solvents such as

decalin at elevated temperatures and upon cooling lamellar UHMW-PE crystals are formed. After crystallization the solvent can be removed, e.g. by extraction, and solid UHMW-PE is obtained which is free of entanglements. In the solid state this so-called disentangled UHMW-PE is ductile and easy to deform into oriented tapes with a high degree of chain alignment. However, upon heating into the melt the favorable chain topology is lost and re-entangling is a very fast, Entropy-driven process and, consequently, in terms of rheology and processing no beneficial effect could be obtained, the melt-viscosity is again prohibitive high.

The use of solvents to generate dis-entangled UHMW-PE is rather cumbersome but used in practice for the production of superstrong polyethylene fibers, e.g. Dyneema® by DSM. A novel and much more elegant route to generate disentangled polymer crystals is via direct synthesis in a reactor as described in **Chapter 2**. Upon polymerization at low temperatures and by using a single site homogeneous catalyst, the growing chains experience a "cold" environment and crystallize individually into folded-chain crystals, most probably monomolecular crystals, viz. one long chain forms one crystal. In fact, this is an easy and direct approach towards complete dis-entangling.

The first aim of this work, as described in **Chapter 2**, is to produce disentangled UHMWPE with different molar mass and narrow polydispersity directly in a polymerization reactor. A single site catalyst, a so called FI catalyst, was used for this purpose. A linear dependency between the polymerization time and the molar mass in the initial stage of the polymerization was observed, indicative of living, or controlled, polymerization. Furthermore, the influence of polymerization parameters such as temperature, co-catalyst to catalyst ratio and type of solvent on molar mass of synthesized polymer have been investigated. By controlling polymerization parameters, polyethylenes with different molar masses up to $9\text{x}10^6$ g/mol and narrow molecular weight distributions in the disentangled state were produced. However, determination of the molar mass and polydispersity becomes a challenge via conventional gel permeation chromatography (GPC).

In **Chapter 3**, a melt rheometry technique based on the "modulus model" was utilized to measure molar mass and PDI and make a comparison with the GPC data. The method works by converting the relaxation spectrum from the time domain to the molecular weight domain, then using a regularized integral inversion to recover the molecular weight distribution curve. These findings are of relevance in determining very high molar masses that cannot be obtained conclusively with the existing chromatography techniques. It is to be noted that in calculating molar mass from relaxation modulus the ill-posed nature of the inverse problem is dealt. Therefore, the possible error in the data obtained might be to check it by other means, such as GPC for molar masses up to $3\text{x}10^6$ g/mol. From the results obtained it was concluded that UHMWPE with different molar masses and narrow distributions has been synthesized successfully. These disentangled materials, so-called nascent or virgin reactor powders, have been studied regarding their rheological behavior, especially addressing the re-entangling process upon heating into the melt.

In **Chapter 4**, an investigation was performed using an oscillatory rheometry on the formation of entanglements and chain dynamics in a disentangled polymer melt. It is demonstrated that the modulus build-up with time at a fixed frequency and at constant strain and temperature shows two distinct regions, defined by two distinct slopes in the modulus build up. Region I, corresponding to the steep slope, arises due to mixing of disentangled chains, whereas Region II shows a slow increase in the modulus build up with time – following the reptation dynamics in the melt. Region I shows a strong dependence on the rate of entropy gain by the crystals on going from the solid to the liquid state. The rate of entropy gain was varied either by heating rate, on annealing of the samples in the vicinity of the equilibrium melting temperature. Molar mass dependence is exhibited during entangling process of the chains, which also shows the influence on the build-up time from the disentangled to the entangled melt state. Further experiments were performed on a disentangled sample to investigate the influence of applied frequency and strain on the entangling process. It was shown that the build-up time to reach a plateau of 2MPa increased considerably at the low frequency of 1rad/s. This difference in the build-up time at the low and the high frequencies suggest differences in the chain dynamics of the different chain regions of the disentangled polymer melt. These observations suggest that the total build-up time will be different for the different chain segments. From the studies of the strain effect, it was observed that the entangled state influences the border of the linear viscoelastic regime and the non-linear region. Disentangled melts show a non-linear regime behavior at much lower strain amplitude, indicative of easier disengagement of chains. These findings suggest a possibility of influencing the entangling process by controlling the mixing of chain segments at different regions – such as slow melting via annealing. The annealing experiment performed on the disentangled polymer in the rheometer showed that the slope of region I for fast heated sample was much higher than the slope of the annealed sample, clearly indicating the influence on the rate of entropy gain during melting of the crystals and its effect on mixing of the initially disentangled chains.

The melting of disentangled crystals and the influence of entanglements on polymer crystallization is discussed in **Chapter 5**. The high melting temperature of nascent UHMWPE has been a matter of debate for a long time. By measuring the melting point of two different molar mass UHMWPEs having narrow polydispersities with the help of DSC the non-linear heating rate dependence of the melting temperature of the nascent polyethylenes was observed suggesting the presence of an activation barrier in melting of the crystals. Furthermore, the effect of annealing below and above the melting temperature was investigated for the nascent polymer. The subsequent heating run on the annealed samples below melting temperature showed two distinct melting peaks suggesting the existence of two populations of crystallites. The subsequent cooling on the annealed samples well above the equilibrium melting temperature resulted in lowering the onset of crystallization. The influence of annealing in the vicinity of melting temperature on the onset of crystallization temperature was also investigated.

**Chapter 6** addresses some of the technological aspects of homogenous polymerization and the disentangled polymer obtained from such a polymerization.

# Chapter 1

# General introduction*

## 1.1 Polymers and entanglements

Polymers are described as long chains of short repeating molecular units linked by covalent bonds. This definition was proposed by Staudinger demonstrating the existence of "long molecules" in 1920.[1] His pioneering work lead to the award of the 1954 Nobel Prize for Chemistry "High Polymers bring High Honors"![2]

From the definition above, it is anticipated that polymers possess different physical and mechanical properties from small molecules. One of the origins of this distinction is the existence of a special type of intermolecular interaction between long chains called "chain entanglement". A schematic representation of an entanglement is depicted in Figure 1.1(a). These entanglements, known as topological constraints, can be considered as temporarily physical cross-links to be distinguished from permanent chemical crosslinks such as present in real networks, e.g. rubbers[3]. However, the properties of uncross-linked polymers such as the plateau modulus, zero shear viscosity and strain hardening can be explained by the concept of physical entanglements. The entanglement theory is regarded as the cradle of the "tube model" and "reptation" theory proposed by Doi-Edward[4] and de Gennes[5] (Nobel prize for Physics in 1991) shed light on the physical properties of polymer melt. This model suggests a virtual tube built up by entanglements and that an assumed chain reptates through this tube, Figure 1.1 (b). The required time for a chain to diffuse through the initial tube and make a new tube is the so called "tube renewal" time that scales with $M^3$, where M is the molar mass of the chain. Taking these concepts into consideration, the zero shear viscosity will scale with the power 3 of molar mass but experimental observations demonstrate a power of 3.4 dependence. Beyond the pure reptation as a dynamic process of entangled chains, there are other mechanisms such as "contour length fluctuation" (CLF) and "constraint release" (CR) which explain the mentioned discrepancy.[6,7]

---

* Reproduced in part from:
Talebi S., Rastogi S. and Lemstra P.J., Book chapter edited by Professor Liuba P. Myasnikova (In press).

For a polymer melt in equilibrium, entanglements are homogeneously distributed along the chain, where the average molar mass between entanglements, $<M_e>$, is considered to be an intrinsic property of the polymer that depends on the molecular configuration of the chain. Thus, with increasing molar mass of the polymer, i.e. with increasing length of the chain, the number of entanglements per unit chain increases. Upon cooling from the melt into the solid state, the entanglements are trapped in the solid. In the case of amorphous polymers, it is anticipated that the entanglement network in the melt is retained in the solid state upon cooling below $T_g$. In the case of crystallizable polymers, folded-chain crystals are formed which leads to partially disentangling, depending on molar mass. Therefore, it is expected, and experimentally observed, that increasing molar mass results in better physical and mechanical properties of polymers. On the other hand, the shear viscosity of polymers increases strongly with increasing molar mass. Consequently, processing of polymers in practice is often a compromise, for the ease of processing a low(er) molar mass is favorable whereas for properties a high(er) molar mass is preferred.

In the case of very high molar mass polymers, conventional melt-processing is not feasible anymore. A prime example in this respect is ultra high molecular weight polyethylene (UHMWPE) with a molar mass, $M_w$, well above $10^6$ g/mole. UHMW-PE possesses excellent wear and fatigue properties, related to the presence of a trapped entanglement network in the solid-state, but it is also considered as an intractable polymer. UHMW-PE products are made by sintering (compression-molding) for prolonged times, up to several days, and machined afterwards into shaped parts.

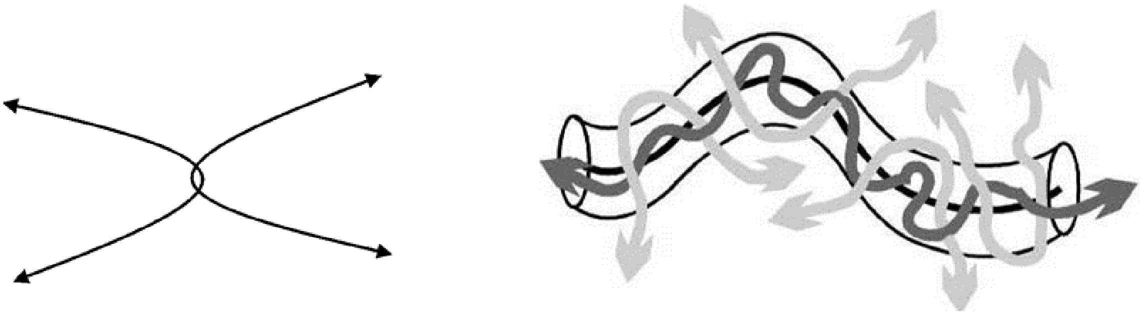
(a) (b)

**Figure 1.1**: (a) Classical model for an entanglement. (b) Chain reptation through the tube imposed by constraints. Reproduced from Strobl[8].

## 1.2 Solution (gel) spinning

As mentioned above, UHMWPE is an intractable polymer. To overcome this problem, dissolution of UHMWPE in a solvent was proposed by Zwick et al. [9] in the early 1960s to shape UHMWPE via solution processes into fibres. Remarkably, he did not consider obtaining better fibre properties by post-drawing, viz. to pursue for chain extension, as is common practice in the fibre industry. Solution-spinning of UHMWPE was revisited at DSM in the late 1970s, see below, resulting in chain-extended UHMWPE molecules which are nearly perfectly aligned in the fibre direction as a result of ultra drawing. However, the route towards these high performance UHMWPE fibres took a tortuous path. In the 1960s, Pennings and Kiel[10] performed fractionation experiments on UHMWPE in dilute solutions. They discovered that upon stirring shish-kebab like structures where obtained, see Figure 1.2.

More experimental[11,12]and fundamental[13,14] studies were performed to understand shish-kebab morphology. These investigations showed that the core structure (shish) consists of (partly) extended chain molecules, whereas the laterally folded chains (kebab) are grown on the core. The shish-kebab type structures are in fact half-way between folded-chain and extended-chain crystals and the mechanical properties are not so impressive, in the order of 25 GPa, due to the lamellar overgrowth.

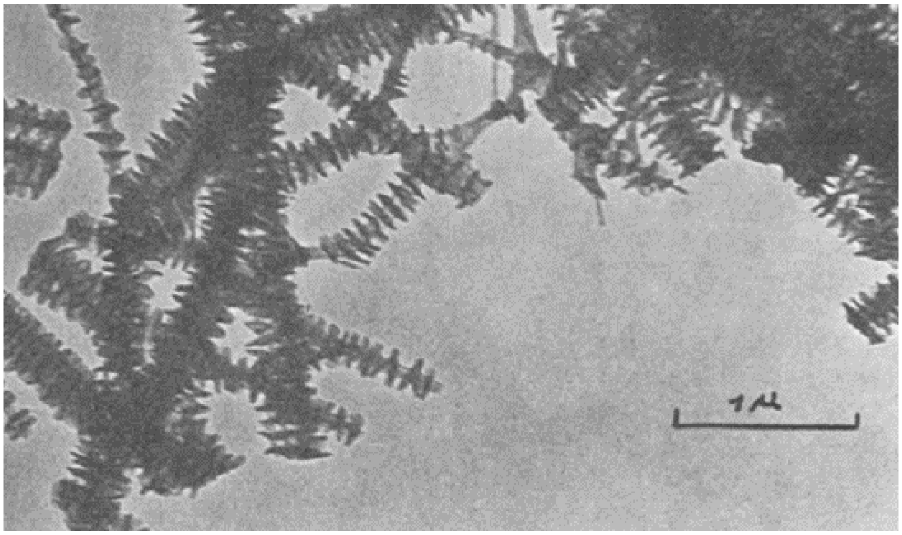

**Figure 1.2**: Shish-kebab structure. (Reproduced from Ref 10)

In 1979, Smith and Lemstra[15,16] made UHMWPE filaments where the molecules were really chain-extended, viz. molecular axis parallel to the fibre axis, with E-Moduli > 100 GPa and a tenacity of 3 GPa. They used a simple cylinder and plunger to pass a very dilute solution (1%) of UHMWPE in decalin through a small nozzle. The spun filaments were stored to dry prior to solid state deformation at higher temperature (but below the melting point) to obtain chain extended structures. Following this route, these authors succeeded in making high modulus, high strength fibres.

Further studies were performed to find out how drawability of extruded filaments varies with polymer concentration in solution, $\varphi$. Smith et al.[17] showed that the maximum drawability, $\lambda_{max}$, was proportional to the square root of the inverse of the initial polymer concentration $\lambda_{max} \sim \varphi^{-0.5}$. This equation shows that the drawability of UHMWPE in the solid state is limited by number of entanglements per unit chain.

Figure 1.3 illustrates schematically three different crystal topologies obtained by crystallization from the melt and solution. The number of trapped entanglements can be controlled depending on the crystallization conditions. Upon crystallization from the melt, the majority of the entanglements are trapped in the solid and act as physical crosslinks preventing draw. Crystallization from very dilute solution (below the critical overlap concentration) results in no entanglements in the amorphous phase and since no connectivity exists between the individual crystals, drawing is not possible albeit that connectivity can be induced by annealing below the melting temperature, see below. Upon crystallization from semi-dilute solutions the number of trapped entanglements is controlled by the initial polymer concentration hence connectivity is provided via trapped entanglements between the crystals but ultra-drawing is not prevented because of the low concentration of entanglements trapped in the solid.

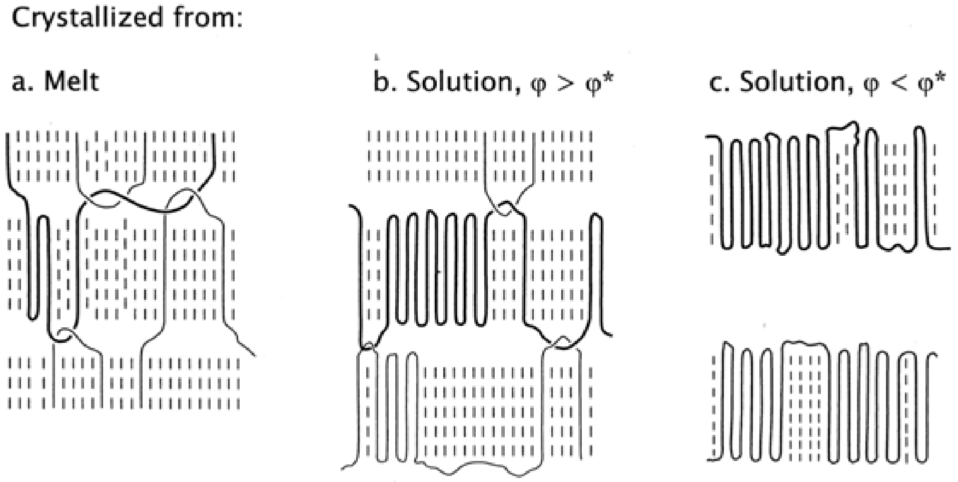

**Figure 1.3**: Crystal topology varies by crystallization from melt and solution at different polymer concentration, φ. φ* is the critical overlap concentration of polymer in dissolution.[18]

## 1.3 Solvent-free processing routes for UHMWPE

The solution spinning process is a successful method to produce high modulus fibres. However, it requires recovery of a large volume of solvent used during processing, about 90%, which poses problems in terms of economy and the environment. To recall, solution spinning is a process in which first a semi-dilute solution (above the critical concentration) of polymer in a solvent is prepared. A semi-dilute solution is a requisite because upon quenching a disentangled state is obtained in which a reduced a number of entanglements is present, see Figure 1.3 (b), providing coherence between lamellar crystals, but sufficient low in number to not resist ultra drawing. Therefore, the first key point in making a high stiffness UHMWPE fibre is making a disentangled polymer. Here, we will address the possibility of producing disentangled polymer in the form of nascent polymer powder directly in the reactor.

The concept of disentanglement of chains dates back to 1967 when Chanzy et al.[19] prepared coherent polymer films of polyethylene on glass slides at low temperature and suggested the potential ability of preparing fibrillar polyethylene during synthesis. The very first heating run of the as synthesized polymers, showed a melting peak close to the equilibrium melting point of polyethylene (142ºC). Chanzy et al. attributed this high melting temperature to the presence of extended chain crystals in the fibrillar morphology of the nascent polymer (for more details, please see Chapter 5 and References[20,21])[*]. Later, Smith et al.[22], by considering the entanglement and disentanglement concept, reported the possibility of preparing high strength/high modulus tapes and filaments. Low temperature polymerization conditions were used for the synthesis. In the late 1980's, Smith et al.[23] reported the high drawability and high E-modulus (about 100 GPa) for UHMWPE nascent powder consolidated below the melting point. Their results suggest the ability of a solvent-free route for generating disentangled polymer powders directly from synthesis. The consolidated disentangled polymer powder below melting point showed considerable drawability and consequently a high E-modulus.

With the development of single-site catalyst, it is now possible to obtain disentangled polymer in a larger scale. The catalyst used for the purpose is a single-site homogeneous catalyst. In such a system, active sites are homogenously dispersed in a solvent medium. By controlling the catalyst concentration, the active sites can be kept far from each other. During the propagation reaction, since the chains are much further apart, they have a lesser chance to entangle. Keeping the polymerization temperature lower than the crystallization temperature, as the growing chain experiences "a cold environment" immediate crystallization results in crystallites having few entanglements. The problem that arises in homogenous polymerization is the fouling, sticking of polymer particles to the reactor walls and stirrer. This is due to the fact that the crystallization process requires a nucleation step. The stirrer and the reactor walls provide "heterogeneous nuclei", while the nucleation barrier is suppressed reactor fouling is promoted.

It was shown in our group that the disentangled UHMWPE obtained directly from the reactor can be consolidated into film below the melting point. It is highly drawable in the vicinity of 125ºC (above the α relaxation temperature and below the melting point). It is convincingly shown that easy drawability in the solid state (more than 20 times) could provide high modulus, high strength tapes[24]. Therefore, it is anticipated that, due to the high drawability of films consolidated from the nascent polymer powder, high modulus of the drawn fibers might be comparable with the modulus of fibers obtained from solution spinning.

The introduction of metallocene, and notably post-metallocene catalysts[25], into polymer chemistry leads to the development of homogeneous polymerization providing disentangled polymers which facilitate solvent-free route to generate high strength fibers and tapes. However, attempts have been made to utilize commercial grade UHMWPE obtained from a Ziegler-Natta catalyst to create tapes possessing high modulus.[26] Kanamoto et al. [27] used bimodal UHMWPE by two stage drawing to obtain high strength tapes (100-140 GPa). Kanamoto et al. showed that UHMWPE obtained from heterogeneous polymerization at low monomer pressure can generate polymers possessing easier drawability in the solid state.[28]

---

[*] Later Engelen and Lemstra (Ref 21) attributed this high melting temperature to the fast reorganization process of crystals prior to melting. Recently, Rastogi et al.(Ref 22) ascribed this phenomenon to the simultaneous detachment of the adjacently re-entrant chain segments within the crystal connected by the amorphous chain segments having restricted chain mobility.

In conclusion, the desired disentangled state, which is a precursor for solid state deformation and is used to obtain extended chain structure to acquire high stiffness fibres or tapes, can be obtained via solution or directly via controlled polymerisation. The ease of solid state deformation suggests the presence of disentangled chains in the amorphous region of the semi-crystalline polymer. A question arises on the melting behaviour of the disentangled crystals. It may be anticipated that melting of the disentangled crystals will lead to the existence of a disentangled melt state, prior to the subsequent entanglement formation. The questions are “how entangling occurs once a polymer exceeds the melting temperature in which chains adopt the random coil state?” and “does disentangled state facilitate melt processing of UHMWPE?”. In the following section, an overview of such a possibility will be provided. Details are discussed in Chapters 4 and 5.

## 1.4 Crossing from the disentangled solid state to the entangled melt state

The similarity between disentangled polymers obtained from a dilute solution and directly from a polymerization reactor is the presence of fewer entanglements in the amorphous phase of the semi-crystalline polymers. Thus, polymers obtained via those two routes show easy solid state deformation. However, they also show differences in the crystal morphology which results in different thermally induced response on melting. It is shown that the solution-cast film obtained from dilute solution shows well stacked lamellar crystals[29] whereas the nascent powder possesses disordered crystals[30]. While on heating before melting point, stacked lamellar crystals facilitate the local mobility of stems and the diffusion of chains between adjacent crystals causes an increase of a lamellar thickness until it is doubled, Figure 1.4. This kind of diffusion is not possible in a nascent polymer due to the chaotic mixture of lamellar structures.

The differences in initial morphology, nascent versus solution cast, results in a different rate of entanglement formation. Bastiaansen et al.[31] found that a memory effect related to the initial disentangle state for solution cast film is lost almost instantaneously upon fast heating. This finding is in good agreement with the Lippits’s work[32] on solution cast films. He suggested that lamellar doubling prior to melt facilitates intermixing of chains on melting resulting in fast entangling. Due to the fact that nascent polymer lacks regular stacking of lamellae, the rate of entanglement formation is longer in comparison with the solution cast film. In this thesis, in continuation of Lippits’s work[32], it is shown that entangling of initially disentangled nascent polymer is a time-dependent process, where the time required for the entanglement formation varies with molar mass and heating rate. It can be concluded that the initial morphology plays a prominent role in the formation of entanglements.

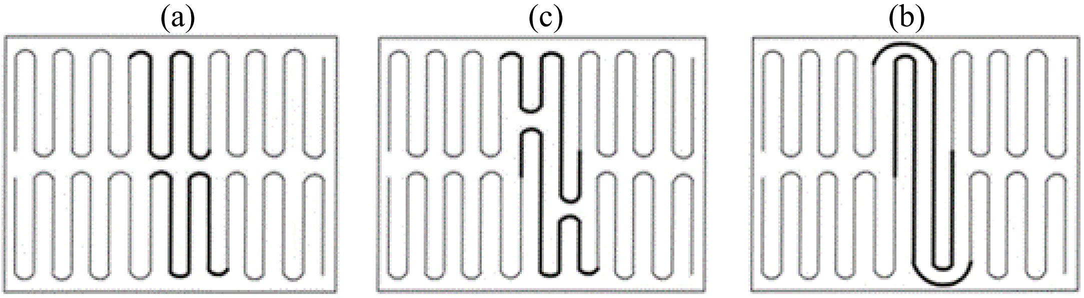

**Figure 1.4**: Schematic model to explain the doubling phenomenon in the regularly stacked adjacent lamellae. The bold line represents the test chain. (a) Before annealing, (b) occurrence of sliding diffusion during annealing and (c) doubled lamellae thickness. Adopted from Ref 29.

In this thesis it is shown that the rate of the entangling process for the initially disentangled polymer can be controlled by the (very) slow and controlled melting process. The UHMW-PE reactor powder consolidated below its melting point shows a gradual increase in the elastic modulus (G′) upon melting in the case of annealed samples in the rheometer. Rastogi et al.[33] attributed this phenomenon to a so-called "heterogeneous" melt. Upon annealing (below the melting point), the crystals start to melt from the sides and becomes partly entangled. This state retards the rate of entanglement formation while the whole crystal is melted (well above the melting temperature).

## 1.5 Scope of thesis

The present thesis is a continuation of the earlier work performed in our group. Kurelec explored a processing route making use of transient meso-phases on the borderline between solid and melt. In her thesis, she discussed about the problem of intractability of UHMWPE[30]. Following the work performed by Gruter and Wang at DSM[34], in the Polymer Chemistry Laboratory at the Eindhoven University of Technology, Sharma succeeded in the synthesis of disentangled UHMWPE.[35] Two different single-site catalysts were used for the synthesis of the disentangled polyethylenes. Lippits, in his thesis, made use of the available disentangled UHMWPE to answer the question "what happens when we start from the non-equilibrium disentangled state and cross the melting temperature into the molten state?" Among several studies performed on these disentangled polyethylenes, he also suggested that a new melt state, the heterogeneous melt, where the thermodynamic equilibrium state can not be reached, is obtained by controlling the melting kinetics.[32]

In this thesis, attempts are made to investigate polymer physics and rheological aspects of these disentangled polyethylenes. To achieve the desired goal, disentangled linear polyethylenes of different molar masses were synthesized. The know-how stated in the work of Sharma[35] has been further modified and routes have been explored to enhance polymer yield – by controlling the polymerization conditions that include the solvent used, the catalyst concentration and the polymerization temperature.

The molar mass and molar mass distribution of the samples thus obtained was determined by melt rheometry. The results are compared with the data obtained from high temperature gel permeation chromatography coupled with multi angle laser light scattering.

The availability of different molar mass UHMWPE with narrow distribution in the disentangled state facilitated to following studies.

- With the help of oscillatory rheometer, the rheology of disentangled UHMWPE in the linear and non-linear viscoelastic regime was investigated.
- The formation of entanglements for disentangled UHMWPE and its influence on crystallization was followed by means of DSC.
- Combination of the results obtained from SAXS/WAXS and solid state NMR with rheometry and DSC complemented our findings.
- Sintering of the disentangled polymer powder above the melting point resulted in a fully fused product.

The thesis is divided into six chapters, where chapters 2 to 5 addresses the issues stated above and the chapter 6 addresses the possible technological aspects of these disentangled polyethylenes. A summary of the chapters is provided in the summary section of the thesis.

## 1.6 References

[1] Staudinger H, *Ber. Deut. Chem. Ges*, **1920,** 53, 1073.

[2] *Chem. Eng. News*, January, **1954**, 11.

[3] Treloar L. R. G., *Trans. Faraday Soc.*, **1940,** 35, 538.

[4] Doi M., Edwards S.F., *The Theory of Polymer Dynamics,* **1986**, Clarendon Press, Oxford.

[5] de Gennes P.G., *Scaling Concepts in Polymer Physics,* **1979**, Cornell University Press, Ithaca, NY

[6] Marrucci G., *J Non-Newtonian Fluid Mech*, 62, **1996**, 279.

[7] Likhtman A. E., Milner S. T. and McLeish T. C. B., *Physical Review Letter*, **2000**, 85, 4550.

[8] Strobl G., *The Dynamics of Polymers*, **1996**, Springer-Verlag Berlin.

[9] Zwick M., **1965**, patent application NL 6501248.

[10] Pennings A. J. , van der Mark J. M. A. and Kiel A. M. , *Kolloid-Z. u. Z.Polymere,* **1965**, *205,* 160.

[11] Peterlin A. J., *J. Polymer Sci*, **1966**, B4, 287.

[12] Keller A. and Odell J. A., *Colloid Polymer Sci.,* **1985**, 263, 181.

[13] Franck F. C., *Proc. Royal Soc. London sec* A, **1970**, 319 , 160.

[14] de Gennes P. G., *J. Chem. Phys,* **1974**, 60, 15.

[15] Smith P., Lemstra P. J., Kalb B. and Pennings A. J., *Polymer Bulletin*, **1979**, 1, 733.

[16] Smith P. and Lemstra P. J, *Makromol. Chem.*, **1979**, 180, 2983.

[17] Smith P., Lemstra P. J. and Booij H. C., *Journal of Polymer Science: Polymer Physics Edition*, **1981**, 19 , 877.

[18] Lemstra P.J., Bastiaansen C.W.M. and Meijer H.E.H., *Die. Angewandte Makromolekular Chmeie*, **1986**,145-146, 343.

[19] (a) Chanzy H., Day A. and Marchessault R. H., *Polymer,* **1967**, 8, 567*; (b)* Chanzy H. and Marchessault R.H., *Macromolecules*, **1969**, 2, 108*; (c)* Chanzy H. D., Revol J. F., Marchessault R. H. and Lamand A , *Colloid& Polymer*, **1973**, 251, 563*; (d)* Chanzy H. D. , Bonjour E. and Marchessault R. H., *Colloid& Polymer,* **1974**, 252, 8.

[20] Engelen M.T.T. and Lemstra P. J., *Polymer Communications*, **1991**, 32, 343.

[21] Lippits D.R., Rastogi S. and Hohne G. W. H., *Physical Review Letters*, **2006,** 96, 218303.

[22] (a) Smith P., Chanzy H. D. and Rotzinger B. P., *Polymer Communications,* **1985,** 26, 258*;(b)* Smith P., Chanzy H. D. and Rotzinger B. P., *PCT International Application, WO 8703288, **1987** (c)* Smith P., Chanzy H. D. and Rotzinger B. P., *J. Materials Science*,**1987** 22, 523.

[23] Smith P., Chanzy H. D. and Rotzinger B. P., *Polymer,* **1989,** *30,*p1814.

[24] Smith P. and Lemstra P. J., *Journal of Material Science,* **1980**, 15, 505.

[25] (a) Matsui S., Tohi Y., Mitani M., Saito J., Makio H., Tanaka H., Nitabaru M., Nakano T. and Fujita T., *Chem. Lett.* **1999**, 1065; (b) Matsui S., Mitani M., Saito J., Tohi Y., Makio H., Tanaka H. and Fujita, T. *Chem. Lett.* **1999**, 1263. (c) Matsui S., Mitani M., Saito J., Matsukawa N., Tanaka H., Nakano T. and Fujita T., *Chem. Lett.* **2000**, 554

[26] (a) Porter R. S. and Kanamoto T., *Polymer Engineering and Science*, **2004**, 34, 266 and (b) Porter R. S. and Kanamoto T. and Zachariades A. E., *Polymer*,**1994**, 35, 4979.

[27] Nakazato K., Kanamoto T. and Porter R. S., *Rep. Prog. Polym. Phys. Jpn.,* **1998**, 41, 317.
[28] Sano A., Iwanami Y., Matsuura K., Yokoyama S. and Kanamoto T, *Polymer*, **2001**, 42, 5859.
[29] Rastogi S., Spoelstra A. B., Goossens J. G. P. and Lemstra P. J., *Macromolecules***,** **1997,** 30, 7880.
[30] Corbeij-Kurelec L., *Chain mobility in polymer system; on the borderline between solid and melt,* **2001**, Ph.D. thesis, Eindhoven University of Technology.
[31] Bastiaansen C.W.M., Meyer H.E.H. and Lemstra P.J., *Polymer*, **1990**, 31, 1435.
[32] Lippits D.R., *Controlling the melting kinetics of polymers; a route to a new melt state,* **2007**, Ph.D. thesis, Eindhoven University of Technology.
[33] Rastogi S., Lippits D., Peters G.W.M., Graf R., Yao Y-F and Spies H.W., *Nature Materials*, **2005**, 4, 635.
[34] Gruter, G.J.M.; Wang, B.; van Beek, J.A.M. *European Patent Application* EP 1057837 A1 **2000.**
[35] Sharma K., *Easily processable UHMWPE with narrow molecular weight distribution,* **2005**, Ph.D. thesis, Eindhoven University of Technology.

This page is intentionally left blank

# Chapter 2

# Synthesis of disentangled polyethylene

## 2.1 Introduction

Polyethylene (PE) is one of the mass production commodity polymers and is a generic name for a class of polymer. Depending on polymerization conditions such as temperature, pressure and catalyst, different kinds of polyethylene can be produced. In a high pressure radical process, various levels of branching is observed leading to Low Density Polyethylene (LDPE). Utilizing organometallic catalysts in the low pressure process yields linear polyethylene, viz High Density Polyethylene (HDPE)[1]. In general, HDPE is prepared by slurry or gas-phase polymerization. Both processes are widely used because of the possibility of producing a wide range of commercial grades including ultra-high molecular weight polyethylene (UHMWPE). In general, UHMWPE is a linear polyethylene with molecular weights over $1x10^6$ Daltons and is known as a high performance polymer with excellent physical properties, such as high toughness, self-lubrication, and abrasion resistance.

The slurry phase production of UHMWPE was first commercialized by Ruhrchemie AG during the 1950s[2]. Generally, classical heterogeneous Ziegler-Natta catalysts are used for this process. Since the active sites in such catalyst systems are relatively close together, the chains also grow in close proximity. This in combination with the relatively high polymerization temperature of 60-100°C, at which crystallization of polymer chains is slower than the chain growth, results in a high degree of entanglement. Due to the high molecular weight and the high degree of entanglement, chain mobility in the melt is limited. This causes difficulty in complete fusion of the polymer particles during processing. Thus, the structure created during synthesis influences the final properties of the polymer. In principle disentangled UHMWPE should have more processability [3].

Chanzy et al. were the first to report the synthesis of disentangled UHMWPE, although they did not attempt any processability test[4]. Smith et al. discovered that high strength/high modulus tapes and filaments can be obtained from disentangled UHMWPE prepared at low temperature[5]. The actual idea to use disentangled UHMWPE to obtain better processability was first explored by Gruter and Wang at DSM[6] and was further developed at the Eindhoven University of Technology[3,7,8]. The principle of the idea is to synthesis polyethylene under conditions where (*i*) the crystallization rate is higher than the propagation rate (*ii*) and the polymers are formed in dilute system. To achieve this, homogenous catalysts have been applied at relatively low temperature. In such a system, active sites are homogenously dispersed in a solvent medium. By controlling the catalyst concentration, the active sites can be kept far from each other. Thus, during the propagation reaction, since the chains are much further apart, they have less chance to entangle. Furthermore, lowering the polymerization temperature favors the formation of disentangled crystals. A comparison of heterogeneous and homogenous polymerization systems are shown schematically in Figure 2.1. It is important to emphasize here that the ability to synthesize disentangled UHMWPE using a homogenous catalyst is strongly dependent on reaction variables such are temperature, monomer pressure and catalyst type.

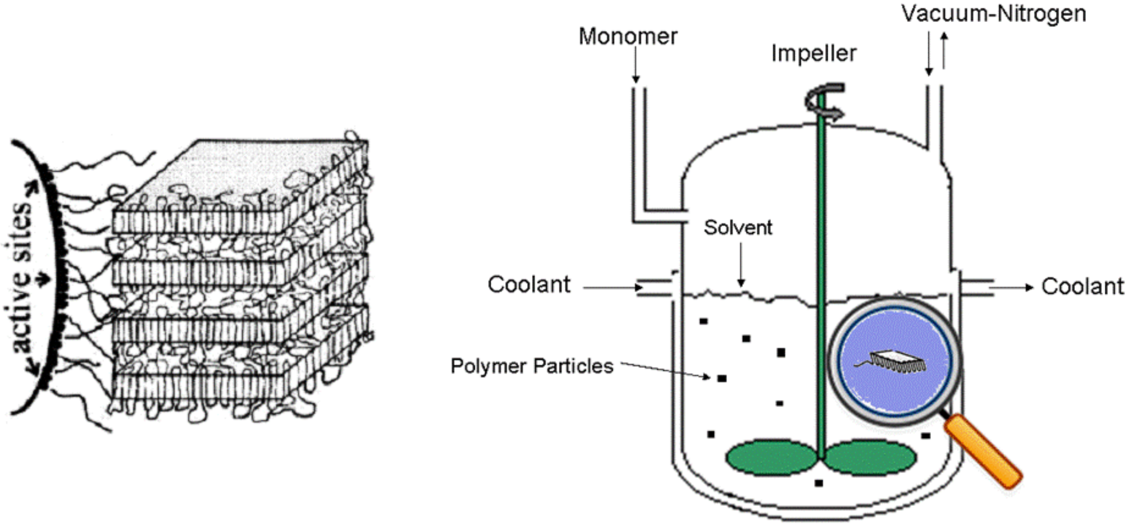

(a) (b)

**Figure 2.1:** Polymerization in (a) heterogeneous[9] and (b) homogeneous systems. In the heterogeneous system active sites are close to each other. Thus, the polymer chains have more chance to meet and entangle. In the homogenous system the chains are far from each other. Thus, the chains have less chance to entangle and are much more likely to form single crystals.

The ability to characterize polymer products is highly important and that is exactly where the bottle neck is for UHMWPE. Due to its poor solubility in common organic solvents molecular weight determination of UHMWPE by means of high temperature GPC has always been cumbersome and a matter of debate. The current state of art has taught us that molecular weight determination of such high molar mass polymers can much more reliably be performed by melt rheometry. Using this technique, it is the objective of this chapter to improve the current synthesis routes to control and predict the molar mass of the product.

## 2.2 Materials and methods

All manipulations were performed under an argon atmosphere using a glove box (Braun MB 150 GI) and Schlenk techniques. Solvents were purchased from VWR. Dry solvents were prepared by passing them over a column containing $Al_2O_3$ and degassed at least twice prior to use. Fluorinated bis(phenoxy imine) titanium complex, Scheme 2.1, as a catalyst, and methyl aluminoxane (MAO), as a co-catalyst, were used as received from MCAT GmbH[10] and Fluka, respectively.

Ethylene (3.5 grade supplied by Air Liquid) was purified by passing over columns of BTS copper catalyst and 4° Angstrom molecular sieves.

Polymer synthesis was performed under an inert atmosphere by using a glass reactor (1 L) equipped with a mechanical stirrer and a temperature probe. Solvent was introduced to the nitrogen-purged reactor and stirred. The solvent was thermostated to the prescribed polymerization temperature, and then the ethylene gas feed (1 bar pressure) was started. Polymerization was initiated by the addition of MAO and catalyst in toluene. After a certain time, polymerization was terminated by the addition of acidified propanol. The resulting polyethylene was collected by filtration, washed with acetone and water then dried under vacuum at 60ºC overnight.

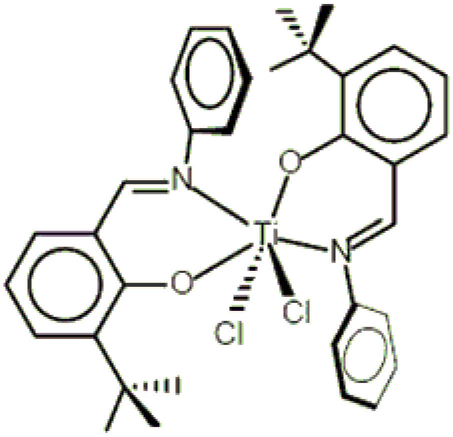

**Scheme 2.1:** shows structure of catalyst used for polymerization. This will be referred as FI catalyst

Molar mass characterization has been performed mainly by melt rheometry using an oscillatory rheometer RMS 800. These data have been confirmed by high temperature size exclusion chromatography (HT-SEC). Molar mass determination will be discussed in detail in chapter 3. It should be mention that in order to obtain reliable SEC data the chromatograph has to be specifically calibrated for very high molar masses. Nevertheless, for molar masses above $5x10^6$ g/mol SEC becomes highly unreliable and deviations on molar mass of over 100% are not uncommon.

## 2.3 Homogeneous versus heterogeneous polymerization

Although the polymer market has been dominated by the multi-sited heterogeneous Ziegler-Natta catalysts, single-site catalysts represented by group 4 metallocene compounds are finding an exceptional role in polymer industry. Metallocene complexes have long been known as olefin polymerization catalysts albeit that initially obtained activities were low. Indeed, these catalysts were discovered by Natta and Breslow independently in the 1950s[11,12]. Dialkylaluminumchloride, the same co-catalyst for heterogeneous polymerization, was initially used to activate metallocene catalysts. The catalyst system was able to produce polyethylene, but the activity was marginal. However, the addition of small amounts of water per mole of aluminum resulted in a considerable increase in activity[13]. The discovery by Kaminsky and Sinn who showed that the reaction of trimethyl aluminum with water resulted in methyl aluminoxane (MAO), a very active co-catalyst for most homogeneous catalyst, marked the beginning of the development of single-site homogeneous metallocene and post-metallocene catalysts[14]. The advantage of single-site catalysts over classical Z-N catalysts is their capability to produce polymers with controlled molecular weight, specific tacticity and improved molecular weight distribution[15]. A special class of single site catalysts is formed by living single-site catalysts.

## 2.4 Living or controlled polymerization

The concept of living polymerization was first described for anionic polymerization of styrene by Szwarc[16]. Living systems are of great interest for a variety of reasons: tuning of molecular weights; end group functionalization; block copolymer formation etc. Due to these great advantages, the living polymerization of olefins has been of major interest. A polymerization is called living when the chain termination and/or transfer reactions are absent. One of the most common strategies to achieve a living system is the lowering of the polymerization temperature. Since the activation energy for the chain transfer reaction is generally higher than that for the propagation reaction, lowering temperature more adversely affects elimination processes relative to enchainment. The design of living catalysts is not trivial and is generally based on empirical and computational method[17]. A classical example of a living olefin polymerization catalyst is group IV metal complexes bearing phenoxyimine ligands invented by scientists at Mitsui[18]. These catalysts have been used in different laboratories and progress in the area of stereo- selective as well as living olefin polymerization has been reported[19, 20]. Fujita et al. has shown that utilizing the FI catalyst living polymerization of ethylene is feasible at room temperature. The highest molar mass that they gained in one minute of polymerization was around $4.5 \times 10^5$ g/mol[21]. Carrying out the same polymerization at room temperature for 5 minutes Sharma[3] produced polyethylene with molar mass above one million. However, due to limited reliability of the used GPC method to determine the molecular weight an accurate estimate of the molar mass could not be obtained. Using melt rheometry as a characterization method, it will be demonstrated that this system is capable of producing UHMWPE with molar mass even exceeding $9 \times 10^6$ g/mol in still a controlled manner.

## 2.5 Effect of polymerization parameters

There are many parameters that control catalyst activity and molar mass of the produced polymer. The parameters that were studied in this work are polymerization time, polymerization temperature, type of solvent and co-catalyst to catalyst ratio.

### 2.5.1 Polymerization time

It has previously been reported that polymerization time had only limited effect on the molar mass for polymers synthesized with the FI catalyst with molecular weight above approximately $10^6$ g/mol. The observed increase of yield with polymerization time was therefore attributed to slow initiation and fast propagation to give products with a molecular weight of $10^6$ g/mol after which heterogenization of catalyst system good severely hamper chain growth as results of mass limitation[3]. In this work, with rheology as an alternative characterization method for high molar mass polymers, the further investigation on the influence of polymerization time on the molar mass has been performed. Figure 2.2 shows the molar mass development with increasing polymerization time based on melt rheology plus GPC specially calibrated for high molar masses. Albeit optimized for ultra high molecular weight polymers, GPC remains unreliable for molecular weights $4\text{x}10^6$ g/mol. Unlike what was reported before the molar mass thus increase with the polymerization time[3]. However, the polydispersity increases considerably with time which indicates that the system starts to deviate from pure living. The reason can be that either the catalyst is not truly living over the full polymerization time, or that the single-site system turns into a multi-site system as the result of heterogenization of the system. This would strongly influence diffusion of ethylene to the living catalyst. This phenomenon could be comparable with self-immobilization of single-site catalysts that has been a subject of interest recently[22]. The trend in Fig 2.2 is quite similar to the published data by Ivanchev et al.[23]. These authors suggested the capture and blocking of active sites by the grown polymer after a certain polymerization time.

### 2.5.2 Polymerization temperature

Polymerization temperature ($T_p$) is one of the most complicated operational factors for the polymerization. The solubility of ethylene monomer in the solvent decreases by increasing temperature and, consequently, the monomer concentration drops at higher temperature[24] (Fig 2.3) causing a decrease in the propagation reaction. On the other hand, raising the temperature increases both the propagation rate as well as the probability of chain transfer reactions. Normally, chain transfer reactions have higher activation energies than insertion reactions and a change in $T_p$ strongly affects the rate of chain termination, hence the molecular weight[25,26, 27]. Consequently catalysts that show living behavior at low temperature might show chain termination at elevated temperature. For example, Fujita et al. reported a certain temperature to get the highest molar mass of the produced polymer, which decreases below or above this temperature[28].

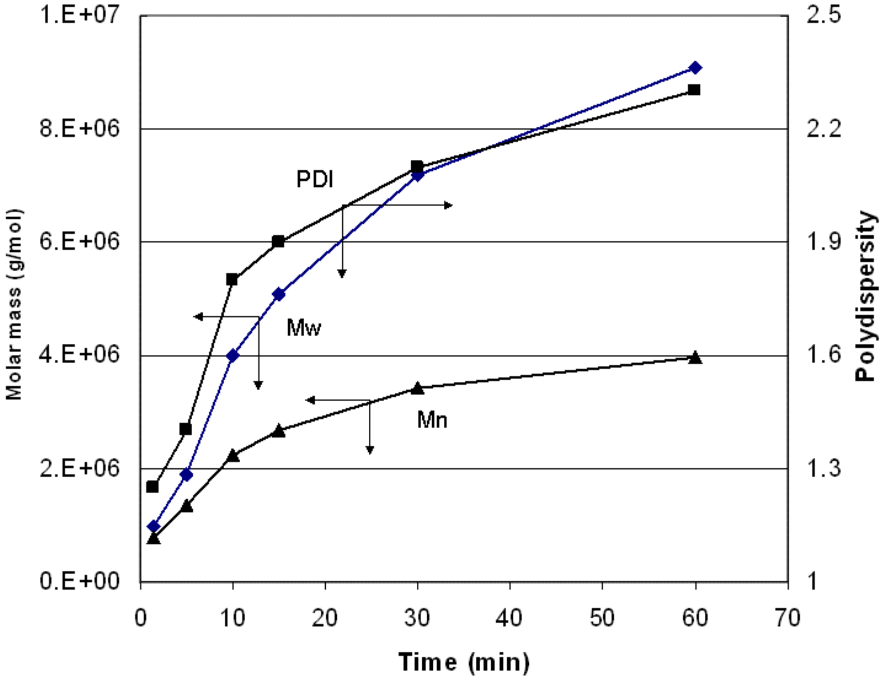

**Figure 2.2:** Effect of polymerization time on the Mw, Mn and PDI of UHMWPE using the FI catalyst (other polymerization parameters are constant: polymerization temperature 20ºC, catalyst concentration 1µmol, Al:Ti molar ratio 8500, atmospheric pressure, in 750 mL of toluene). Polymer characteristics, such are Mw, Mn and PDI, have been determined using GPC and melt rheometry as described in Chapter 3. GPC measurements were performed at Erlangen University in the group of Prof Münstedt.

In Figure 2.4, the effect of the polymerization temperature on the MW and PDI of the obtained polymer by using the FI catalyst is illustrated. The average molecular weight increases with increase in polymerization temperature, illustrating that increasing the temperature does not lead to termination processes. This can be explained by a very low probability of chain transfer reactions for this catalyst. Because increasing temperature causes an increase in the propagation rate and since there is no chain transfer reaction due to the existence of a tert-butyl group at the 3-position of the phenoxy moiety as reported by Fujita et al.[29] producing high molar mass at shorter time is feasible. Surprisingly at temperature exceeding 30ºC a dramatic drop in polymer yield was observed suggesting the thermal decomposition of the catalyst. Using petroleum ether as a solvent instead of toluene Sharma observed a significant catalytic activity for the same catalyst at temperature as high as 70ºC. This is probably the result of a difference in thermal stability of the catalyst for the different solvents. The solvent effect will be discussed later in this chapter.

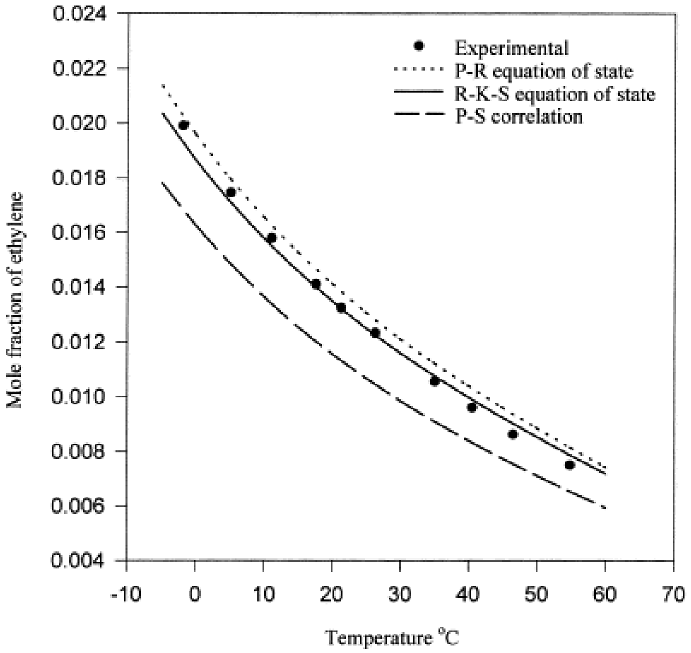

**Figure 2.3:** Solubility of ethylene in toluene at 1 atm. Data from Ref 24.

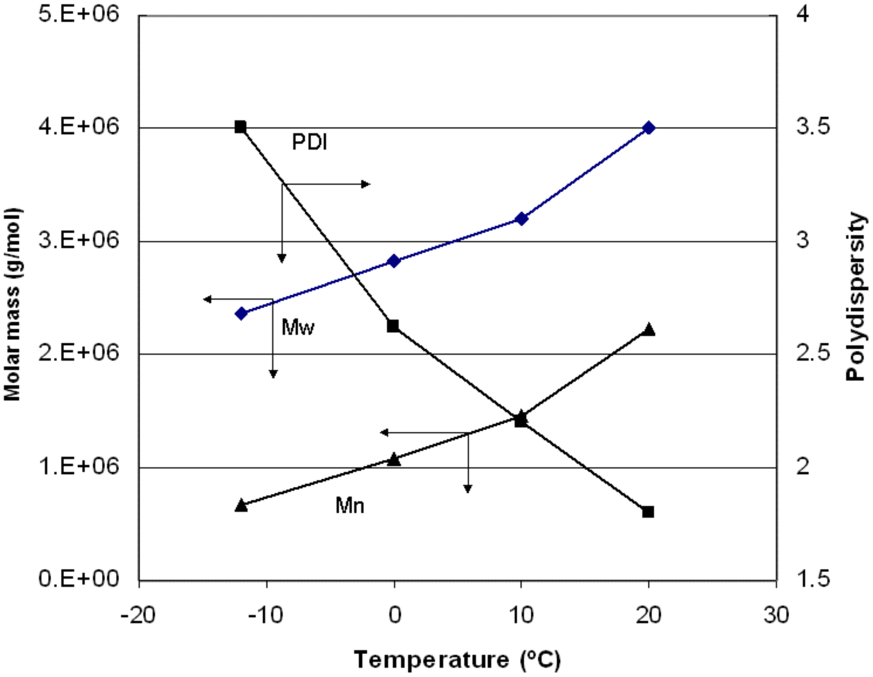

**Figure 2.4:** Effect of the polymerization temperature on the Mw, Mn and PDI of UHMWPE prepared using the FI catalyst. (Other polymerization parameters are constant. Polymerization time 10 minutes and Al:Ti molar ratio 8500 at atmospheric pressure, 750 mL of toluene).

Another interesting feature is the dramatic increase of the polydispersity with lowering of the polymerization temperature (Figure 2.4). At lower temperature, the solubility of the grown chains in the solvent decreases resulting in more rapid precipitation of the polymers chains from solution. Such heterogenization of the catalyst at low temperature can impede the controlled nature of a living polymerization resulting in broadening of the molecular weight distribution. An alternative cause of the broadening of PDI forms slow or partial catalyst activation at low temperature.

### 2.5.3 Type of solvent

The nature of the solvent affects the polymerization system in two ways. First of all the solubility of ethylene depends on the type of solvent (Figure 2.5). Furthermore, since we are dealing with cataionic catalytically active species the polarity of the solvent will strongly determine the solvatation and ion separation of the catalyst[24,25,30].

One of the striking phenomena that was observed in this work is that using toluene as a polymerization medium instead of heptane, hexane or petroleum ether results in a remarkable increase on yield of the polymer. The results are summarized in Table 2.1. Considerable increase in the yield of synthesized polymer using toluene can not be explained by the varying of solubility of monomer resulted of solvent type because the solubility of ethylene in toluene is comparable with other solvents, such as benzene and cyclohexane, and even slightly lower than hexane, Figure 2.5. This effect may be ascribed to the higher polarity of toluene, resulting in more effective separation of the cationic active species and the counterion. This is in accordance with the results published by Fujita for a zirconium catalyst[28].

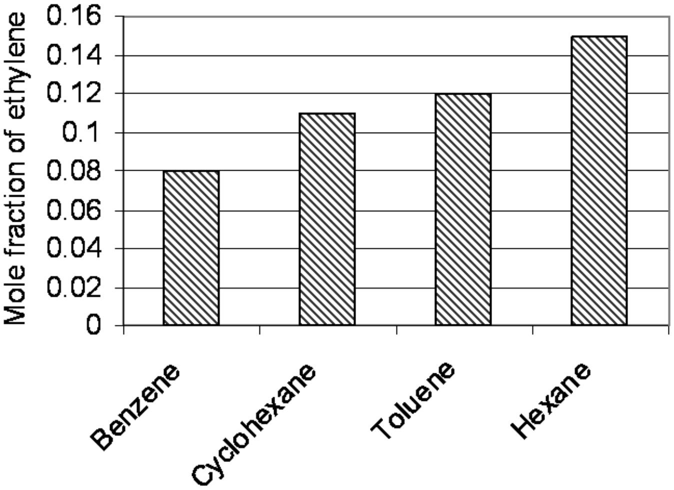

**Figure 2.5:** Solubility of ethylene in different solvents at 10 atm and 30ºC. Data from Ref 24 and 30.

**Table 2.1:** Polymerization of ethylene using the FI catalyst with two different solvents

| Run | Mw (g/mol) | PDI | Yield (g) |
|---|---|---|---|
| 1(a) | $9.1x10^6$ | 2.3 | 12 |
| 2(b) | $5.5\ x10^6$ | 2.4 | 3 |
| 3(c) | $3.4\ x10^6$ | 2.4 | 1.7 |

(a) 750 mL of toluene as solvent at 20ºC, 1 hour polymerization time, MAO:Cat ratio 8500.
(b) 750 mL of petroleum ether as solvent at 20ºC, 1 hour polymerization time, MAO:Cat ratio 54,000.
(c) 750 mL of petroleum ether as solvent at 0ºC, 30 min polymerization time, MAO:Cat ratio 17,000.

### 2.5.4 Co-catalyst to catalyst ratio

Methyl aluminoxane (MAO) is the most widely used co-catalyst in homogenous polymerizations. Its structure is not clearly known, however, some possible structures are proposed in the literature[31]. Beside acting as a scavenger, the role of MAO comprises alkylation of the catalyst precursor, generation of cationic active species and stabilization of these species by coordinative contact with its Cl-MAO$^-$ (and / or Me-MAO$^-$) counter-ion. It is likely that the necessary excess of MAO shifts the reaction equilibrium towards the active species[32,33]. Other additional roles for MAO are reflected by the larger amounts of it required for higher activity. It is proposed by several authors that the metallocene (or post-metallocene catalysts such as the FI catalyst) is surrounded by MAO in the outer-sphere preventing deactivation of the catalyst that may arise due to bimolecular processes between metallocenes[25,27,33]. However it should not be forgotten introducing a large excess of MAO affects the polarity of reaction mixture. For example, Sharma[3] found that the polymer yield continues to increase with increasing amount of MAO even up to a staggering Al:Ti ratio of 130,000, which is difficult to explain by effects other than polarity.

The effect of the aluminum:metal ratio for the metallocene catalyzed polymerization of ethylene has been explored by Chein and Wang[34]. However, the effect of the Al:M ratio on the molar mass of the polymer produced is still ambiguous and different data have been reported[35]. Decrease of molar mass by increasing the Al:M ratio can be explained by chain transfer reactions due to high concentration of methyl aluminoxane. In the case of the FI catalyst increasing the amount of MAO results in an increase in molar mass rather than a decrease (Figure 2.6). Clearly, in the case of FI catalyst chain transfer to aluminum does not occur. Assuming that the catalyst is intrinsically living, the observed increase in yield and molar mass with increasing Al:Ti ratio can be explained by the increased in the polarity of medium with increasing MAO concentration. The increase in PDI is assumed to be the result of heterogenization of the system.

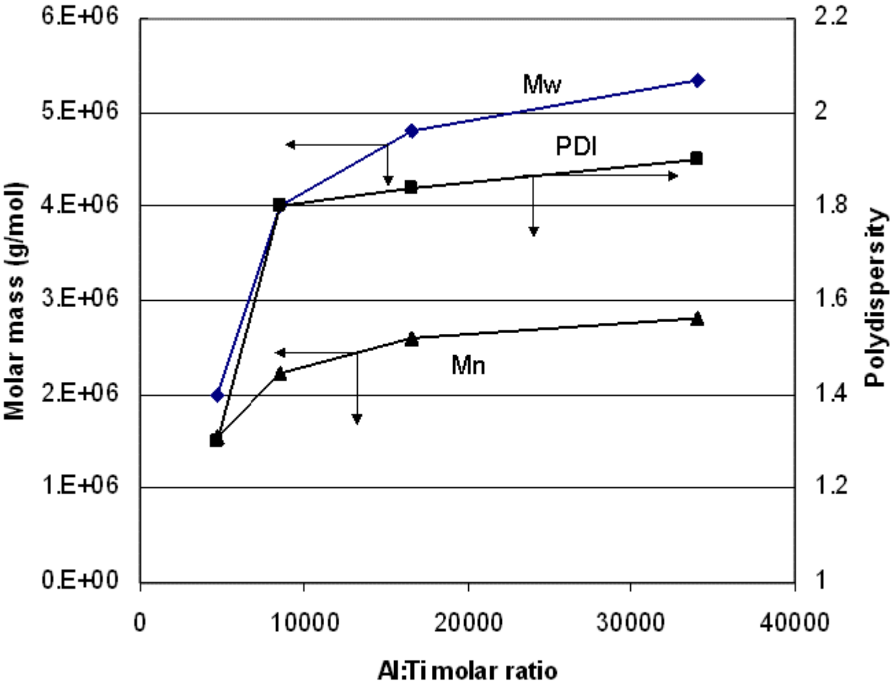

**Figure 2.6:** Effect of MAO:catalyst ratio on the Mw, Mn and PDI of UHMWPE using the FI catalyst (other polymerization parameters were kept constant, polymerization temperature 20ºC, polymerization time 10 minutes at atmospheric pressure in 750 mL of toluene)

## 2.6 Conclusions

In this chapter we have shown that by controlling the polymerization parameters and [3-*t*-Bu-2-O-$C_6H_3CH=N(C_6F_5]_2TiCl_2$/MAO as the catalyst system it is indeed possible to tune and predict the molar mass of the polyethylene formed.

For short reaction times, a linear dependence between the polymerization time and the molar mass was observed, indicative for living behavior. The polymerization rate is fast and a molar mass above $1x10^6$ g/mol is already obtained after 5 minutes. Consequently, the polymer rapidly precipitates leading to heterogenization of the catalyst system, which results in broadening of the PDI. The polydispersity is also broadened when the polymerization is carried out at low temperature. This is most probably caused by slow and partial of activation of precatalyst at this temperature.

Besides polymerization time and temperature, solvent type and co-catalyst:catalyst ratio are two additional parameters that influence the molar mass of the polymer. The polymerization rate is considerably faster in toluene than in aliphatic solvents, which is assumed to be caused by the higher polarity of the former. Likewise, increasing the amount of MAO also increases the polarity of the reaction medium affording better ion separation and therefore a higher observed activity. Hence, since we are dealing with a living catalyst system, a higher polymerization rate leads to a higher molecular weight for the same reaction time.

Summarizing, by tuning polymerization time and temperature and choosing the appropriate solvent, using the FI catalyst UHMWPE can be obtained with extremely high molar masses of up to $10^7$ g/mol with an acceptable PDI of around 2. In chapter 4 it will be shown on the basis of rheology measurements that the polyethylenes produced using the protocol described in this chapter are indeed highly disentangled.

## 2.7 References

[1] Odian G., *Principles of Polymerization*, **2004**, Fourth Edition, John Wiley & Sons.

[2] Kurtz S.M., *The UHMWPE handbook*, **2004**, Elsevier Academic Press.

[3] Sharma K., *Easily processable UHMWPE with narrow molecular weight distribution,* **2005**, Ph.D. thesis, Eindhoven University of Technology.

[4] (a) Chanzy H., Day A. and Marchessault R. H., *Polymer,* **1967**, 8, 567,*; (b)* Chanzy H. and Marchessault, *Macromolecules*, **1969**, 2, 108*; (c)* Chanzy H. D., Revol J. F., Marchessault R. H. and Lamand A , *Colloid& Polymer*, **1973**, 251, 563,*;(d)* Chanzy H. D. , Bonjour E. and Marchessault R. H., *Colloid& Polymer,* **1974**, 252, 8.

[5] (a) Smith P., Chanzy H. D. and Rotzinger B. P., *Polymer Communications,* **1985,** 26, 258 *(b)* Smith P., Chanzy H. D. and Rotzinger B. P., *PCT International Application, WO 8703288, **1987** (c)* Smith P., Chanzy H. D. and Rotzinger B. P., *J. Materials Science,***1987** 22, 523; *(d)* Rotzinger B. P., Chanzy H. D. and Smith P., *Polymer,* **1989,** *30,*p1814.

[6] Gruter, G.J.M.; Wang, B.; van Beek, J.A.M. *European Patent Application* EP 1057837 A1 **2000.**

[7] Corbeij-Kurelec L., *Chain mobility in polymer system; on the borderline between solid and melt,* **2001**, Ph.D. thesis, Eindhoven University of Technology.

[8] Lippits D.R., *Controlling the melting kinetics of polymers; a route to a new melt state,* **2007**, Ph.D. thesis, Eindhoven University of Technology.

[9] Loos J., Arndt-Rosenau M., Weingarten U., Kaminsky W. and Lemstra P.J., *Polymer Bulletin*, **2002**, 48,191.

[10] www.metallocene.de

[11] Natta G., Pino P., Mazzanti G. and Giannini U., *J. Am. Chem. Soc.*, **1957**, 79, 2975.

[12] Breslow D. S., Newburg N. R., *J. Am. Chem. Soc.*, **1957**, 79, 5072.

[13] Long W. P., and Breslow, D. S., *Justus Liebigs Ann. Chem.*, **1975**, 463.

[14] Sinn H., Kaminsky W., Vollmer H. and Woldt R., *Angew. Chem. Int. Ed.*, **1980**, 19, 390.

[15] Matsugi T. and Fujita T., *Chemical Society Reviews*, **2008**, 37, 1264.

[16] Szwarc M. (a) *J. Am. Chem. Soc.*, **1956**, 78, 2656; (b) *Nature*, **1956**, 178, 78.

[17] (a) Domskia G. J., Rosea J. M., Coates G. W., Boligb A. D., Brookhartb M., *Prog. Poly. Sci.*, **2007**, 32, 30; (b) Coates G. W., Hustad P. D. and Reinartz S., *Angew. Chem. Int. Ed.*, **2002**, 40, 2236.

[18] (a) Matsui S., Tohi Y., Mitani M., Saito J., Makio H., Tanaka H., Nitabaru M., Nakano T. and Fujita T., *Chem. Lett.* **1999**, 1065 (b) Matsui S., Mitani M., Saito J., Tohi Y., Makio H., Tanaka H. and Fujita, T. *Chem. Lett*. **1999**, 1263 (c) Matsui S., Mitani M., Saito J., Matsukawa N., Tanaka H., Nakano T. and Fujita T., *Chem. Lett.* **2000**, 554. (d) Fujita, T., Tohi, Y., Mitani, M., Matsui, S., Saito, J., Nitabaru, M., Sugi, K,., Makio, H. and Tsutsui, T., *Eur. Pat. Appl.* 874005 (e) Nakano T., Tanaka H., Kashiwa N. and Fujita T., PCT Int. Appl. WO2001055231.

[19] (a) Tian J., Coates G. W., A*ngew. Chem.*, **2000**, 112, 3772 (b) *Angew. Chem. Int. Ed.*, **2000**, 39, 3626.

[20] (a) Mitani M., Mohri J-I., Yoshida Y., Saito J., Ishii S., Tsuru K., Matsui S., Furuyama R., Nakano T., Tanaka H. , Kojoh S-I., Matsugi T., Kashiwa N., and Fujita T. ,*J. Am. Chem. Soc.*, **2002**, 124, 7888; (b) Mitani M., Nakano T. and Fujita T., *Chem. Eur. J.*, **2003**, 9, 2396.

[21] Saito J. , Mitani M., Mohri J-I., Yoshida Y., Matsui S., Ishii S-I., Kojoh S-I., Kashiwa N. and Fujita T., *Angew. Chem.,* **2001**, 113, 3002.

[22] Zhang J., Wang X., Jin G-X. , *Coord. Chem. Rev.,* **2006**, 250, 95.

[23] (a) Ivanchev S. S., Badaev V. K., Ivancheva N. I. and Khaikin S. Ya., *Diklady Physical Chemistry*, **2004**, 394, 46; (b) Ivanchev S. S., Trunov V. A., Rybakov V. B., Al'bov D. V. and Rogozin D. G., *Diklady Physical Chemistry,* **2005**, 404,165.

[24] Atiqullah M., Hammawa H. and Hamid H., *Eur. Polym. J.,* **1998**, 34, 1511.

[25] Huang J. and Rempel G.L., *Prog. Polym. Sci.,* **1995**, 20, 459.

[26] Kaminsky W., Kulper K. and Niedoba S., *Makromol. Chem., Macromol. Symp.,* **1986**, 3, 377.

[27] Chein J.C.W. and Sugimoto R., *J. Polymer Science, polymer chemistry Ed.* **1990**, 28, 15.

[28] Saito J. , Mitani M., Matsui S., Tohi Y., Makio H., Nakano T., Tanaka H., Kashiwa N., Fujita T., *Macromol. Chem. Phys.*, **2002**, 203, 59.

[29] Furuyama R., Saito J., Ishii S-I., Mitani M., Matsui M., Tohi Y., Makio H. , atsukawa N., Tanaka H., Fujita T., *Journal Molecular Cayalysis A: chemical*, **2003**, 31, 200.

[30] Zhuze T. P. and Zhurba A.S., *Russian Chemical Bulletin*, **1960**, 9, 335.

[31] (a) Kaminsky W. and Steiger R., *Polyhedron*, **1988**, 7, 2375; (b) Corradini P. and Guerra G., *Prog. Poly. Sci.,* **1991**, 16, 239.

[32] Dos Santos J. H. Z., Grecco P.P., Stedile F.C. and Chornik B., *J Mateials Online*, **2006**, 2, 1.

[33] Kaminsky W. (a) *J Molecular Cat.*, **1992**, 74, 109; (b) *Macromol. Symp.,* **1995**, 97, 79; (c) *Macromol. Chem. Phys.*, **1996**, 197, 3907.

[34] Chein J. C. W. and Wang B-P., *J. Polym. Sci. Part A*, **1990**, 28, 15.

[35] (a) Rieger B. and Janiak C., *Angew. Makromol. Chem.,* **1994**, 215, 35; (b) Estrada J. M. V. and Hamielec A. E., *Polymer*, **1994**, 35, 808; (c) D'Agnillo L., Soares J. B.P., Penlidis A., *Macromol. Chem. Phys.,* **1998**, 199, 955.

# Chapter 3

# Molar mass and molecular weight distribution determination from melt rheometry

## 3.1 Introduction

From the chemical structure point of view there is no distinction between paraffin oil, high density polyethylene (HDPE) and ultra high molecular weight polyethylene (UHMWPE). However, physical and mechanical properties of the material vary significantly from paraffin oil to UHMWPE. Paraffin oil flows at room temperature, but HDPE can be processed via normal polymer processing machines, extrusion and injection molding, to produce a tough polymer. However, with further increase of the molar mass ($> 10^6$ g/mol) it becomes nearly impossible to process the material via conventional routes. A general figure for the dependency of polymer properties on molecular weight is shown on figure 3.1.

Differences in the molar mass and molecular weight distribution (MWD) play important roles in the processing characteristics of the polymer, which will ultimately influence the physical and mechanical properties of the material. For instance, in melt spinning a low molecular weight polymer with a broad MWD is needed, whereas to produce fiber by solution spinning a very high molecular weight polymer with narrow MWD is a requisite. Moreover, a fundamental understanding of chain dynamics also requires the molecular characteristics of the polymer. Therefore, it is important to determine these two physical parameters.

## 3.2 Basic Definitions

Contrary to organic molecules, there are different definitions for the molecular weight of polymers. This is because most of the polymeric materials are mixtures of various molecular sizes. This distribution of molecular weights is a result of the statistical nature of the polymerization process. Consequently, characterization of molecular size in a polymer requires the measurement of its molecular weight distribution.

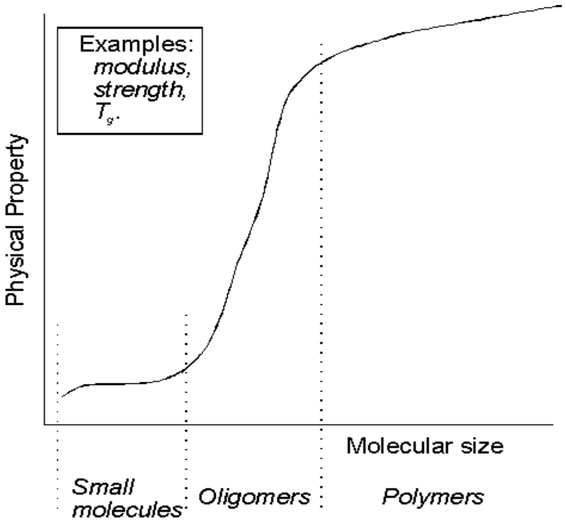

**Figure 3.1:** Polymer properties of polymers, such are modulus, strength, glass transition, increases with increasing molecular size.

One of the simplest ways to present a distribution is to plot the number of molecules of size Mi (a polymer chain with i repeat unit) against Mi, giving the number or frequency distribution. An alternative way of representing the distribution is to assign statistical weightage to the molecules according to their chain length and to plot Wi (the total weight of molecules of length i) against Mi. This yields the weight distribution of the polymer.

To have better insight in the physical characteristics of the polymers, it is often necessary to measure weight average (Mw), number average (Mn), viscosity average (Mv), highest molar mass component (Mz) of the polymer.

For a polydisperse polymer

Mw > Mv > Mn

where the differences between the various average molecular weights increases as the molecular-weight distribution broadens. A typical polymer sample will have the molecular weight distribution shown in Fig. 3-2. The approximate positions of the different average molecular weights are indicated on this distribution curve[1,2,3,4].

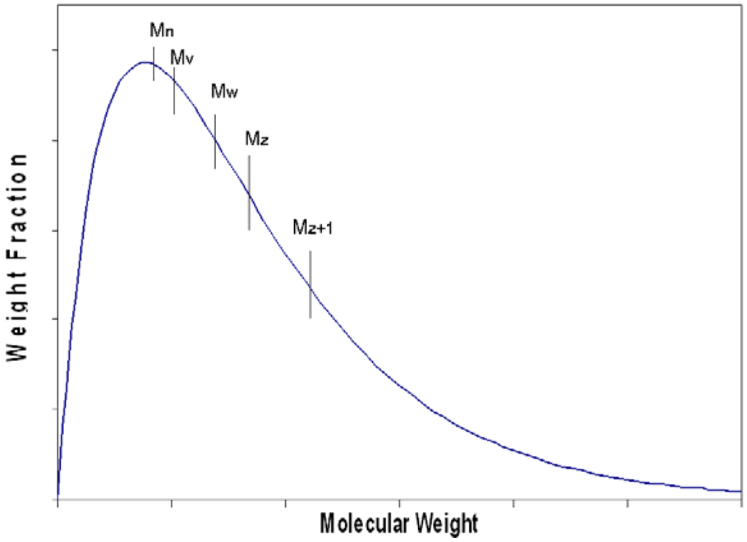

**Figure 3.2:** Schematic plot of a distribution of molecular weights along with the rankings of the various average molecular weights.

There are many methods and types of equipment to determine the molecular weights of polymers as mentioned. They include light scattering, osmometry, solution viscosity, size exclusion chromatography (SEC) also called gel permeation chromatography (GPC) and melt Rheometry. The pros and cons of some of these methods are briefly summarized in Table 3.1.

**Table 3.1:** Some basic advantages and disadvantages of different methods that are normally applied to determine molar mass of polymers.

| | **Gel Permeation Chromatography** | **Solution Viscometry** | **Melt Rheometry** |
|---|---|---|---|
| Advantage | More accurate data with coupling by MALDI* or MALLS** and can be used for branched polymers | Instrument is simple and cheap | Highly sensitive to the high molar mass tail,<br>Applicable for insoluble polymers |
| Disadvantage | Cannot be used for very high molar mass and insoluble polymers | Less accuracy,<br>PDI cannot be measured,<br>Needs soluble polymers | Inaccuracy in the case of branched polymers, needs initial estimation |

* Matrix-assisted laser desorption/ionization.

** Multi-angle laser light scattering

## 3.3 Experimental techniques

*Rheometry*

Oscillatory shear measurements and stress relaxation in the linear viscoelastic (LVE) regime have been performed using a Rheometrics RMS 800 strain controlled spectrometer over a broad range of temperature (140°C-220°C), angular frequencies (0.001 to 100 rad/s) and strains (0.5 to 2%). By performing strain sweeps on the disentangled and fully entangled samples, the LVE region was obtained. Due to high sample stiffness, parallel plate geometry was used with a disk diameter of 8 mm and a sample thickness of 1 mm. The time-temperature superposition was applied at a reference temperature of 190°C. For the high molar mass materials, stress relaxation experiments were performed to expand the time window of the measurements. All experiments in this chapter were performed on the fully entangled sample. Prior to measurements, the disentangled nascent powders were first sintered at 50°C and 200 bars and the resulting disks of 8 mm diameter were heated fast (~ 30ºC/min) to well above the equilibrium melting temperature in the rheometer. Time sweep experiment, at fixed frequency and strain, was performed on the initially disentangled samples until no change in elastic modulus was observerd. No change in the elastic modulus was indicative of the fully entangled state. Stress relaxation and frequency sweep experiments were performed on the fully entangled polymers by applying strain amplitude in the linear viscoelastic regime.

The slippage between the sample and rheometer discs was checked with the help of an oscilloscope. During dynamic experiments two output signals from the rheometer i.e. one signal corresponding to sinusoidal strain, and the other signal to the resulting stress response, were monitored continuously by an oscilloscope. A perfect sinusoidal stress response, which can be achieved at low values of strain was an indicative of no slippage between the sample and discs.

For all samples 0.5 wt% Irganox 1010 was added and measurements were performed under a nitrogen atmosphere in order to prevent thermo-oxidative degradation. To make sure that no degradation has occurred during experimentation frequency sweep experiments performed at beginning and end of the experiments were compared. No change in the elastic modulus, viscous modulus and phase angle of the fully entangled polymer overruled the possibility of thermal or chemical degradation. In past Infrared spectroscopy followed by dissolution of the polymer after experimentation were also performed[5,6]. The findings suggest no change in molecular characteristics arising due to degradation.

*GPC*

The measurements were carried out in group of Prof. Münstedt at the Institute of Polymer Materials, Erlangen University. A high temperature GPC (150ºC, Waters Inc.) coupled with a high temperature multi-angle light scattering apparatus (MALLS, Dawn EOS, Wyatt Technologies) was used for the measurements. The measuring temperature was 140ºC and 1,2,4 trichlorobenzene was used as a solvent. The flow rate was chosen to be 0.5 ml/min and 325:l of the polymer solution was injected onto the column system consisting of three columns: Shodex UT806M (Showa Denko, exclusion limit in polystyrene molar mass $5\times10^7$ g/mol) and one high molar mass separation column Shodex UT807 (exclusion limit $2\times10^8$ g/mol). The concentration of the polymer eluted from the columns was measured by means of two concentration detectors using different detection techniques (infra red absorption, polyCHAR IR4, and, an internal differential refractive index detector.

The evaluation of the measurements was performed using ASTRA 4.73 analysis software (Wyatt Technologies). The concentration signal from the IR-detector was used in the evaluation of the data because of its higher sensitivity. The determination of the absolute molar mass and of the radius of gyration, $<r_g^2>^{0.5}$, for each eluted fraction was done in a linear Zimm-plot[7]. In parallel, the same concentration signal was evaluated via the calibration curve connecting elution volume with the molar mass of polymer standards using the WinGPC 6.20 software (Polymer Standard Services). The GPC was calibrated with polystyrenes of narrow molar mass distribution characterized by Mw/Mn values below 1.1. The calibration curve spans a molar mass range from 580 g/mol to 11,300,000 g/mol. For the measurements of polyethylene samples, the polystyrene calibration was converted into a polyethylene calibration using the universal calibration technique. The following Mark-Houwink parameters of K=0.0196 and a=0.73 (units for K chosen in such a way that M is g/mol for the Staudinger index in $cm^3/g$) were used to correct for the different hydrodynamic volumes of polystyrene and polypropylene in solution. All chromatograms were corrected with respect to the elution volume of the internal standard[*].

## 3.4 Methods of determining MWD from melt rheology

Many attempts have been devoted to the estimation of rheological properties of polymer melts utilizing molecular weight and MWD data for a given polymer. However, molecular weight characterization from the rheological data, an inverse problem, has been given less attention.

There are two typical models to determine MWD from the polymer melt rheology: the “Viscosity Model” and “Modulus Model”. The viscosity model is based on the work of Bersted[8] and Bersted and Slee[9] in which the molecular weight is related to the observed behavior in the shear rate dependent viscosity. This model has been developed by Colby, Fetters and Graessley[10], Malkin and Teishev[11], Tuminello[12] and Nichetti and Manas-Zloczower[13].

Zero shear viscosity is related to weight average molecular weight according to Equation (3.1):

$$\eta_0 = K_1(\overline{M}_w)^{3.4} \tag{3.1}$$

---

[*] From the private report kindly provided by Dr. J. Kaschta, Group of Prof. H. Münstedt in the Institute of Polymer Materials at the Erlangen University.

In this chapter the “modulus model” will be emphasized. According to literature this model reflects viscoelastic properties of a polymer which correspond to the high molecular weight component. This model can be presented in terms of relaxation modulus, G (t). This method works by converting the relaxation spectrum from the time domain to the molecular weight domain, then using a regularized integral inversion to recover the MWD curve, Eq (3.2):

$$\frac{G(t)}{G_N^{\circ}} = \left( \int_{\ln(M_e)}^{\infty} F^{1/\beta}(t,M) w(M) d(\ln M) \right)^{\beta} \qquad (3.2)$$

In Equation (3.2), G(t) is normalized by the plateau modulus, $G_N^{\circ}$, F(t,M) is a kernel function describing the relaxation behavior of a monodisperse component of molecular weight M, where time is related to M by equation (3.3).

$$t = k_4 (M)^{3.4} \qquad (3.3)$$

*w*(M) is the weight fraction of the MWD function. The exponent, β, is a parameter which corresponds to the mixing behavior of the chains. For example, β is 1 for simple reptation and 2 for the double reptation theory. $M_e$ is the average molecular weight between entanglements.

For equation 3.2, the following kernel functions have been proposed in literature.
**a.** One of the simplest models is the Step-Function[14]. This model, presented in equation 3.4 (a) and (b), assumes that the relaxation of the monodisperse component with molecular weight M is an instantaneous process. However, this simplification results in a theoretical data that does not match with the experimental measurements, as shown in Figure 3.3.

$$F_1(t,M) = 1 \quad \text{if} \quad t < \tau_0(M) \qquad (3.4a)$$

$$F_1(t,M) = 0 \quad \text{if} \quad t \geq \tau_0(M) \qquad (3.4b)$$

**b.** The exponential relaxation behavior of polymer chains is more realistic than the step function. In this category, the Single Exponential[15] is the simplest model, Eq (3.5).

$$F_2(t,M) = \exp[-t / \tau_0(M)] \qquad (3.5)$$

**c.** The Doi kernel is based on a discrete summation of single exponential functions[16], Eq (3.6).

$$F_3(t,M) = \frac{8}{\pi^2} \sum_{n \in odd}^{\infty} \frac{\exp[-tn^2 / \tau_0(M)]}{n^2} \qquad (3.6)$$

**d.** There are two more models describing relaxation functions of polymers, the BSW[17] and the des Cloizeaux[18] kernel models. These models, by introducing more mathematical terms, are providing more flexibility in studying relaxation behavior, but also make it more complicated.

Figure 3.3 illustrates the kernel functions according to models described as $F_1$, $F_2$ and $F_3$. As stated in literature[19], the BSW and des Cloizeaux kernel functions also show comparable trends with $F_3$. These functions are not shown in the figure as they are not used in this thesis.

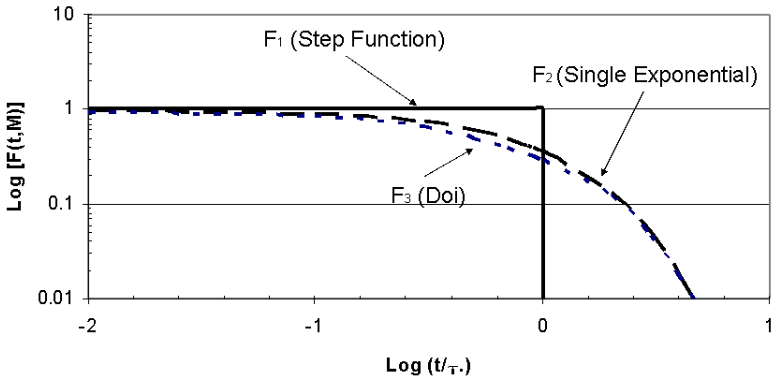

**Figure 3.3:** Kernel functions $F_1$, $F_2$ and $F_3$ against time

Next to the kernel function, the exponent, β in the Eq (3.2), is a parameter that has a significant effect on the molar mass determination based on "modulus model". Indeed, β indicates the nature of the polymer dynamics. Wu[20] made the molecular weight distribution calculations based on the classical (simple or single) reptation model, proposed by de Gennes[21], that suggests β equals 1.

Besides the pure reptation, another relaxation mode has been proposed by Doi and Edwards [16] named "constraint release" or the "double reptation" by Rubinstein and Colby[22], des Cloizeaux[23] and Tsenoglou[24]. The double reptation theory imposes the exponent β to a value of 2. A higher β value, slightly higher than 2, has been also proposed in the literature[25, 26, 27, 28] representing the contribution of higher-order entanglements or due to the tube dilation.

One the most successful algorithms in predicting molar mass distribution of nearly monodisperse, broad and bimodal polymer melts was developed by Mead[29]. His calculations are based on the double reptation model, $\beta=2$, and the single exponential kernel function, Eq (3.5).

Mead's algorithm was commercialized by Rheometrics Scientific for incorporation in their Orchestrator software[30] and was used in this chapter.

Frequency sweep experiments on the molten sample provide the elastic (G′) and loss (G″) moduli as a function of frequency, which is the base input for the software to evaluate molar mass. As stated by Carrot and Guillet[31], the accuracy of the weight average molecular weight prediction is mainly determined by the low frequency limit of the measurements, which in this case is $10^{-3}$ (rad/s). Since in this thesis high molar mass polymer is of interest, experiments are performed at low frequencies to determine the rheological data. For this purpose, a stress relaxation experiment was performed on the fully entangled sample followed by conversion of the data from the time scale domain to the frequency domain. In this respect, we were able to extend the low frequency data to two decades, up to $10^{-5}$ (rad/s).

## 3.5 Rheological measurements

a. *Frequency sweep*: Small amplitude sinusoidal oscillatory measurements with varying frequency are a rapid and often used method to measure the viscous and elastic properties of a polymer simultaneously. In this type of experiment a sinusoidal strain, $\gamma(t) = \gamma_0 \sin(\omega t)$, is applied on the sample and the stress response, which should be a sinusoidal shear stress, $\tau = \tau_0 \sin(\omega t + \delta)$, is recorded. Two parameters that are most often reported are the storage (elastic) modulus, (G′ (ω)), and the loss modulus, (G″(ω)). These parameters represent the relative degrees of the material to recover (elastic response) or flow (viscous response), respectively.

The double logarithmic plots of the loss and storage modulus versus frequency, see Figure 3.4, show a crossover between G′ and G″ at a specific frequency. This is obviously a well-defined point and conveniently this "cross-over" frequency and modulus has been shown to depend on the molecular weight and molecular weight distribution for linear polymers.

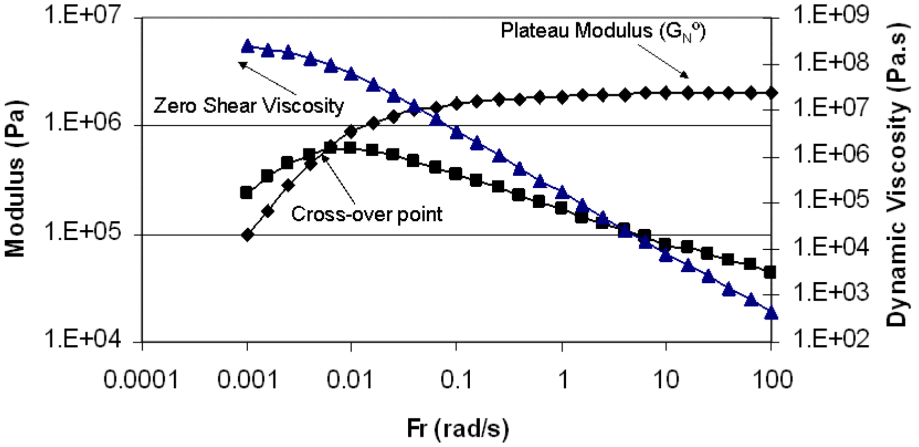

**Figure 3.4:** Double logarithmic plots of viscoelastic properties versus frequency for UHMWPE sample having molar mass of $2 \times 10^6$ g/mol at 160ºC, G′ ♦),G″ (■) and η′ (▲).

Another way to view the same experiment is in terms of a sinusoidal strain rate, $d\gamma/dt$. Then a dynamic viscosity material function is defined[32]. The viscous and elastic parts of the complex viscosity are defined in Equations (3.7) and (3.8), respectively.

$$\eta' = \frac{G''}{\omega} \tag{3.7}$$

$$\eta'' = \frac{G'}{\omega} \tag{3.8}$$

One of the most typical effects in polymer viscoelasticity is the non-Newtonian character of the viscosity function. The dynamic viscosity decreases as the frequency increases. At very low frequency, $\eta'$ tends toward an invariant value. So, below some critical frequency, $\eta'$ does not depend on the frequency and the material exhibits a Newtonian behavior. The Newtonian viscosity of a polymer melt, $\eta_0$, named the zero shear viscosity, is defined by Equation (3.9).

$$\lim_{\omega \to 0} \eta'(\omega) = \eta_0 \tag{3.9}$$

It is well known that the zero shear viscosity scales with polymer molecular weight (Mw) to a power of 3.4, if Mw>Mc where Mc is the critical molecular weight, which is related to the onset of molecular entanglements.[33] Thus, in case of a very high molecular weight polymer, such as UHMWPE, the plateau to determine $\eta_0$ occurs at a very low frequency which is beyond the instrument range. As shown in Figure 3.4, the cross-over of elastic and viscous moduli occurs at significantly higher frequencies than the point at which a constant value of shear viscosity occurs. Therefore, the cross over point gains an advantage over zero shear viscosity in polymer molar mass characterization by means of melt rheology.

Figure 3.5 shows series of frequency sweep experiments performed on samples with different molar masses. Samples having lower molar masses, batch No. 1 and 2, show a cross-over point in the range of accessible frequency of instrument, below $10^{-3}$ (rad/s), but for higher molar mass, batch No. 3 and 4, this point is shifted to lower frequency and does not occur in the measurable frequency range. Furthermore, Figure 3.6 shows that elastic modulus of samples batch No. 3 and 4 does not fall-off and the dynamic viscosity does not level-off, which is a good indication of having very high molar mass.

These results show us that different molar mass polymers have been synthesized following the route explained in chapter 2.

In order to obtain the rheological data at a lower frequency range, it is essential to perform stress relaxation experiments.

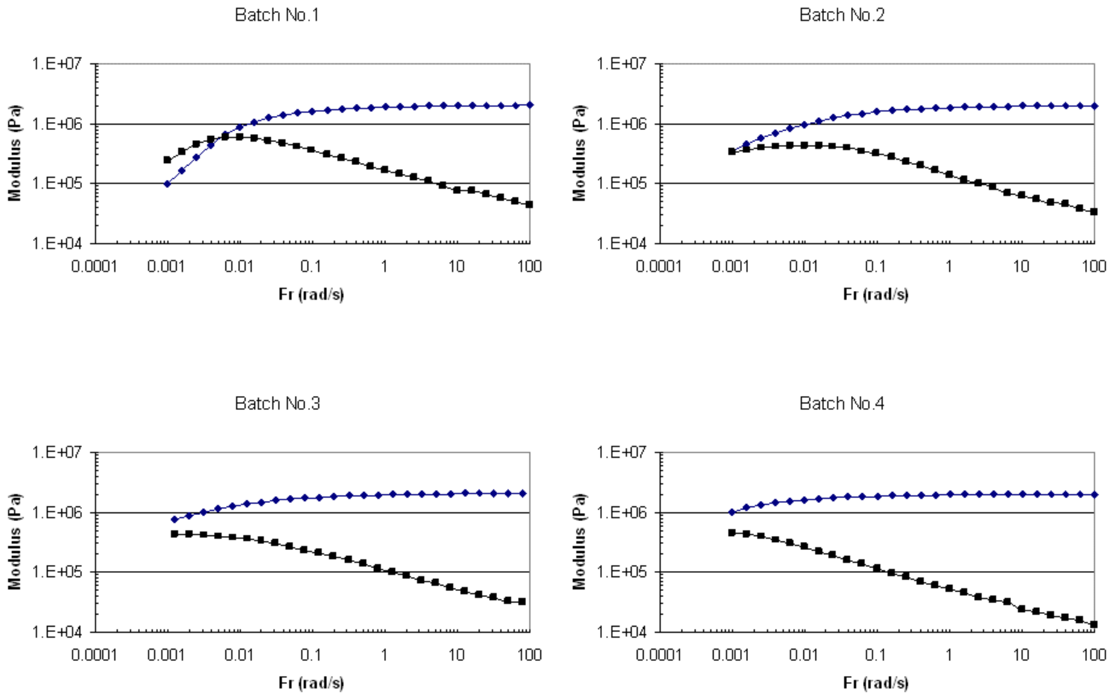

**Figure 3.5:** Series of frequency sweep experiments on different molar mass UHMWPE. (♦)G′ and (■)G″. The Cross over point shifts to lower frequency from batch No.1 to batch No.2. In the case of batches No. 3 and 4, although the cross over point is not observed in the measurable frequency region, but the onset of terminal region shifts to lower frequency. Therefore, from the shown dynamic data the expected increase in molar mass for different samples can be estimated, i.e. the average molar mass of batch No.1< batch No.2< batch No.3< batch No.4.

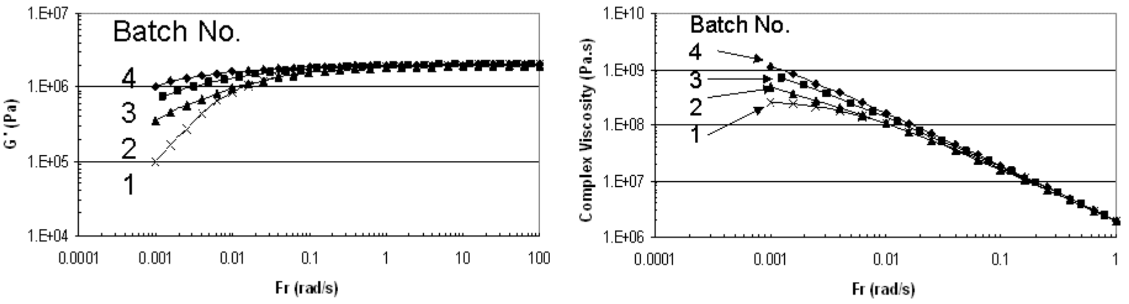
(a) (b)

**Figure 3.6:** Comparison of (a) the elastic modulus and (b) the complex viscosity for different molar masses UHMWPE. From batches No.1 to No.4, in figure (a) the onset of terminal zone shifts to lower frequency and, in figure (b) with increasing batch number complex viscosity shows higher value at lower frequency. Therefore, from the shown dynamic data the expected increase in molar mass for different samples can be estimated, i.e. the average molar mass of batch No.1< batch No.2< batch No.3< batch No.4.

b. *Stress Relaxation*: In this experiment, a single transient deformation (step strain) is applied and maintained on the sample and the time dependent decay of stress is recorded. The data are often displayed as the relaxation modulus versus time. Integration of the modulus versus time function is a rapid means of determining the zero shear viscosity and hence the average molecular weight, Equation (3.10).

$$\eta_0 = \int_0^{\infty} G(t)dt \qquad (3.10)$$

Figure 3.7 shows the relaxation modulus versus time for samples having different molar masses. The relaxation profile and the area under the relaxation modulus, $\eta_0$, for different samples are distinct. The figure reveals that batches No. 4 and 5, require a very long time to be relaxed under the applied strain, compared to batch No. 1 relaxes in considerably shorter time. It should be noted that the required time to reach the lowest level of relaxation modulus for HDPE is still lower than for batch No.1. The characteristic relaxation time for each sample can be obtained from the corresponding relaxation spectrum for each sample, although it is known that in case of higher molar mass data uncertainty in determination of the relaxation time exists.

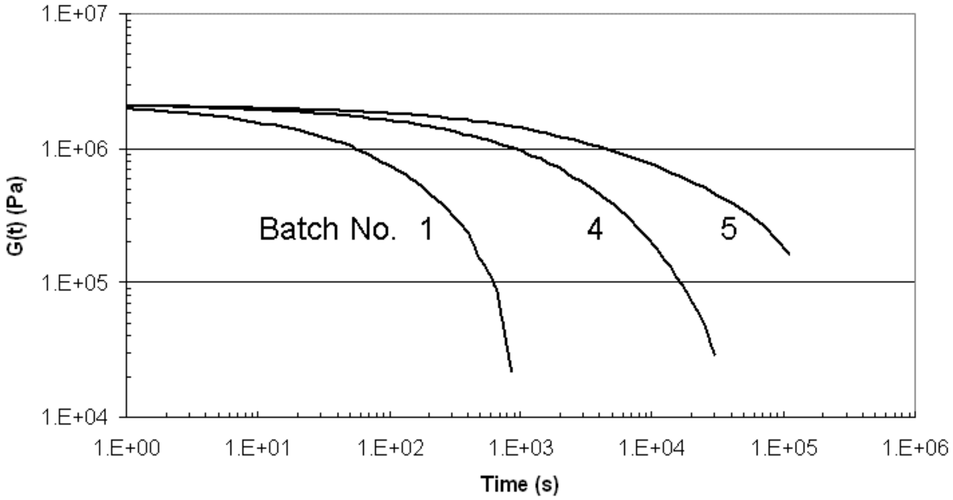

**Figure 3.7:** Relaxation profiles for three different batches. Data reported here is reproducible for different samples of the same batch. At least three fresh samples for each batch were investigated. Distinctive trend of the relaxation curves for batches No.1, No.4 and No. 5 clearly suggest differences in the molar mass of the three batches. From the data it is evident that the area under the relaxation curve increases with the increasing batch number. The full relaxation curve of the batch No.5 could not be obtained due to the desired long relaxation times. Time required for obtaining the complete relaxation curve for the batch 5 becomes beyond the experimental limitations of the provided rheometer time.

As stated earlier in this chapter, static data such as creep and stress relaxation can be converted to dynamic properties such as the dynamic modulus or dynamic viscosity and vice versa. Detailed studies on such conversion are provided in the literature[34,35,36] especially by Ferry[33]. Figure 3.8 illustrates the dynamic data over a very large range of frequency. The data in the range of 100 to $10^{-3}$ (rad/s) was collected directly from the frequency sweep experiment and the data in the range of 1 to $8*10^{-5}$ (rad/s) was obtained by converting static data to dynamic data. The two sets of data when plotted together show a good overlap. Following this method, it is possible to obtain dynamic data over almost 7 decades. Although these data are sufficient to calculate the molar masses of synthesized samples, in the next part another approach, time-molar mass superposition, explaining how to extend dynamic data to even lower frequency such is $10^{-7}$ (rad/s) will be addressed .

## 3.6 Molar mass data obtained from melt rheometry and GPC

To recall, the molar mass determination is based on Eq (3.2) which assumes a single exponential as the kernel function and double reptation as the framework of chain dynamics. The molar mass data obtained from the melt rheometry and GPC are summarized in Table 3.2. The GPC data was kindly provided by Dr. J. Kaschta, Group of Prof. H. Münstedt, Erlangen University. The data that are provided include weight and number average molecular weights, Mw was obtained by two different techniques – light scattering and the conventional calibration method. These data and the reproducibility of the GPC runs are given in the Appendix 1.

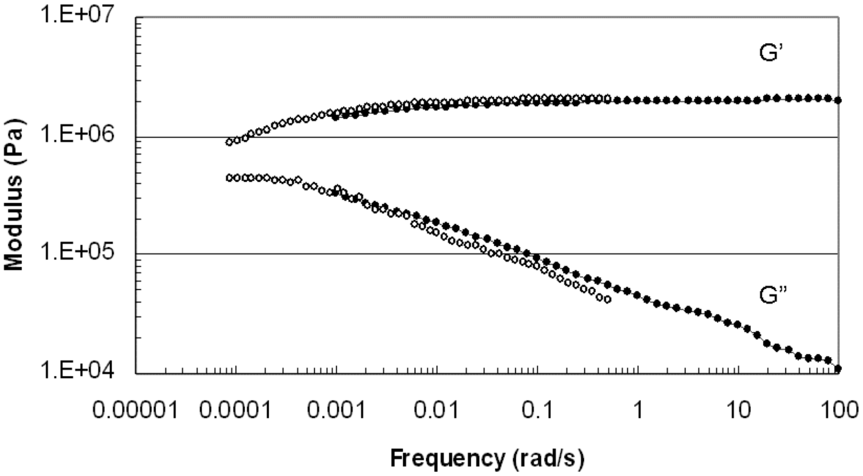

**Figure 3.8:** Dynamic data obtained from frequency sweep, (direct data), (closed circles) and stress relaxation experiments, (converted data), (open circles) for sample batch No. 5. Both experiments were performed at 160°C.

**Table 3.2:** Comparison of molecular weight obtained from GPC and melt rheometry

| Sample Batch No. | GPC | | Melt Rheometry | |
|---|---|---|---|---|
| | Mw* (g/mol) | PDI | Mw (g/mol) | PDI |
| 1 | $2.3\text{x}10^6$ | 1.9 | $2.0\ \text{x}10^6$ | 1.4 |
| 2 | - | - | $2.8\text{x}10^6$ | 2.6 |
| 3 | - | - | $3.8\text{x}10^6$ | 2.3 |
| 4 | $4.3\text{x}10^6$ | 2.3 | $5.3\ \text{x}10^6$ | 1.9 |
| 5 | $5.7\text{x}10^6$ | 2.1 | $9.1\text{x}10^6$ | 2.3 |
| 6 | $2.4\text{x}10^6$ | 1.3 | $1.9\text{x}10^6$ | 1.3 |
| 7 | - | - | $1.1\text{x}10^7$ | 6.5 |

*From universal calibration.

In case of three batches, No 1, 4 and 6, acceptable agreement exists between the rheological and GPC results. From figure 3.7 it is clear that the relaxation modulus for batch No.5, falls one decade within $10^5$ second. Thus, an extremely high molar mass is expected for this sample. From melt rheometry, the calculated molar mass for this sample is around $9\text{x}10^6$ g/mol, whereas the GPC estimates it of about $6\text{x}10^6$ g/mol. The discrepancy between results obtained from GPC and rheology might be explained by the mass recovery from the GPC columns, r, of the injected polymer. The mass recovery is the ratio of detected mass obtained by the integration of the concentration signal and injected mass, ($r = \frac{m_{\text{detected}}}{m_{\text{injected}}} \times 100\%$).

Comparing the detected mass, $m_{\text{detected}}$, with the injected mass, $m_{\text{injected}}$, it can be concluded how large is the amount of gel/insoluble material or if material is being absorbed on the columns. Table 3.3 summarizes the percentage of mass recovery for the measurements of the different polymers. The obtained molar mass from both GPC and rheology methods for samples having molar mass around $2\text{x}10^6$ g/mol is in very good agreement. The r value for those samples, batch No.1 and 6, are around 95%, indicating all material is eluted from the columns and that no gel is present. The difference between the measured molar mass from two methods for batch No. 4, having a molar mass of $5.3\text{x}10^6$ g/mol (from rheology) is about 20% and the r value is about 90%. The r value for the sample with highest molar mass, $9.1\text{x}10^6$ g/mol, is less than 90% and this might be an explanation for the observed discrepancy between data obtained from GPC and rheometry.

**Table 3.3:** The percentage of mass recovery, r, for different molar masses (obtained from rheology) for two different experiments: Inject1 and Inject2. These experiments were performed in the group of Prof Münstedt at Erlangen University.

| Sample Batch No. (Mw from melt rheometry) | Inject 1( %) | Inject 2 (%) |
|---|---|---|
| 1 ($2x10^6$ g/mol)) | 95.7 | 92.7 |
| 4 ($5.3 x10^6$ g/mol) | 89.2 | 92.4 |
| 5 ($9.1x10^6$ g/mol) | 85.0 | 86.7 |
| 6 ($1.9x10^6$ g/mol) | 96.8 | 91.4 |

Figure 3.9 shows GPC chromatograms and molecular weight distributions obtained from rheometry for batch No. 1, 4, 5 and 6. The radius of gyration is also plotted in the chromatogram. Fig 3.9 (a), (c), (e) and (g) show chromatograms with radius of gyration for the corresponding samples. Within the region where molar mass and molar mass distribution has been determined the light scattering data shows linear variation in the radius of gyration with molar mass. However, at lower molar mass region deviation in the linear relationship of the radius of gyration against molar mass is observed. This deviation in the molar mass represents existence of molar mass component that possess higher radius of gyration than the expected value.

Detailed studies on deviation of the radius of gyration with increasing molar mass have been performed for the branched polymers[37,38]. The authors have conclusively demonstrated that with increasing branch content radius of gyration falls below the anticipated value for the linear polymer. Contrary to the decrease in the radius of gyration the polymer synthesized in our laboratory shows increase in the radius of gyration at the lower molar mass region. At this stage there is no proper explanation for the deviation, however from physical viewpoint this may be related to the difference in chain swelling process of the disentangled state of the synthesized polymer that may cause increase in the radius of gyration. This calls for further experimental studies that will be pursued in the near future. Further experimental details are provided in the appendix 1.

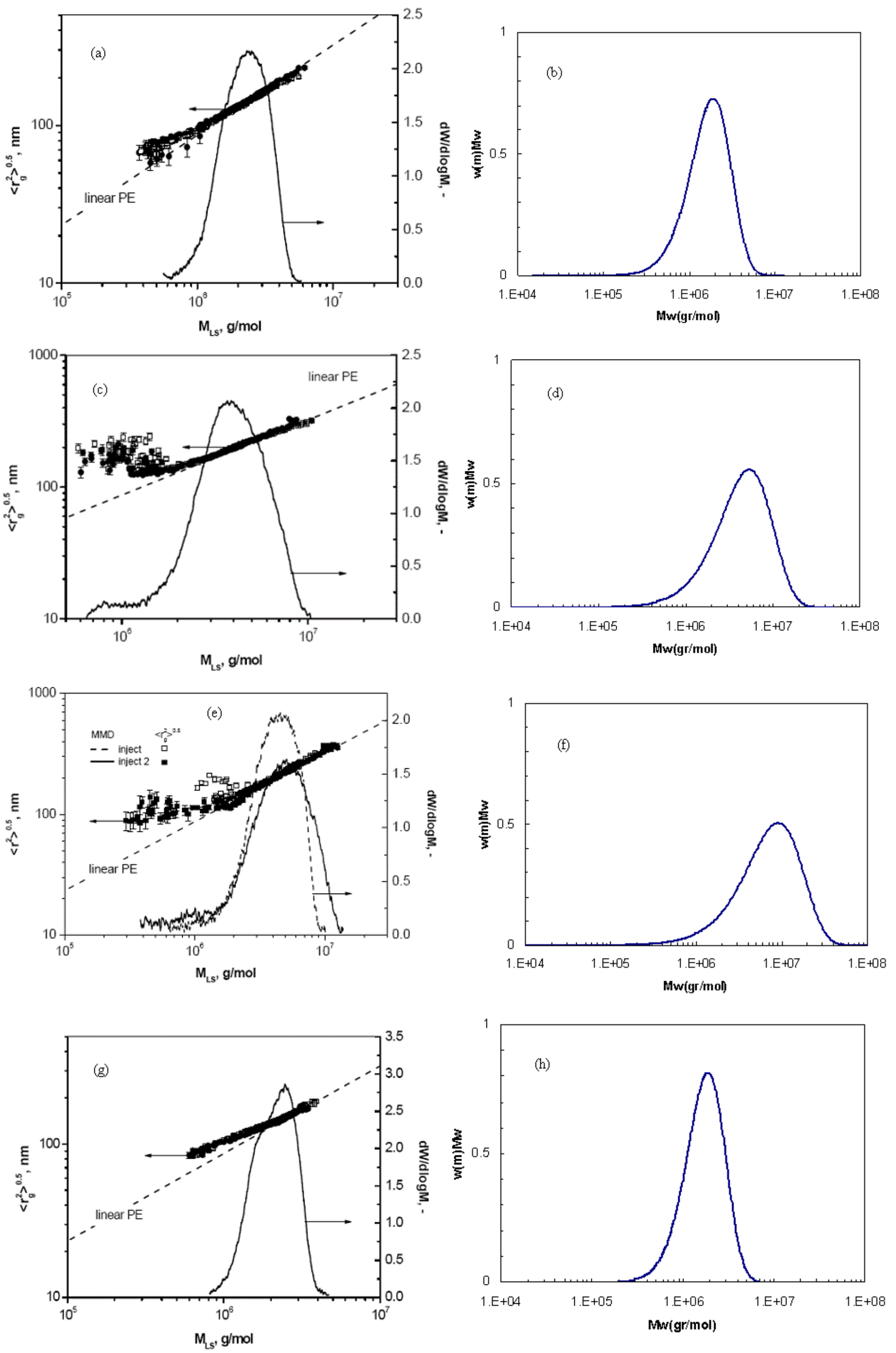

**Figure 3.9:** Comparing (a), (c), (e) and (g) chromatograms for batches No. 1,4,5 and 6 resepectively. Figures (b), (d), (f) and (g) represent w(m)xMw calculated using algorithm of Mead[29] for the respective batches.

## 3.7 Creating a master curve from time-molecular weight superposition

To check the molar mass determined from the melt rheometry an alternative approach to the dynamic behavior of UHMWPE was applied. The alternative approach combines dynamic data obtained for different molar masses. A master curve is created by shifting dynamic data to the curve for the highest molecular weight. The dynamic data for the low molar mass polyethylenes was retrieved from the experiments performed earlier in our group$^5$. Figure 3.10 shows the elastic and loss moduli of linear polyethylenes having molar mass lower than $10^5$ g/mol. From Fig 3.10, it is clear that G′ and G″ show a similar trend for different molar masses of polyethylenes, except that they are shifted to lower frequency with the increasing molar mass. This shows that the dynamic behavior of polymer chains with different molar mass is governed by similar underlying physics. Similar to the time-temperature superposition where one converts the temperature domain to the time domain, the molecular weight was converted to the time domain. It can be assumed that the polymer chains follow the Maxwell model where the relaxation time is $\tau_0 = \frac{\eta}{E}$.

E (the modulus of the spring) is independent of the molar mass because the average molar mass (Mw) is well above the critical molar mass for entanglements formation (Mc). However, η (the viscosity of the dashpot) will vary with the molar mass. Thus, a shift factor can be found empirically for polymers having different molar masses, but similar polydispersities. Thus, dynamic characteristics, such as the cross over point and the zero shear viscosity of high molar mass polymers can be predicted using a shift factor.

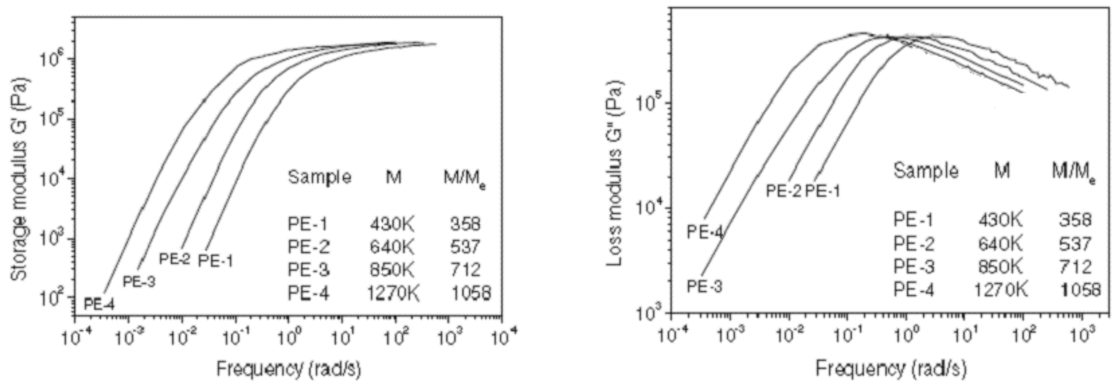
(a) (b)

**Figure 3.10:** (a) Storage modulus, G′, and (b) loss modulus, G″, data for the narrow molecular weight polyethylenes (PDI~1.2), adopted from Ref 5.

It is assumed that the synthesized UHMWPE samples possess similar polydispersities as low mass polyethylenes described in Figure 3.10. Considering GPC data and frequency sweep results, Figure 3.5, and taking similar synthesis conditions (controlled polymerization) into consideration, this assumption seems to be reasonable. Thus, it is expected that the chain dynamics in UHMWPE having a low polydispersity (where number average molar mass is in the vicinity of a $10^6$ g/mol) should be similar to the linear monodisperse polyethylene shown in Fig 3.10, except that the terminal region will be shifted to much lower frequencies. The result of time-MW superposition for highest molar mass sample, batch No. 5 having molar mass of $9.1 \times 10^6$ g/mol, is illustrated in Figure 3.11(a). The terminal region representing the overall chain dynamics is extended to very low frequency, $10^{-7}$ rad/s.

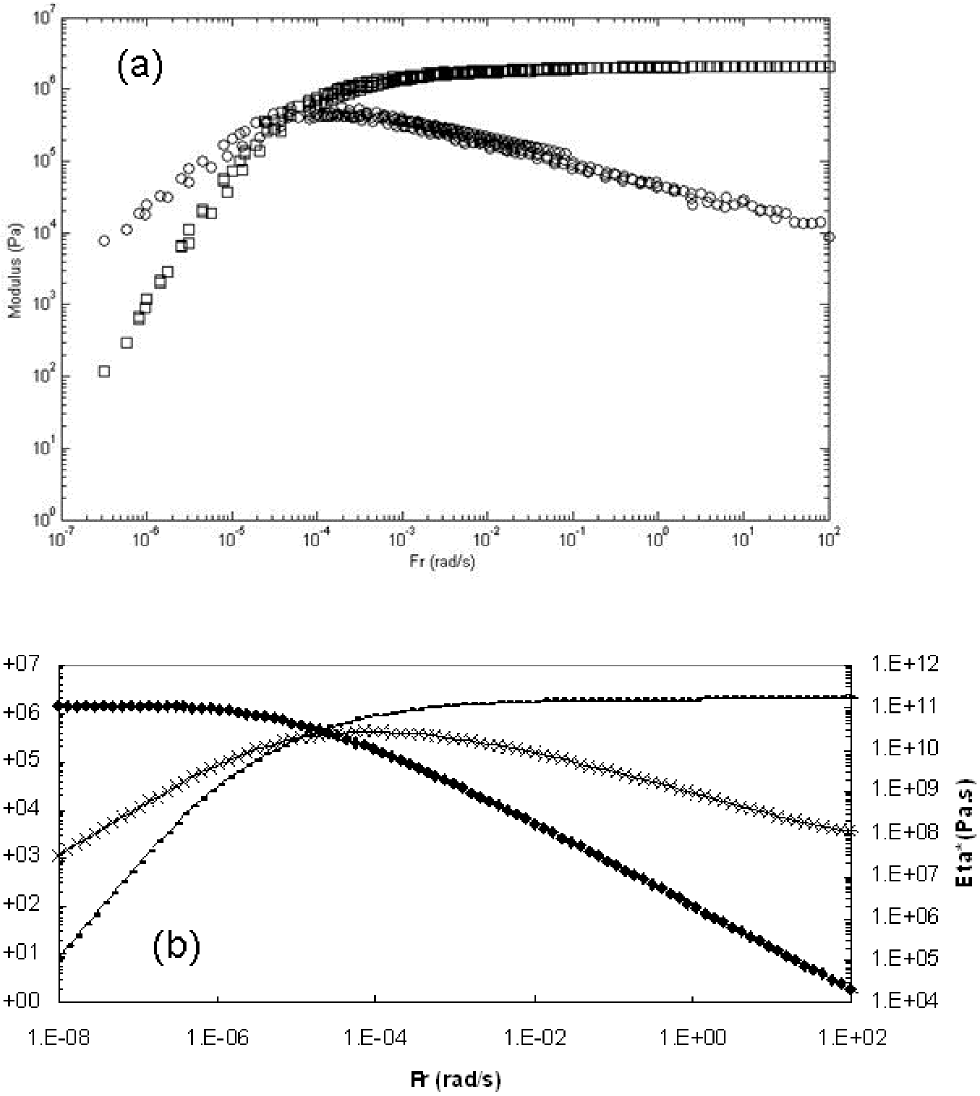

**Figure 3.11:** Master curves for the reference sample, batch No. 5, having molar mass of $9.1 \times 10^6$ g/mol. Figure (a) depicts G′ (open squares) and G″(open circles), respectively. The storage and loss modulus over the wide frequency region were obtained by shifting the modulus data horizontally for a range of polymers. Figure (b) shows theoretically determined dynamic data from molar mass data. G′, G″ and Eta* are shown by dash, cross and closed squares, respectively. Cross over point matches well from both methods that it occurs at frequency around $1 \times 10^{-5}$ to $2 \times 10^{-5}$ (rad/s).

Figure 3.11(b) shows extended dynamic data obtained theoretically from the model (equation 3.2) which determines the molecular weight of the as synthesized polymer. From Figures 3.11, it is apparent that the theoretical data (Figure 3.11b) matches well with the experimental results described in Figure 3.11a. Interestingly, the value of the cross over point and zero shear viscosity obtained experimentally ($2.1\text{x}10^{-5}$ rad/s, $9.5\text{x}10^{10}$ Pa.s) and theoretically ($1.1\text{x}10^{-5}$ rad/s, $1.3\text{x}10^{11}$ Pa.s) are quite similar.

Figure 3.12 illustrates the double logarithmic plot of zero shear viscosity versus molar mass. The figure shows a linear dependency between zero shear viscosity and molar mass with the slope of approximately 3.6, on a log scale. This finding is close to the 3.4-power law experimental scaling of polymer melt viscosity with molecular weight[33]. However it disagrees with the reported studies on the high molar mass polymers. The discrepancy might be explained by possessing of higher polydispersity for the investigated samples in this chapter in comparison with the polymers were utilized in the literature.[39]

The horizontal shift value required to plot the master curve in Figure 3.11a is shown in Figure 3.13. The horizontal shift value shows a slope of 3.5. Results reported in Figures 3.12 and 3.13 justify the entanglement nature of the samples used for the study in this chapter.

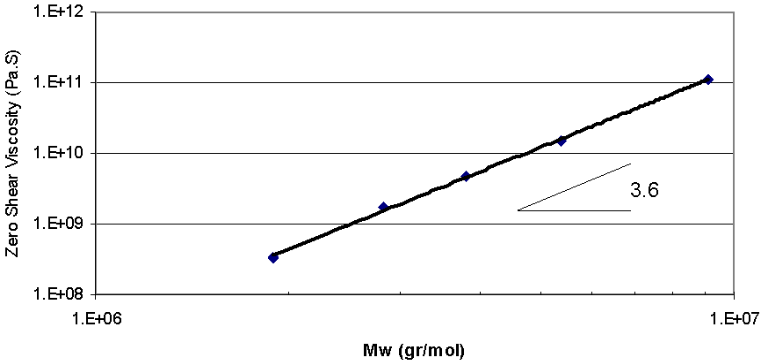

**Figure 3.12:** Zero shear viscosity versus molar mass. Here the viscosity is determined from Figures similar to the Figure 3.11b for different samples.

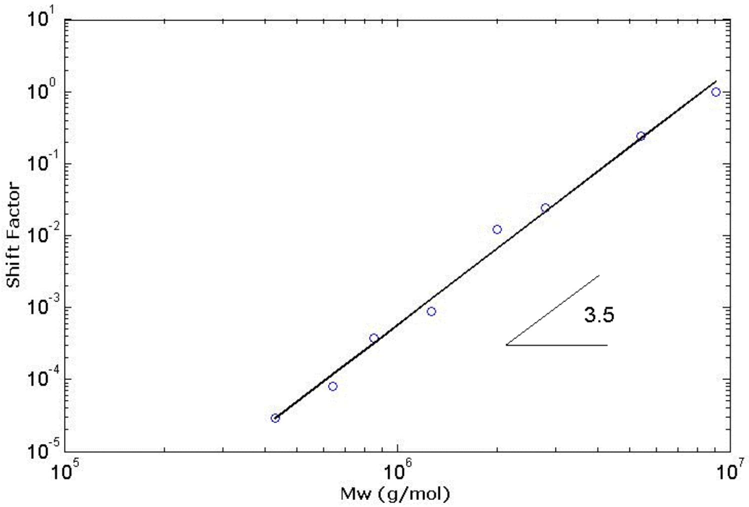

**Figure 3.13:** Horizontal shift factor versus molar mass. Here the horizontal shift applied to draw the master curve depicted in figure 3.11a is shown. The shift was applied to draw the curve for the highest molar mass investigated in this chapter, i.e. Batch No 5 (having molar mass of 9.1x$10^6$ g/mol).

## 3.8 Conclusions

In this chapter, the basic definition of molecular weight and different methods to measure molar mass of polymers is reviewed. Our preferred method is melt rheometry which can be based on a viscosity model or a modulus model. The modulus model was emphasized in this chapter. Two important parameters in this model are the kernel function describing the relaxation behavior of a monodisperse component and β exponent indicating the nature of the polymer dynamics.

Considering the good match (within experimental limitations) between the experimental and theoretical data, it was concluded that the applied rheological techniques to determine the high molar mass works reasonably good for the chemistry applied in the synthesis of relatively low molar mass distribution. These findings are of relevance in determining very high molar masses that cannot be obtained conclusively with the existing chromatography techniques. An important factor to determine such high molar masses via melt rheological methods is the availability of the onset of the terminal region data in the modulus-frequency diagram. The onset of the terminal region data is obtained by converting the static data into the dynamic data. The static data are obtained from stress-relaxation measurements.

## 3.9 References

[1] Peebles L. H., *Molecular Weight Distributions in Polymers*, **1971**, Wiley-Interscience, New York.

[2] Eastmond G.C., *Comprehensive Polymer Science*, **1989**, Oxford.

[3] Odian G., *Priciple of Polymerization*, Fourth Edition, **2004**, Wiley-Interscience.

[4] *Encyclopedia of Polymer Science and Technology*, **2002**,John Wiley & Sons, Inc

[5] Lippits D.R., *Controlling the melting kinetics of polymers; a route to a new melt state,* **2007**, Ph.D. thesis, Eindhoven University of Technology.

[6] Corbeij-Kurelec L., *Chain mobility in polymer system; on the borderline between solid and melt,* **2001**, Ph.D. thesis, Eindhoven University of Technology.

[7] Zimm B. H., *J. Chem. Phys.*, **1948**, 16, 1099.

[8] Bersted B. H., *J. Appl. Polymer Sci*, **1975**,19, 2167.

[9] Bersted B. H. and Slee J. D., *J. Appl. Polymer Sci.*, **1977**,21, 2631.

[10] Colby R.H., Fetters L.J. and Graessley W.W., *Macromolecules*, **1987**, 20, 2226.

[11] Malkin A. Ya. and Teishev A.E., *Polymer Eng. Sci.*, **1991**, 31, 1590.

[12] Tuminello W.H., *Polymer Eng. Sci.* **1991**, 31, 1496.

[13] Nichetti D. and Manas-Zloczower I., *Journal of Rheology*, **1998**, 42, 951.

[14] Tuminello W.H., *Polymer Eng. Sci.,* **1986**, 26, 1339.

[15] Tsenoglou C., *Macromolecules*, **1991**, 24, 1762.

[16] Doi M. and EDWARDS S. F., *The Theory of Polymer Dynamics,* **1986,** Clarendon Oxford.

[17] Baumgaertel M., Schausberger A. and Winter H.H., *Rheol. Acta*, **1990**, 29, 400.

[18] des Cloizeaux J., *Macromolecules*, **1990**, 23, 4678.

[19] Tuminello W.H., *Society of Rheology meeting,* **1999**, Madison, Wisconsin, US.

[20] Wu S., *Polymer Eng. Sci*., **1985**, 25, 122.

[21] de Gennes P.G., *Scaling Concepts in Polymer Physics,* **1979**, Cornell University Press, Ithaca, NY

[22] Rubinstein M. and Colby R.H., *J. Chem. Phys.*, **1988**, 89, 5291.

[23] des Cloizeaux J., (a) *Europhys. Lett.*, **1998**, 5, 417; (b) *J. Phys. I France*, **1993**, 3, 61.

[24] Tsenoglou C., *Journal of Polymer Science: Part B: Polymer Physics*, **1988**, 26, 2329.

[25] Marrucci G., *J. Polym. Sci.*, **1985**,23, 159.

[26] Rubinstein M., Helfand E. and Pearson D.S., *Macromolecules*, **1987**, 20, 822.

[27] van Ruymbeke E., Keunings R., Stéphenne V., Hagenaars A. and Bailly C., *Macromolecules*, **2002**, 35, 2689.

[28] van Ruymbeke E., Keunings R. and Bailly C., *J. Non-Newtonian Fluid Mech.*, **2002**, 105, 153.

[29] Mead D. W., *Journal of Rheology*, (a) **1994**, 38, 1739 and (b) **1994**, 38, 1797.

[30] Rheometric Scientific Inc., Product Brirf.

[31] Carrot C. and Guillet J., *Journal of Rheology,* **1997**, 41, 1203.

[32] Macosko C. W., *Rheology Principles, Measurements, and Applications*, **1994**,Wiley-VCH, Inc.

[33] Ferry J. D., *Viscoelastic Properties of Polymers*, **1980**, Wiley, New York.

[34] Plazek D. J., Raghupathi N. and Orbon S. J., *Journal of Rheology,* **1979**, 23, 477.

[35] Schwarzl F. R., *Rheol. Acta*, **1975**, 14, 581.

[36] Kraft M., Meissner J. and Kaschta J., *Macromolecules*, **1999**, 32, 751.
[37] Stadler F.J., Piel C., Klimke K., Kaschta J., Parkinson M., Wilhelm M., Kaminsky W. and Münstedt H., *Macromolecules,* **2006**, 39, 1474.
[38] Stadler F.J., Piel C., Kaminsky W. and Münstedt H., *Macromolecular symposia* , **2006**, 236, 209.
[39] Milner S.T. and McLeish T.C.B., *Physical Review Letter*, **1998**, 81, 725.

# Chapter 4

# Rheological aspects of disentangled polymer melts

## 4.1 Introduction

An unperturbed single chain of polyethylene of molar mass 300,000 g/mol will have a density of approximately $8.8 \times 10^{-3}$ g/cm$^3$. However, the bulk density of the linear polyethylene is approximately 0.96 g/cm$^3$. The difference in density arises due to difference in the free volume, which is due to presence of the physical contact points between the neighboring chains. These contact points between the chains in a polymer melt are termed as physical entanglements and are considered to be the folklore of rheological concepts in polymer science. In a polymer melt, entanglements are homogeneously distributed along the chain, where the molar mass between entanglements is considered to be an intrinsic property of the polymer that depends on the molecular conformation of the chain. Thus, with increasing molar mass of the polymer, i.e. with increasing length of the chain, the number of entanglements per unit chain increases. Since these physical entanglements are the friction points in the chain dynamics of the polymer, melt viscosity shows a fundamental relationship with molar mass. See Eq 4.1.

$$\eta = kM^{3.4} \tag{4.1}$$

This fundamental relationship which holds good for polymer melts[1] shows an increase in zero shear viscosity by a factor of 1000 with an ten times increase in average molar mass by 10. This makes the processability of the high molar mass polymers nearly impossible via conventional routes. One of the methods to decrease the number of entanglements per unit chain is to make use of a solvent. The quest has been to retain the disentangled state even after removal of the solvent.

In an amorphous polymer, attempts[2] have been made to freeze the disentangled state by adopting quenching methods, such as the freeze-drying process. In this process, a polymer solution, where the polymer concentration is lower than the chain overlap concentration, is quenched rapidly from the solution state to the glassy state. The quenching is done fast to maintain the disentangled chain conformation. A fluffy disentangled polymer from the quenched solution is obtained on the removal of the solvent. This method has been successfully applied to obtain disentangled polystyrenes. Such disentangled polymer has been used to investigate the influence of entanglements on the glass transition temperature. Although rheological studies have been performed on the thus obtained disentangled materials, but because of the low molar mass of the polymer used fast interpenetration (entangling) of chains caused difficulty in following the entanglement formation process.[3]

Unlike amorphous polymers, in crystalline polymers fast quenching often leads to crystallization. Depending on the chain overlap concentration, entanglements residing in the amorphous phase can be manipulated. For an example, in the ultra high molar mass polyethylenes having an average molar mass greater than $10^6$ g/mol, the addition of only 1wt% of the polymer in a solvent provides a viscous solution, which on cooling forms a gel. The solvent removal leads to regular stacking of crystals where the entanglements reside in the amorphous domains. Solid state deformation of the thus obtained semi-crystalline polymer film, below the melting point and above the alpha relaxation temperature, shows a strong dependence on the entanglements present in the amorphous region[4], Figure 4.1. The figure shows easy drawability of the solution cast film compared to the melt crystallized sample. Strain hardening in the melt crystallized film indicates the presence of entanglements in the amorphous domains of the polymer. Detailed studies performed by Rastogi et al.[5] on such polymer films show regular stacking of crystals, where the crystals tend to thicken below the melting point leading to lamellar doubling, Fig 4.2. Such a thickening process facilitates the development of the physical contacts in the neighboring chains prior to melting. Thus, on melting, an "immediate" loss in the disentangled state occurs.

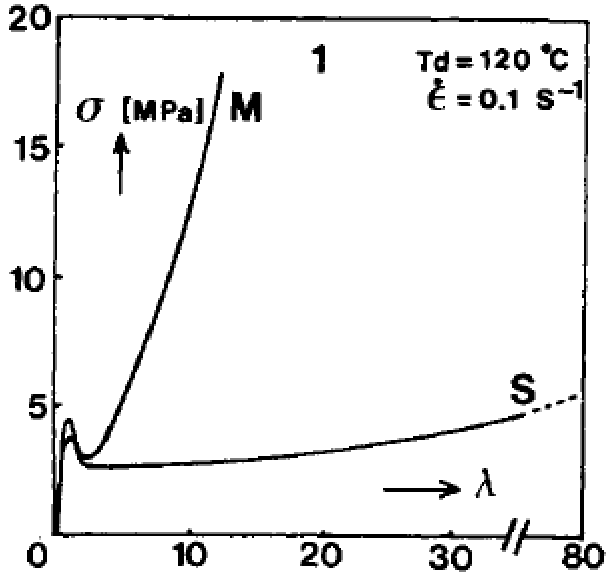

**Figure 4.1:** Stress-strain curve for melt-crystallized (M) and solution-cast (S) films at 120ºC. Adopted from Ref 4.

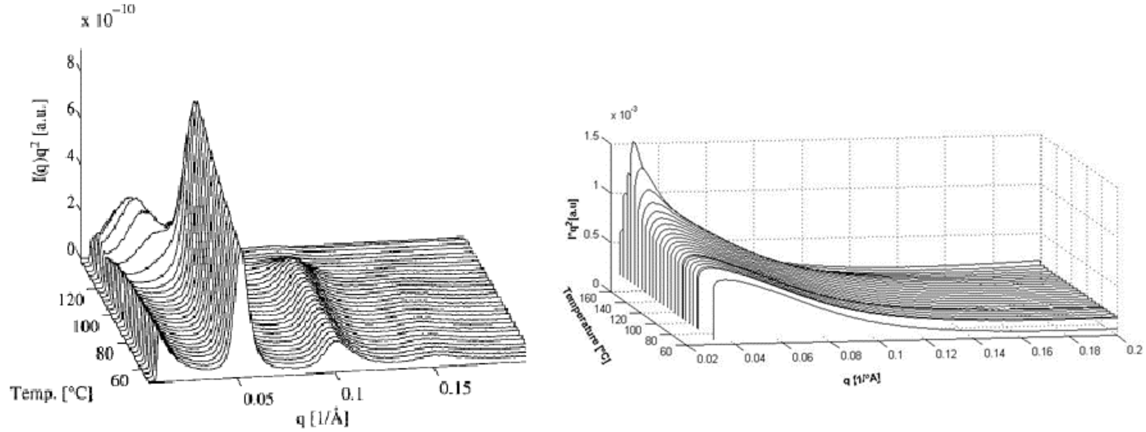

(a) (b)

**Figure 4.2:** (a) SAXS patterns at room temperature (first frame in the three dimensional picture) obtained from the solution cast film shows a well defined peak at Bragg spacing of 12.5nm. Higher orders in the SAXS pattern confirm the regular stacking of crystals having well defined crystal thickness. On heating, the sample thickens and a broad peak at 25nm is observed with diminishing of the peak intensity at 12.5nm and the associated higher orders. Adapted from Ref 5. (b) SAXS patterns obtained from the nascent disentangled UHMWPE shows no well defined peak. On heating, the intensity increases due to different thermal expansions of the crystalline and the amorphous regions in the semi-crystalline polymer. No significant shift in the broad intensity distribution, prior to melting is observed. A comparison with figure (a) confirms the considerably different morphology in the two disentangled samples. This can be attributed to differences in their origin.

In the previous chapter, an elegant route via controlled synthesis was demonstrated to achieve the "disentangled" nascent crystals, where the entanglements residing in the amorphous regions of the semi-crystalline polymer are to an extent similar to the solution cast films which can be deformed in the solid state. However, unlike solution cast films, these crystals do not show regular periodicity. The difference in the regular stacking of crystals in the solution cast films and the nascent crystals become apparent from the SAXS data summarized in the Figure 4.2. It is to be noted that unlike solution cast films no well defined peak having higher orders in the SAXS patterns arising due to regular stacking of the crystals is observed. On heating, the nascent crystals neither show lamellar doubling nor considerable thickening. This difference in thickening behavior that can be attributed to a difference in the morphology provides a possibility to explore entanglement formation in the initially disentangled melt state on melting of the disentangled polymer. For sake of simplicity the term disentangled polymer is used in this thesis, but in reality it might not be fully disentangled. From here onwards experimental studies are performed on the disentangled polymers directly obtained on synthesis. The synthesis route adopted is described in Chapter 2 of this thesis.

## 4.2 Experimental techniques

*Rheometry*

Oscillatory shear measurements in the linear viscoelastic (LVE) regime were carried out using a Rheometrics RMS 800 strain controlled spectrometer for a broad range of temperatures (140°C-220°C), angular frequencies (0.001 to 100 rad/s) and strains (0.1 to 100%). By performing strain sweep on the disentangled and fully entangled samples the LVE region is obtained. Due to high sample stiffness, parallel plate geometry was used with a disk diameter of 8 mm and a sample thickness of 1 mm. Disk samples were prepared by compressing the disentangled nascent powders at 50°C and 200 bar. The build-up (increase) of the elastic modulus with time was investigated via oscillatory shear measurement in order to follow the entanglement formation in the melt.

A constant strain was applied at a fixed angular frequency in the time sweep experiment. The chosen frequency for the time sweep experiment was in the plateau region of the fully entangled material. The change of the modulus is followed in time. Special care has been taken to avoid experimental artifacts such as non-linear effects. The slippage between the sample and rheometer disks was checked with the help of an oscilloscope. For all samples, 0.5 wt% Irganox 1010 was added and investigations were performed under a nitrogen atmosphere in order to prevent thermo-oxidative degradation.

## 4.3 Following entanglement formation in disentangled polymers

One of the characteristics of disentangled semi-crystalline polymers is the easy deformation in the solid state (see Figure 4.1). Unlike commercially available entangled polymers the nascent disentangled samples could be compressed easily below the melting temperature, providing a relatively tough transparent film that can be drawn in the solid state, Figure 4.3. Film samples synthesized in chapter 2 show easy solid state deformation.

The films thus obtained were used to investigate rheological aspects of the disentangled polymer melt. Samples were obtained from the films to follow changes in the elastic modulus during the entanglement formation. As described in the experimental section, samples of 8mm diameter cut from the film were placed between the plates of the rheometer. The smaller sample diameter compared to the conventionally used diameter of 25mm was chosen to avoid torque instabilities that can arise in the UHMWPE due to the high melt viscosity.

In general, on melting of the entangled polyethylene placed between the plates of the rheometer (where the gap between the plates is kept constant), the normal force increases. Increase in the normal force occurs due to volume expansion on the solid to liquid transformation. Once the sample was molten the normal force stays constant. Similar to the entangled samples, melting of the nascent disentangled sample also shows an increase in the normal force on melting, but with time the normal force decreases gradually. This gradual decrease in the normal force arises due to change in the free volume of the disentangled melt during entanglement formation. In the same material when it is fully entangled no such changes in the normal force were observed. This difference suggests different behavior of the disentangled and entangled polymer after melting. These findings are further strengthened by x-ray scattering data summarized in the Appendix 2.

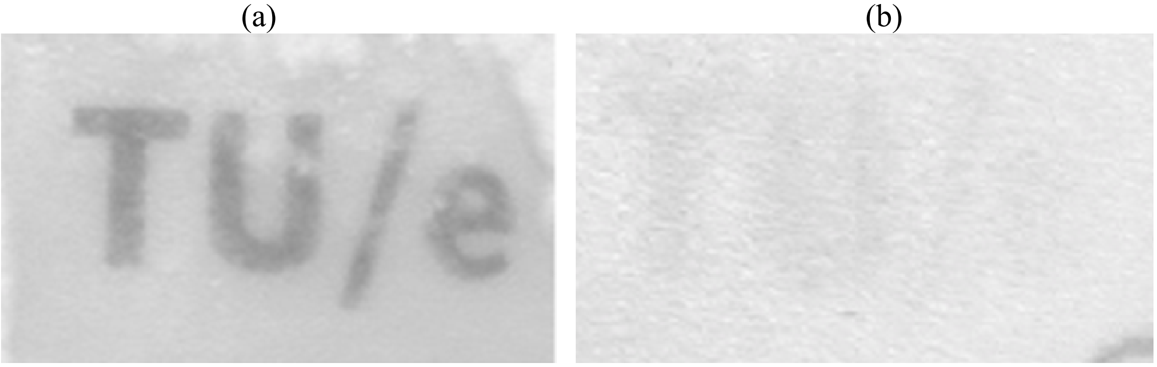
(a) (b)

**Figure 4.3:** Compaction results of different nascent UHMWPE powders at 50°C and 200 bars. Figure (a) refers to a compact film obtained from the sample synthesized using a metallocene catalyst. Figure (b) refers to a compact film obtained from the commercial Ziegler–Natta grade. A comparison of the two figures shows difference in the translucent nature of the two films. This difference arises due to different refractive indices of the two films prior to melting process, i.e. the film b possess more air voids compared to film a. The film shown in figure (a) possesses considerably higher mechanical strength compared to figure (b). The highly mechanical strength of the film in figure (a) combined with the disentangled nature of the polymer facilitates easy drawability of the sample. Both samples show the same melting temperature and enthalpy desired for melting process, suggesting similar crystallinity.

Experimental observations on the disentangled polyethylenes, though not recorded due to instrumental limitation, are that the time required for the normal force to decay to the equilibrium state after melting depends on the molar mass of the polymer. The higher the molar mass the longer is the time required for the normal force to decay to the equilibrium state. These observations have been instrumental in the formulation of the experiments that follow below.

### 4.3.1 Modulus build-up

One of the salient features in linking the chain dynamics with the polymer melt viscosity is the number of entanglements per unit chain. Brownian motion occurs in the chain segments between the entanglements. The presence of the entanglements (i.e. physical contacts between the neighboring chains) restricts the all possible conformations that a single chain can adopt (or the time required for the adoption of different conformations increases dramatically). The restriction thus imposed facilitates cooperative motion between the neighboring chain segments, a requirement for chain reptation. These concepts have been elegantly presented in the tube model proposed by de Gennes[6], Doi and Edwards[7]. The model reduces the topological constraints to the notion of a virtual tube, where the diameter of the virtual tube is defined by the constraints on the test chain with its neighbors. The constrained chain dynamics give rise to a characteristic time ($\tau_d$), for a chain to diffuse one tube length. A salient feature of the theory is that it requires very few parameters: the tube diameter, $a$ (or equivalently the average molecular weight between topological constraints, $<M\mathrm{e}>$, or the plateau modulus, $G_N^o$ ), and the monomeric friction coefficient, $\zeta_0(T)$ (or equivalently $\tau_e(T)$, the characteristic relaxation time for a segment between two entanglements). The average molecular weight between entanglements, $<M\mathrm{e}>$, is inversely proportional to the entanglement density. This is related to the elastic modulus in the rubbery plateau region, $G_N^o$, according to:

$$G_N^o = \frac{g_N \rho R T}{< M_e >} \tag{4.2}$$

where $g_N$ is a numerical factor (1 or 4/5 depending upon convention), ρ the density, $R$ the gas constant, and $T$ the absolute temperature[1]. From these basic concepts it appears that the plateau modulus is an intrinsic property as it arises from the elastic response of the entangled polymer melt. It is, therefore, independent of the total number of entanglements per chain, which increases with molar mass.

As stated earlier, the adopted synthesis route provides a disentangled semi-crystalline polymer, which on melting will provide disentangled polymer melt – a thermodynamically unstable state. To achieve the thermodynamically stable state, chains will tend to entangle as a function of time. Fewer entanglements in the disentangled melt will lead to higher molar mass between entanglements, thus a lower elastic modulus could be anticipated. See equation 4.2. However, it has to be realized that equation 4.2 has been derived for the polymer melt in the thermodynamically stable state.

To follow the entanglement process in the disentangled melt, a constant strain of 1.0% at a fixed frequency of 10 rad/s was applied to the polymer melt placed between the plates in the rheometer. Torque applied to maintain the constant strain increases with time – i.e. with the formation of entanglements the elastic modulus of the melt increases. Variation in the elastic modulus as a function of time at a constant gap between the plates is shown in Figure 4.4.

The figure 4.4 shows two distinguishable rates of modulus build up. The initial sharp increase in modulus may be associated with the mixing of the chains on melting of the disentangled crystals – i.e. mixing process of the disentangled chains. This process will be dependent on the rate at which the chains are brought in contact with each other, a subject that will be addressed in detail at the end of this Chapter. After the mixing process of the chains a gradual increase in the modulus occurs, where the gradual increase corresponds to the entanglement formation during the chain reptation process.

Annexure 3 shows a series of data recorded on different molar masses[*]. Similar concepts have been proposed by the Hiroshima[8] group, where the authors followed the variation in nucleation density with the increasing number of entanglements in an initially disentangled polyethylene. Considering the concepts of mixing of chains followed by chain reptation, it may be anticipated that the time required for the modulus build up will be molar mass dependent. What follows are the observations on the modulus build up in a series of disentangled polymers having molar masses greater than $2\times10^6$ g/mol.

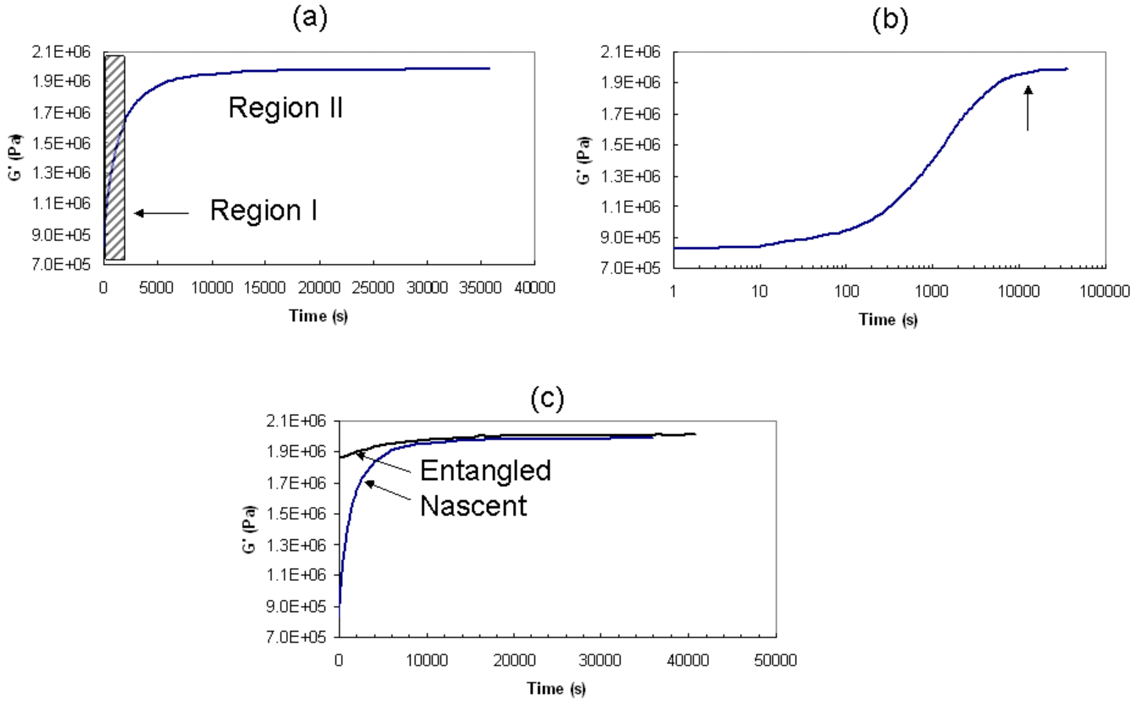

**Figure 4.4:** Modulus build-up in the initially disentangled polymer having a molar mass of $2\times10^6$ g/mol as a function of time. Figure (a), plotted in the linear-linear scale, two regions can be distinguished in the curve a sharp and a gradual build up, named Region I and Region II, respectively. The hatched area shows Region I. In Region I steep increase in the modulus is associated to mixing of disentangled chains on crystal melting, whereas increase in modulus in the Region II is mainly dominated by the chain reptation now in the partially entangled melt. It could be anticipated that after a certain time the modulus will reach the plateau value. To have a clear indication of the modulus reaching the plateau value the same figure (a) is now plotted in the linear-log scale, figure (b). The time required to reach the build up of modulus is termed as the build up time which corresponds to 98% of the asymptotic equilibrium (marked by an arrow) value of the fully entangled melt. Figure (c) shows difference in the change in modulus of the initially disentangled nascent polymer melt and the fully entangled melt. The fully entangled melt was obtained on melting of the sample crystallized after reaching the plateau modulus in figure (b).

---

[*] The Annexure summarizes the reproducibility of the data for two different molar masses.

### 4.3.2 Dependence on the build-up of modulus on molar mass

Figure 4.5 shows a series of time sweep experiments performed on three different disentangled polyethylenes having molar masses 2x$10^6$, 5.3x$10^6$ and 9.1x$10^6$ g/mol. All the samples were synthesized using the same catalyst and polymerization conditions. Different molar masses were obtained by varying the polymerization time as described in chapter 2. Molar masses of these samples were determined by melt rheology and size exclusion chromatography, as described in chapter 3.

From the linear-linear plot of the time sweep experiments, it is evident that the time required for the modulus build up increases with the increasing molar mass. All three molar masses show a mixing region, where the Rouse dynamics[9] will be more prominent, followed by the entanglement formation via chain reptation. It may be anticipated that the mixing zone, Region I, will be lesser molar mass dependent compared to the entanglement formation via chain reptation, Region II. However, from the given data due to the initial instability in the measurements the molar mass dependence on the difference in the Region I of the samples could not be established. A clear distinction in the chain reptation zone, Region II, with increasing the molar mass was observed. From Figure 4.5, it is evident that with increasing molar mass the time required for the establishment of the entangled state increases.

The build-up time required for the samples with different molar masses is summarized in Figure 4.6. The figure shows a set of data points showing build up time for seven different molar masses summarized in Table 4.1. Two data points have been taken from our earlier work[10].

Here the adopted procedure to determine the build time is recalled. From Figure 4.4, the build up time can be approximately determined. The arrow in Figure 4.4 (b) illustrates the time required to reach 98% of the asymptotic equilibrium value of the fully entangled melt.

It is to be noted that in the determination of the modulus build-up with increasing molar mass the total time that includes Regions I and II have been taken. Considering the molar masses greater than a $10^6$ g/mol, the mixing time required in Region I will be considerably less compared to the time required in Region II. The power law established in Figure 4.6 is likely to arise due to chain reptation i.e. the time needed in the Region II. It is surprising that power law holds in the partially disentangled polymer melts, where all samples have been synthesized using single site catalyst. However, the stated power law may not hold if different synthesis conditions, such are concentration, temperature, monomer pressure are used. Because using the different polymerization conditions initial morphology of the samples will defer that will have implications on mixing of chains and the corresponding modulus build up time.

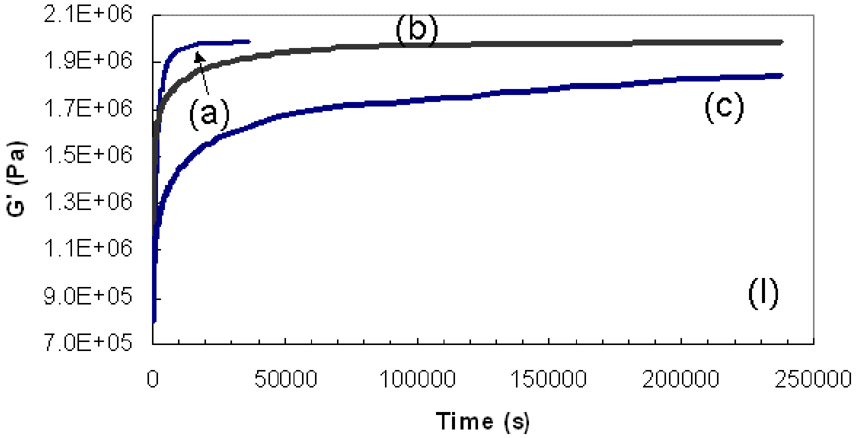

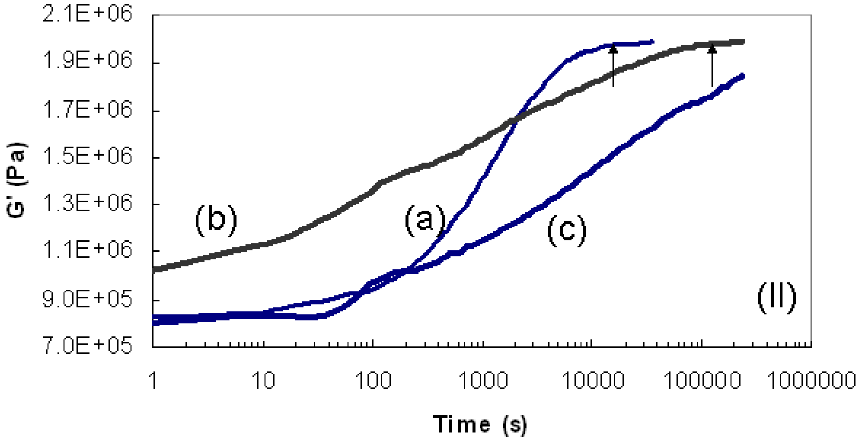

**Figure 4.5:** Modulus build-up in an initially disentangled polymer having molar mass of (a) $2x10^6$, (b) $5.3x10^6$ and (c) $9.1x10^6$ g/mol as a function of time. Experiments were performed at constant temperature 160ºC and fixed frequency and strain of 10 rad/s and 1%, respectively. Similar to figure 4.4 to have clear distinction between the build up time for different molar masses linear-log scale figure (II) is drawn. Arrows marked here refer to the modulus build up time in the initially disentangled melt. The absolute values of elastic modulus at t = 0 are questionable because of the uncertainties associated to the time required for reaching the thermal stability.

These observations on molar mass dependence and build up time are in accordance with our previous publications and work performed in our group[11]. To recall, Lippits showed that the time required for the chain dynamics in the two different melts is the same, though in the disentangled melt initial chain dynamics is faster than in the entangled melt state[11].

**Table 4.1:** Characteristic build-up time of initially disentangled polymers studied at constant temperature 160ºC and fixed frequency and strain of 10 rad/s and 1%, respectively.

| Mw (g/mol) | Build up Time (s) |
|---|---|
| $8\text{x}10^{5\,(a)}$ | 800 |
| $1.4\text{x}10^{6\,(a)}$ | 4000 |
| $2\text{x}10^{6}$ | 15000 |
| $2.4\text{x}10^{6}$ | 20000 |
| $3.8\text{x}10^{6}$ | 50000 |
| $4\text{x}10^{6}$ | 80000 |
| $5.3\text{x}10^{6}$ | 150000 |

(a) Data obtained from Ref 10.

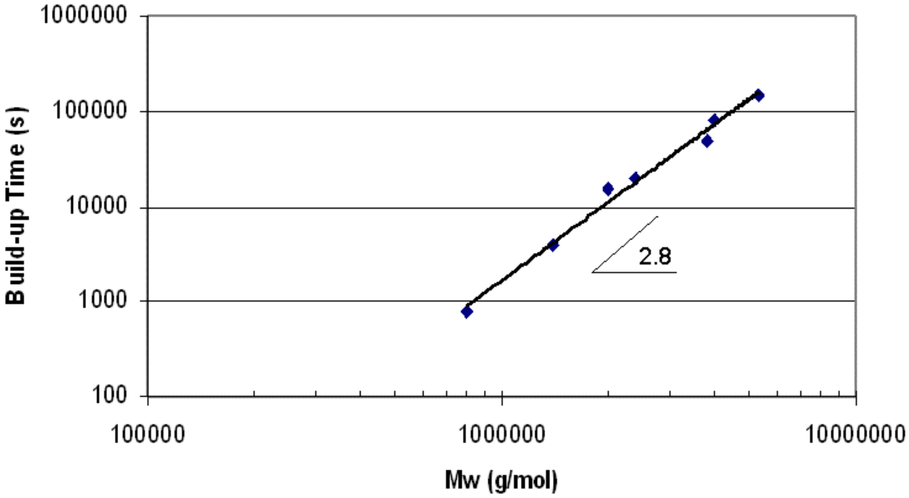

**Figure 4.6:** Required build-up time for different molar masses. Data obtained from Table 4.1.

## 4.4 Effect of frequency and strain on modulus build-up

Figure 4.7 summarizes frequency sweep experiments performed on the partially disentangled melt. To follow changes in the modulus in a certain frequency range during the entanglement formation, a region from 0.1 to 100 rad/s was chosen to get the maximum numbers of data points in a short interval. The successive frequency sweep experiments performed within this region show a gradual increase in the modulus. Once a modulus of 2 MPa was achieved, the polymer melt was considered to be fully entangled. The successive frequency sweep experiment on the thus obtained polymer melt shows the anticipated behavior from an entangled melt.

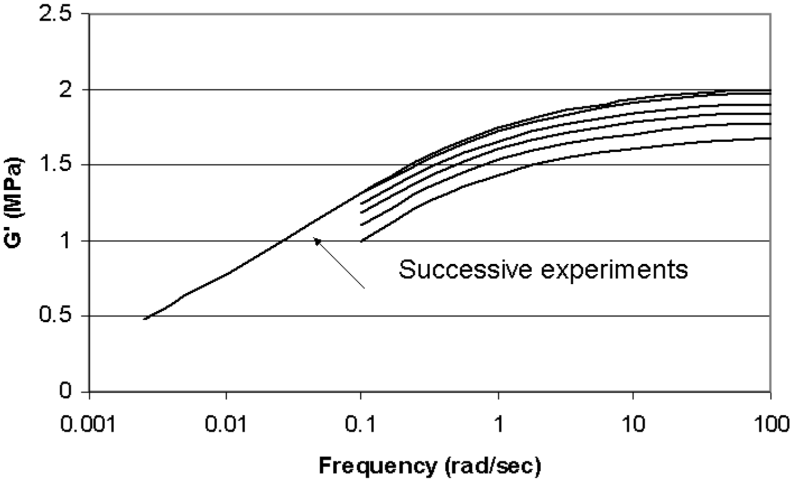

**Figure 4.7:** Successive frequency sweep experiment on a disentangled sample, having molar mass of 2x10$^6$ g/mol, at 160ºC and 0.5% strain. For the fully entangled sample the experiment was performed over a larger frequency range (100-.001 rad/s). Data shown here correspond to the first, second, fourth, 8th and nth cycle of the frequency sweeps ranging between 0.1 to 100rad/sec. Time between the successive cycles was approximately 500 seconds, whereas the nth cycle was performed on the sample when the fully entangled state was obtained.

### 4.4.1 Frequency effect

A frequency sweep experiment provides information about the response of the chains at different time scales, from local to cooperative motion. Such information is depicted in Figure 4.8 [12]. Beyond reptation as a dynamic process of entangled chains there are other mechanisms such are "contour length fluctuation" (CLF), "constraint release" (CR) and under very fast (or strong) flows the tube stretching and "convective constraint release" (CCR)[13,14]. Considering the high molar mass that is investigated, for a fully entangled melt state reptation dynamics will be the most prominent feature. To probe how the local and cooperative motions change in the disentangled melt time sweep experiments have been performed at different frequencies for constant strain and temperature.

Figure 4.9(i) shows the frequency sweep experiment on a fully entangled polymer melt having molar mass of 5.3x10$^6$ g/mol at constant temperature (160ºC) and strain (1%). From the frequency region from 3 to 100 rad/s a plateau region was observed for this sample, whereas change from elastic to viscous region occurs in the vicinity of 1rad/s. From the figure, the plateau region followed by the terminal region at low frequencies is evident. Segments of the chain dynamics that cause the overall change in modulus with frequency (or time) is described in the figure 4.8.

Figure 4.9(ii) shows a series of time sweep experiments performed on an initially disentangled polymer melt having a molar mass of 5.3x10$^6$ g/mol at three different frequencies: 100, 10 and 1 rad/s at a constant strain (1%) and temperature (160ºC). The three frequencies refer to chain dynamics associated to different regions of the chain as described in Figure 4.8. From figure 4.9 (i), the frequencies 100 and 10 rad/s correspond to chain dynamics associated to plateau region, whereas at the frequency 1 rad/s chain dynamics is related to the terminal region. Thus purpose of performing time sweep experiments at the chosen frequencies is to follow entanglements formation at different chain lengths.

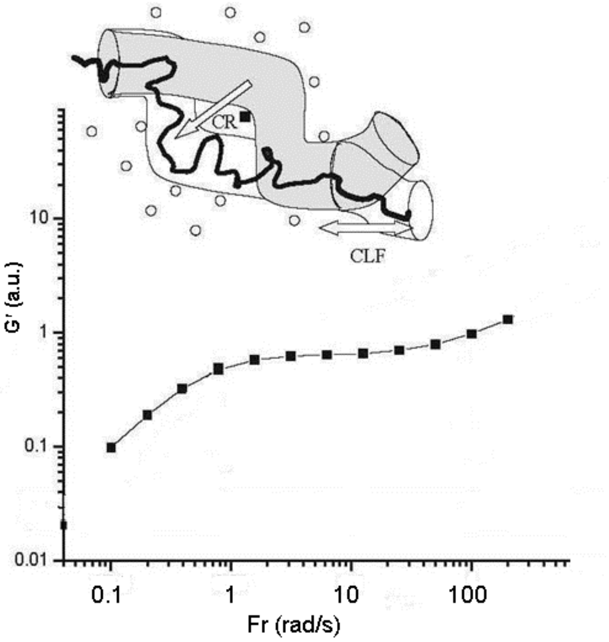

**Figure 4.8:** Schematic illustration of relaxation of flow of a linear polymer, as reproduced from Ref 12. The figure is a typical example that one observes in a linear polymer. In an entangled polymer melt, different chain lengths are anticipated to have different chain dynamics, thus a different response to the applied stress. For an example, due to large chain conformations that chain segments between the entanglements can adopt, on application of the stress these chain segments show high modulus (glassy region) – a high frequency region. The presence of entangled network, where the overall chain dynamics in a specific time zone appears to be stationary, plateau region is realized. At the low frequency region, transition from elastic to viscous region is observed due to chain reptation that leads to tube renewal – causing a drop in modulus.

Figure 4.9 (ii) shows modulus build-up time for the three frequencies. Clear differences exist in the time required for the modulus build-up. Compared to the build up time at the high frequencies, 10 and 100 rad/s, the build-up time to reach a plateau of 2MPa at the low frequency of 1rad/s is significantly higher. This difference in the build-up time at the low and the high frequencies suggest differences in the chain dynamics of the different chain regions of the disentangled polymer melt. From Figure 4.9(iii) it is apparent that the slope of the modulus build-up in the mixing region (Region I) shows a strong dependence on the applied frequency, i.e. with decreasing frequency the slope of the modulus build-up time decreases. With the decrease in the slope, the time required for the modulus to reach the plateau value increases. These observations suggest that the total build-up time will be different for the different chain segments.

Considering the frequencies of 10 and 100 rad/s representing chain segments in the plateau region and the frequency of 1 rad/s at the onset of the terminal region, the frequency dependence of the modulus build-up time in Region I suggest that mixing of smaller chain segments is faster than the mixing of the larger chain segments. The larger chain segments will require greater cooperative motion. These findings are in agreement with the NMR studies performed to follow the entanglements formation, where the studies showed faster entanglements formation between few methylene units, independent of molar mass[10]. Considering the frequency dependence on the modulus build-up the influence of applied strain at a fixed frequency on the modulus build-up will be investigated.

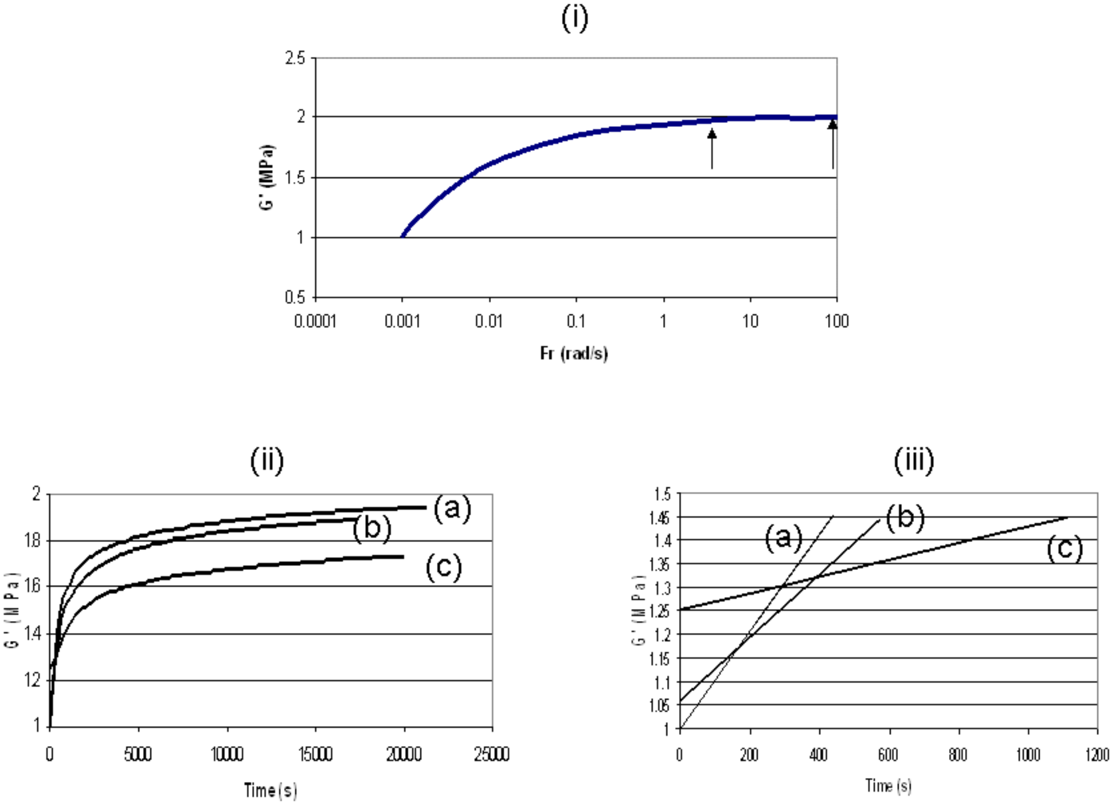

(i)

(ii)

(iii)

**Figure 4.9:** Shear oscillatory experiments on a sample having molar mass of 5.3x$10^6$ g/mol. Figure [i] shows frequency-sweep experiment on the fully entangled sample, strain 1%, temperature 160ºC. Plateau modulus is observed in the frequency range marked by arrows (approximately above 1rad/s). Figure [ii] depicts time-sweep experiment performed on the disentangled sample at (a) 100, (b) 10 and (c) 1 rad/s at constant temperature (160ºC) and fixed strain (1%). Figure [iii] shows magnified Region I illustrating three different slopes for the three different frequencies. The slope ratio (a):(b):(c) is 10:7:2.

### 4.4.2 Strain effect

To recall, on melting a disentangled polymer the entangling process leads to an increase in the modulus with time. These time sweep experiments were performed at a fixed strain, constant frequency and temperature. It is well known that with increasing strain above a critical value the elastic modulus decreases and phase angle increases, Figure 4.10. The region above the critical strain is suggested to be the non-linear viscoelastic region of the polymer melt. The decrease in the storage modulus is associated with the alignment (partial disengagement) of chains in the shear direction[15]. Since the alignment (partial disengagement) process will be dependent on the chain relaxation. The critical strain desired for the non-linear viscoelastic region is anticipated to be influenced by the number of entanglements per unit chain. Thus, the disentangled polymer melt provides a unique opportunity to follow the influence of entanglements on the critical strain.

Figure 4.11 shows the strain sweep for a disentangled sample at fixed frequency (10 rad/s) and temperature (160ºC). Experimental observations are that with the increasing number of strain sweep cycles the value of the critical strain increases. To quote, in the very first applied strain sweep cycle the phase angle increases at a strain of 3%. With the increasing number of the strain sweep cycles as the number of entanglements per unit chain increases the desired critical strain for chain disengagement shifts to higher values. Ultimately, for an entangled polymer melt having a molar mass of 9x10$^6$ g/mol, the critical strain reaches a value of 10%. These observations further confirm the disentangled state of the polymer melt.

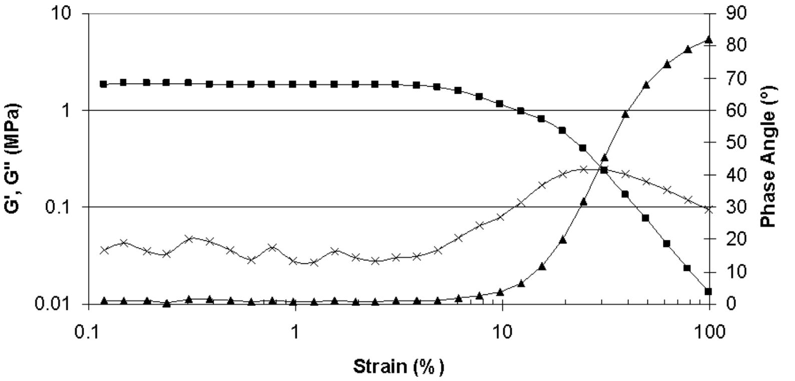

**Figure 4.10:** Strain-sweep for a fully entangled sample having a molar mass of 5.3x10$^6$ g/mol at constant temperature 160ºC and a fixed frequency 10 rad/s. (■) Elastic modulus, (×) loss modulus and (▲) phase angle. The peak observed in the loss modulus in the non-linear viscoelastic region is unique and reproducible. Probably this is specific to the high molar mass of the sample. More detailed studies are needed to explain this feature.

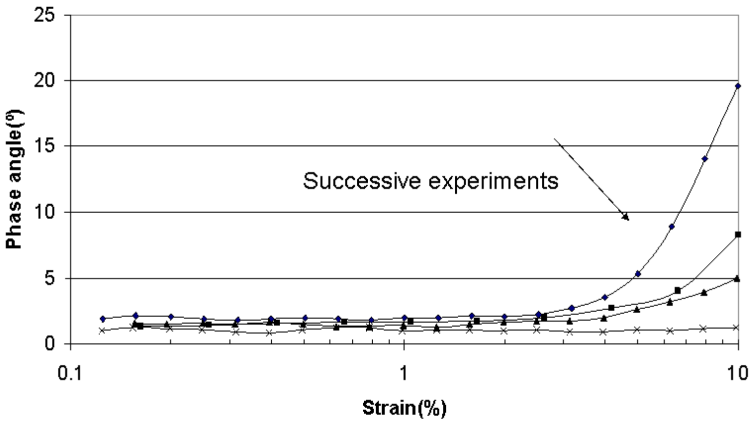

**Figure 4.11:** Successive strain sweep experiments on a disentangled sample having a molar mass of 9x$10^6$ g/mol, at 160ºC and frequency 10 rad/s. By the entangling process, the required strain to switch from the linear viscoelastic region (LVR) to the non-linear viscoelastic region shifts to higher values. Where (♦), (■) and (▲) in the figure correspond to the first, second and 20th sequence, respectively. The cross points (×) indicates the entangled polymer.

Figure 4.12 shows the modulus build-up in a disentangled polymer melt on the application of different strains in the linear and non-linear viscoelastic regions. When the applied strain is in the linear viscoelastic region, the time sweep experiment shows similar trend in the build up of modulus as reported earlier (Figure 4.5, for different molar masses). No strain dependence in the modulus build-up was observed. Whereas, when the applied strain is in the non-linear viscoelastic region (strain greater than 2% for the disentangled polymer, Figure 4.11), the disentangled polymer melt shows a lower initial elastic modulus which is expected for the non-LVR. However, the modulus increases initially due to the entanglement formation process followed by an unusual decrease. The increase in modulus arises due to the increase in the number of entanglements per unit chain in the initially disentangled polymer melt. In the non-linear viscoelastic regime of the applied strain, the decrease in the modulus is expected due to partial disengagement (or alignment) of the entangled chains, leading to shear thinning. The resultant two competing effects, (build up of modulus in the disentangled melt and disengagement of the entangled chains) influence the time sweep experiment reported in Figure 4.12.

From the experimental observations above, it is apparent that the strain required for the shift from the linear to the non-linear viscoelastic regime depends on the entanglements in the melt, i.e. the strain required for the shift is lower for the initially disentangled melt state compared to the melt in the entangled state. Thus, a cause for the lower modulus at the very initial state of the disentangled melt may also arise due to the applied strain used in the experiments. Here the caution needs to be taken to make use of the lowest possible strain.

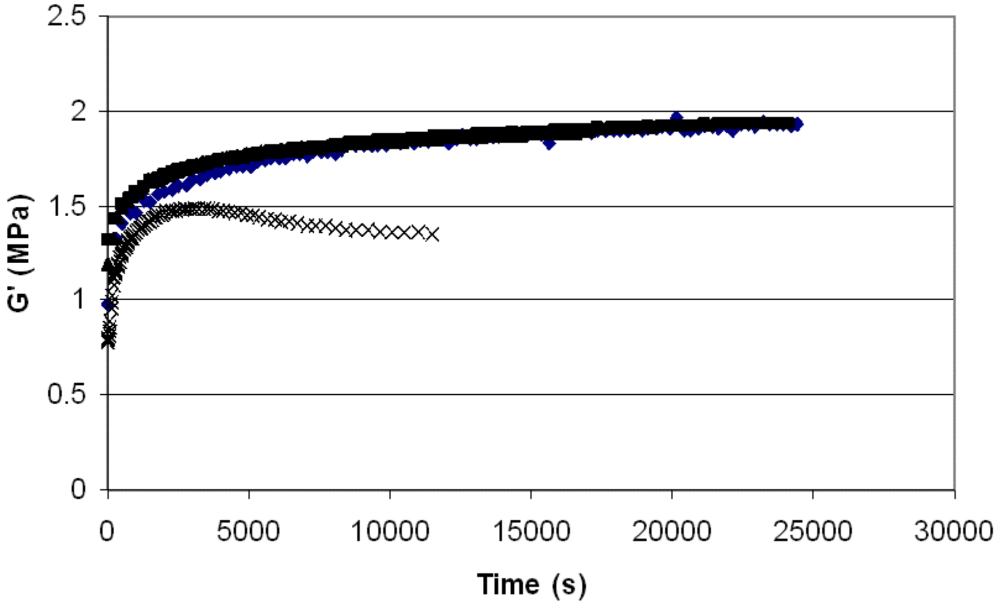

**Figure 4.12:** Time-sweep experiments on the disentangled sample having a molar mass of $5.3 \times 10^6$ g/mol at (♦) 0.2, (■) 1, (▲) 2 and (×) 5% strain. Constant temperature (160ºC) and fixed frequency (10 rad/s).

The important observation in this series of experiments is the independence of the time sweep modulus build-up profile on application of applied strain in the linear viscoelastic regime. What follows is the influence of melting process of the disentangled crystals on the mixing process of the chains in Region I, and the resultant build-up time in the disentangled polymer melt.

## 4.5 Annealing experiments

Before proceeding further, some of the salient features of the melting process of the disentangled linear polyethylenes is presented. To quote, the melting of spherulitic structures is a complicated process because the chains are shared between different crystalline zones, where the entanglements reside in the amorphous regions. Toda et al[16] showed that contrary to the complicated melting of a spherulitic structure the melting of single crystals is the reversal process of crystallization, where detachment of chain segments from the crystal surface has to overcome the entropic barrier. Thus, it is stated that kinetics plays an important role in melting process of the crystals.

Similar melting kinetics has been observed by us independently in the disentangled linear polyethylenes. Where it was shown that when given sufficient time ("slow" melting) melting in the disentangled crystals occur by continuous detachment of chain segments from the crystal surface followed by their reeling-in into the melt. Whereas the "fast" melting results in cluster melting where 7-8 chain segments are involved[17]. Influence of melting kinetics on modulus build-up time has been investigated further here.

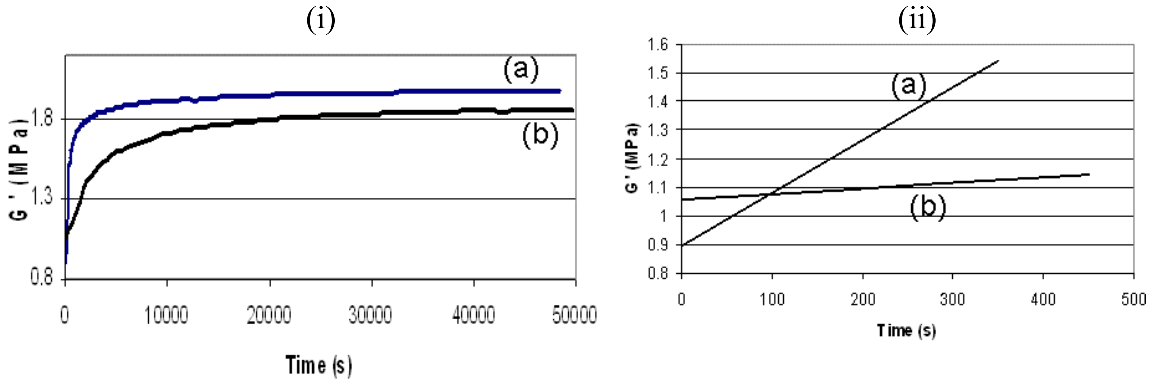

**Figure 4.13:** Figure (i) shows time sweep experiment on disentangled the sample having a molar mass of 3.8x$10^6$ g/mol at 160ºC, 10 rad/s and 1% strain. (a) Fast heated sample, (b) annealed sample. Figure (ii) shows the magnified Region I where the two different slopes can be recognized, the slope ratio (a):(b):: 10:1.

To achieve the "slow" melting aspects, the annealing experiments in the vicinity of the onset of melting temperature recorded by DSC during a normal heating rate of 10ºC/min were performed. In the disentangled sample, the occurrence of slow melting during the annealing process was followed in the rheometer. With melting on annealing once the material softens, due to better contact between the plate and the polymer, an increase in the elastic modulus was recorded. With time, as the material melts further, the modulus decreases and a simultaneous decrease in the phase angle was observed.

Figure 4.13(i) shows the different time scales for Region I for the two samples heated to melt at two different heating rates. The polymer heated fast shows a smaller Region I along the time axis compared to the sample annealed in the vicinity of the equilibrium melting point. However, once the polymer melts and reptation dynamics comes into picture, the slope in Region II becomes nearly parallel. Considering the parallel lines and lower modulus of (b) in Region II, where the lower modulus could be due to physical or experimental reasons, it can be debated that the annealed polymer acquires the heterogeneous melt state as has been stated earlier[18]. Figure 4.13(ii), shows the magnified Region I. It is evident that the slope of (a) is much higher than the slope of (b), clearly indicating the influence on the rate of entropy gain during melting of the crystals and its effect on mixing of the initially disentangled chains. The figure also shows that at t = 0, i.e. when the polymer is heated to 160ºC either by fast heating (slope (a)) or slow heating (slope (b)), the initial modulus for (a) is lower than the initial modulus for (b).

A cause for this difference is depicted in Figure 4.14, where the slow heating causes the formation of entanglements due to the difference in the melting kinetics of the crystals on slow or fast heating. [17,18,19]

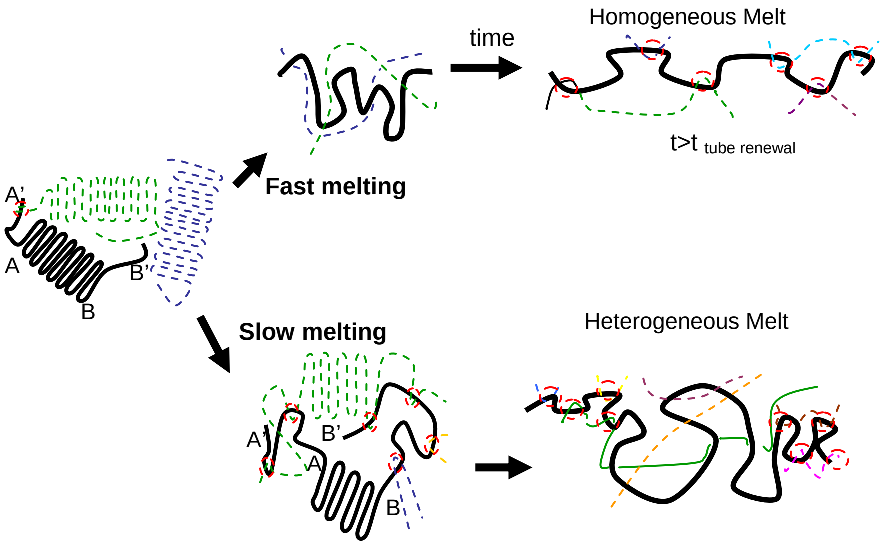

**Figure 4.14:** Depicting the melting process of the disentangled nascent crystals during fast and slow heating. On slow heating, the evolution of the heterogeneous distribution of entanglements occur, which leads to differences in the local mobility of the amorphous component. Adopted from Ref 18.

## 4.6 Conclusions

From the rheological studies performed in this chapter, it is evident that the melting of disentangled polymer initiates entangling of chains. A melt initially in the disentangled state entangles with time. Entanglement formation is followed by an increase in modulus. Modulus build-up with time at a constant frequency, strain and temperature shows two distinct regions, defined by two distinct slopes. Region I, corresponding to the steep slope, arises due to mixing of disentangled chains, whereas Region II shows a slow increase in the modulus build-up with time – following the reptation dynamics in the melt. Region I shows a strong dependence on the rate of entropy gain by the crystals on going from the solid to the liquid state. The rate of entropy gain is varied either by the heating rate, or annealing of the samples in the vicinity of the equilibrium melting temperature. Even molar mass dependence is realized during the entangling process of the chains, which also shows influence on the build-up time from the disentangled to the entangled melt state. Once mixing of the disentangled chains takes place, further build-up of the modulus follows the reptation dynamics. This is realized as a power law in the modulus build-up time and molar mass. The exponent was 2.8.

The initially disentangled melt (as stated earlier in this Chapter the term disentangled melt does not mean that the chains are fully disentangled) shows a lower elastic modulus indicative of higher molar mass between entanglements (Me), where the Me decreases with the entanglements formation. Since a disentangled chain is not a thermodynamically stable state the existing rheological models are not fully applicable. The critical strain at a fixed frequency, required for the shift from linear to the non-linear viscoelastic region, shows a strong dependence on the entangled state of the polymer melt.

## 4.6 References

[1] Ferry J. D., *Viscoelastic Properties of Polymers*, **1980**, Wiley, New York.

[2] (a) Richardson M. J., *Proc. R. Soc. London, Ser. A* , **1964**, 279, 50, (b) Jachowicz J. and Morawetz H., *Macromolecules*, **1982**,15, 828, (c) Chang P. L. and Morawetz H., *Macromolecules*, **1987**, 20, 428, (d) Liu C.-Y. and Morawetz H., *Macromolecules* , **1988**, 21, 515, (e) Rong W., *J. Polymer Sci. B*, **2005**, 43, 2243.

[3] Kotliar A.M., Kumar R. and Back R.A., *J. Polymer Sci. part B*, **1990**, 28, 1033.

[4] Lemstra P.J, Bastiaansen C.W.M. and H.E.H. Meijer, *Die Angewandte Makromolekulare Chemie*, **1986**, 1451/146, 343.

[5] Rastogi S., Spoelstra A. B., Goossens J. G. P., and Lemstra P. J., *Macromolecules*, **1997**, 30, 7880.

[6] de Gennes P.G., *Scaling Concepts in Polymer Physics,* **1979**, Cornell University Press, Ithaca, NY

[7] Doi M., Edwards S.F., *The Theory of Polymer Dynamics,* **1986,** Clarendon Press,Oxford.

[8] Yamazaki S., Gu F., Watanabe K. , Okada K., Toda A. and Hikosaka M., *Polymer*, **2006**, 47, 6422.

[9] Rouse P. E., *J. Chem. Phys.,* **1953**, 21, 1272.

[10] Dirk R. Lippits, Controlling the melting kinetics of polymers; a route to a new melt state*, PhD thesis, Eindhoven University of Technology*, **2007**.

[11] Lippits D.R., Rastogi S., Talebi S. and Bailly C., *Macromolecules,* **2006**, 39, 8882.

[12] Bent J., Hutchings L. R., Richards R. W., Gough T., Spares R., Coates P. D., Grillo I., Harlen O. G., Read D. J., Graham R. S., Likhtman A. E., Groves D. J., Nicholson T. M., McLeish T. C. B., *Science*, **2003**, 301, 1691.

[13] Marrucci G., *J Non-Newtonian Fluid Mech*, **1996**, 62, 279.

[14] Likhtman A. E, Milner S.T. and McLeish T.C.B., *Physical Review Letter*, **2000**, 85, 4550.

[15] Hyun K., Kim S.H., Ahn K. H.and Lee S. J., *J. Non-Newtonian Fluid Mech.*, **2002**, 107, 51.

[16] Toda A., Kojima I. and Hikosaka M., *Macromolecules*, **2008**, 41, 120.

[17] Lippits D.R., Rastogi S. and Hohne G.W.H., *Physical Review Letters*, **2006**, 96, 218303.

[18] Rastogi S., Lippits D., Peters G.W.M., Graf R., Yao Y-F and Spies H.W., *Nature Materials*, **2005**, 4, 635.

[19] McLeish T. C. B., *Soft Matter*, **2007**, 3, 83.

This page is intentionally left blank

# Chapter 5

# Melting of disentangled crystals and its implications for crystallization

## 5.1 Introduction

In the previous chapters, the synthesis of disentangled polyethylenes with varying molar mass was presented. One of the characteristics of these materials is the high melting temperature during their first heating run. To recapitulate, several studies performed on the nascent polymer clearly show a high melting temperature of 141ºC, a value close to the equilibrium melting temperature. For a long time such a high melting temperature has been a matter of dispute. In the past, the high melting temperature has been attributed to a larger degree of perfection and a greater thermodynamic stability gained during polymerization[1], extended chain crystals[2] or a fast reorganization process of the crystals prior to melting[3]. Later, it was proposed that mainly the local kinetics of polymer formation at the active catalyst sites, which is controlled by the polymerization conditions (e.g. the synthesis process and polymerization temperature), and the subsequent crystallization determines the thermal properties and the morphology of the nascent state[4]. Recently, it has been shown that the melting temperature in the semi-crystalline polymers depends not only on the crystal thickness, but also on the morphological aspects of the amorphous phase[5,6].

## 5.2 High melting temperature in nascent polymers

To investigate the morphological features of the amorphous phase, solid state NMR studies have been performed on the nascent samples. Considering the unknown morphology of the nascent polymer, solution cast films as a model system were investigated by NMR[7,8]. Studies performed on the films showed restricted local dynamics in the amorphous regions compared to the melt crystallized sample of the same polymer. Though in the films local dynamics in the amorphous regions is restricted, chain diffusion between amorphous and crystalline regions is observed to be much faster. Considering the same enthalpic barrier between the crystalline and the amorphous regions of the solution and the melt crystallized samples, the fast chain diffusion process in the films was attributed to a lower entropic barrier. Similar to the solution cast films the nascent samples also show restricted local dynamics in the amorphous region and fast chain diffusion between the crystalline and the amorphous regions[9].

Combining these NMR studies with the studies performed by Rastogi et al.[10] the high melting temperature of the nascent polymers was attributed to the simultaneous detachment of the adjacently re-entrant chain segments within the crystal connected by the amorphous chain segments having restricted chain mobility. Such a possibility is depicted in a schematic drawing shown in Figure 5.1. The figure depicts differences in the topological constraints that reside in the amorphous regions of the semi-crystalline polymers. The polymer crystallized from the melt shows hardly any connectivity between the adjacent chains within the same crystal. Whereas, the restricted local mobility in the amorphous region of the nascent sample suggests adjacent re-entry of chains within the crystal.

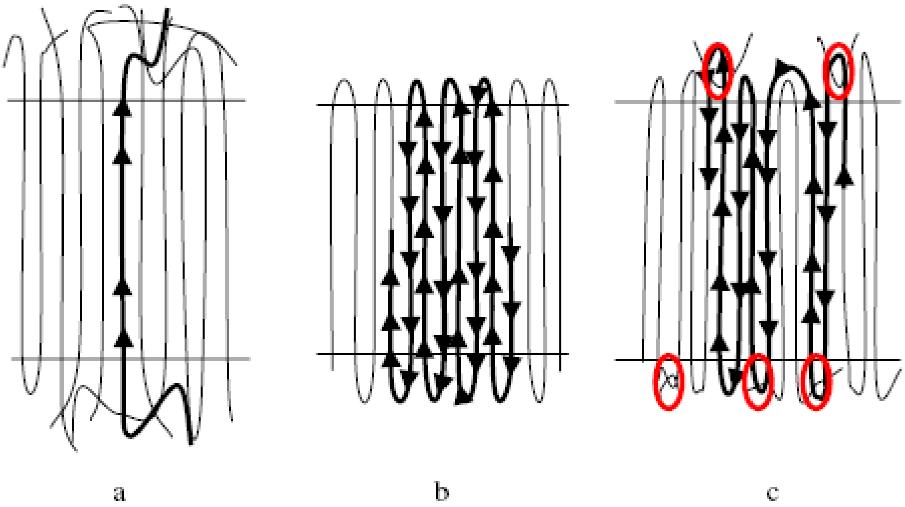

**Figure 5.1** Illustration of the crystal structure of (a) a melt-crystallized sample having inter-crystal molecules and loose loops, (b) nascent disentangled sample having tight folds and (c) nascent entangled sample having tight folds. The depicted entanglements in the figure are circled. Adapted from Ref 10.

Thus, while the melting of the melt-crystallized sample requires detachment of a single chain stem from the crystal, melting of the nascent sample occurs by simultaneous detachment of several adjacently re-entrant chains connected by the amorphous region having restricted local mobility. Therefore, during melting, the number of $CH_2$ units that need to be detached from the crystal substrate having similar thickness in the nascent samples is much larger than the melt crystallized samples. Therefore, at the normal heating rates (10ºC/min or higher) the melting temperature of the adjacently re-entrant chains is much higher than the one anticipated by the Gibbs-Thomson equation, which takes into consideration crystal thickness and the surface free energy only. However, this high melting temperature is lost on second heating run in DSC because such a sample is representative of melt crystallized polymer, Figure 5.2.

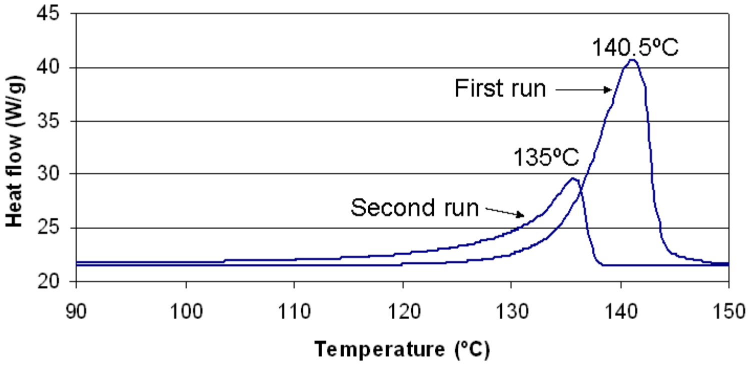

**Figure 5.2:** DSC curve obtained on the first and second heating runs on a disentangled UHMWPE (2x$10^6$ g/mol). Heating rate (10ºC/min). It is to be noted that similar DSC curves are observed for different molar masses and are independent of the polymerization conditions.

## 5.3 Heating rate dependence in melting of polymers

A general notion in the melting process of crystals is the absence of any activation barrier in the detachment of chains from a crystal surface. Chains residing at the interface, of crystal and melt, encounter a different environment compared to the chains residing within the crystal. This difference favors melting (detachment of chains) at the interface. The time required for the melting process of a crystal is, therefore, believed to be limited by the thermal diffusion process, where melting is often explained as a simple transport phenomena.

Pioneer work by Wunderlich[11] showed that in polymers the melting temperature is often dependent on the heating rate. The reported melting temperature is often higher than the true value due to thermal lag between the pan of the instrument and the sample. These findings lead to the concept of superheating[12]. Recently, Toda et al[13] by meticulously avoiding the instrumental heat lag showed the non-linear dependence in the melting temperature of a polymer at different heating rates. The non-linear dependence that cannot be simply explained by the thermal diffusion, leads to the concept of the activation barrier for chain detachment from the crystal surface during melting of crystals. This non-linearity in the melting process was further observed during melting of a single crystal. Non-linear dependence of the melting temperature with the heating rate, i.e. time dependent melting of the crystals, lead to the concept of kinetics in melting, where the activation barrier is solely entropic, rather enthalpic.

Similar melting kinetics was also observed in our disentangled ultra-high molecular weight samples, where the melting kinetics showed a dependence on the topological constraints (entanglements) residing in the amorphous regions of the semi-crystalline polymers. A strong heating rate dependence of the melting process of these crystals leads to the development of differences in melting during slow and fast heating. While in fast heating, melting occurs by detachment of several chain segments i.e. cluster melting, whereas in slow heating, melting proceeds via successive detachment of chains from a crystal surface followed by the reeling in of chains in the melt. The time required for the slow melting process shows a dependence on the topological constraints[6].

During synthesis of samples in Chapter 2 considerable precautions have been taken to obtain disentangled polymers. The physical concepts applied to obtain the desired morphology are the polymerization temperature is lower than the crystallization temperature, where prior to entanglement formation chains should crystallize. The single-site catalyst facilitates the process, where ideally a single chain forming a single crystal can be anticipated. The melting of such a crystal will be similar to the melting process observed in a single crystal.

Figure 5.3 shows a non-linear heating rate dependence on the melting temperature of the nascent polyethylenes of two different molar masses, $2x10^6$ and $3.8x10^6$ g/mol having a narrow polydispersity of 2.0 for such high molar masses. This non-linear melting temperature dependence confirms the presence of an activation barrier in melting of the crystals. It is to be noted that the melting temperature of the two samples at zero heating rate is below 139ºC (the lower melting temperature becomes apparent on annealing the samples, as described in the following section), while linear extrapolation of the line gives value in the vicinity of 139.8ºC. Considering the restricted local mobility of the amorphous phase and high chain diffusion between the crystalline and the amorphous regions [8], as investigated by NMR, the origin of this high melting temperature for the chain folded crystals can be explained by the schematic figure above, Figure 5.1.

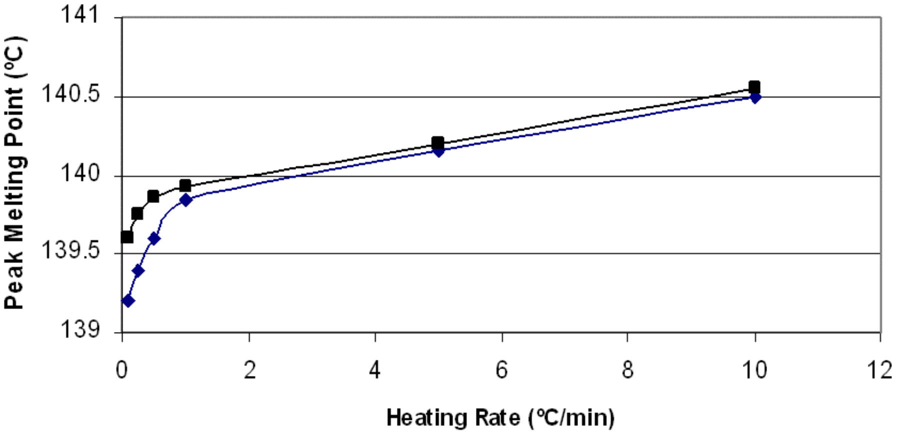

**Figure 5.3:** Dependence of the peak melting point on the heating rate for disentangled UHMWPE. Samples having molar mass of (♦) $2x10^6$ and (■) $3.8x10^6$ g/mol. The accuracy of measured value at heating rates above 1ºC/min is ± 0.5ºC and below 1ºC/min is ± 0.2ºC.

## 5.4 Annealing experiment below the melting point

To follow the kinetics of the melting process, the samples were annealed at a fixed temperature for different times and subsequently cooled to room temperature. On heating the annealed sample (annealed at and above 137ºC) two melting peaks were observed as shown in Figure 5.4. The peak at the lower melting temperature is attributed to the melting of the regions that crystallized on cooling the annealed sample, whereas the peak at the higher temperature arises from regions of the sample that did not melt during on annealing process. The ratio of the two peaks showed strong a dependence on the annealing temperature, annealing time and molar mass. One of the striking observations in these samples has been that on annealing the high temperature peak shifts to the higher values. The shift observed during the annealing process also showed a strong dependence on the annealing temperature, annealing time and molar mass. Figure 5.4 shows this dependence for two different annealing times and annealing temperatures for the disentangled sample of molar mass 2x$10^6$ g/mol.

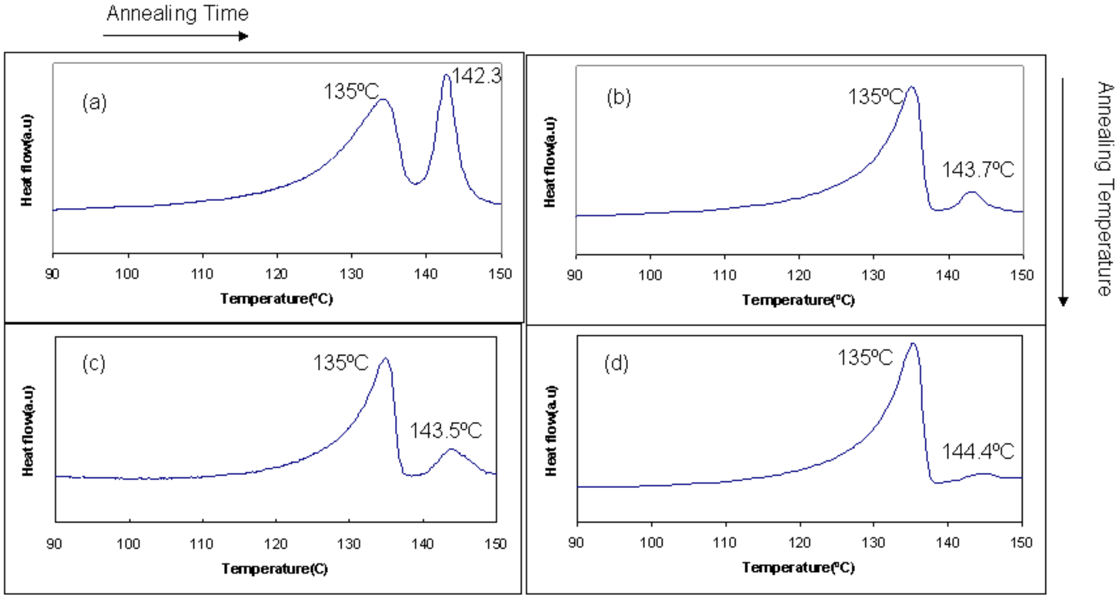

**Figure 5.4:** Heating runs of the nascent disentangled UHMWPE (2x$10^6$ g/mol), after annealing at (a) 137ºC for 50min, (b) 137ºC for 900min, (c) 138ºC for 50min and (d) 138ºC for 900min. By increasing the annealing time, or annealing temperature, the high temperature peak shifts to the higher values.

### 5.4.1 Influence of annealing time at a constant annealing temperature

Table 5.1 summarizes the observations on a disentangled polyethylene sample. The polymer was annealed at 138ºC for different times. After the requisite annealing temperature and time, the samples were cooled to room temperature. The subsequent heating run of the thus cooled sample showed two melting peaks as shown in Figure 5.4. Peak melting temperatures, with the corresponding enthalpies are shown in Table 5.1. With increasing annealing time, while the enthalpy of the low melting peak increases the melting temperature remains constant. Whereas, with annealing time, the enthalpy of the high melting peak decreases and the peak temperature shows a gradual shift to higher values at the usual heating rate of 10ºC/min. Change in the total enthalpy of the nascent and the annealed sample arises due to decrease in crystallinity of the melt crystallized polymer. This decrease in crystallinity is in agreement with Figure 5.2, where the drop in crystallinity in the melt crystallized sample (2nd heating run of Figure 5.2) occurs by nearly 50%.

**Table 5.1:** Influence of annealing time on the peak melting point.

| Annealing time (min) | Peak melting point | |
|---|---|---|
| | Lower Peak (Enthalpy) | Higher Peak (Enthalpy) |
| Without annealing | 140.5ºC<br>(223 J/g) | |
| 5 | 135ºC<br>(63.2 J/g) | 141.7ºC<br>(19.3 J/g) |
| 20 | 135ºC<br>(96.2 J/g) | 142.7 ºC<br>(4.9 J/g) |
| 50 | 135ºC<br>(99.5 J/g) | 143.5 ºC<br>(4.5 J/g) |
| 900 | 135ºC<br>(103 J/g) | 144.4 ºC<br>(2.5 J/g) |

Annealing temperature 138ºC. Molar mass of sample 2x$10^6$ g/mol. Heating rate 10ºC/min. The accuracy of measured values are ± 0.5ºC.

### 5.4.2 Influence of annealing temperature at a constant annealing time

Similar to Table 5.1, Table 5.2 summarizes the two melting events on the annealed samples at different annealing temperatures for the same annealing time. It is to be noted that with increasing annealing time (beyond 15hrs) the observed changes in the melting peak decreased substantially, Table 5.1. Thus, the chosen annealing time for different annealing temperatures is 15hrs. It is to be noted that with increasing annealing temperature the enthalpy of the high melting peak decreases substantially, whereas the peak melting temperature shifts to a higher value. These observations are in accordance with our earlier findings[6] and their applicability in this chapter for different molar masses has been addressed in the following sections of this chapter.

**Table 5.2:** Influence of annealing temperature on the peak melting point.

| Annealing Temperature (ºC) | Peak melting point | |
|---|---|---|
| | Lower Peak (Enthalpy) | Higher Peak (Enthalpy) |
| Without annealing | 140.5 ºC<br>(223 J/g) | |
| 136 | 132 ºC<br>(15.5 J/g) | 142.9 ºC<br>(98.2 J/g) |
| 137 | 135 ºC<br>(98.3 J/g) | 143.7 ºC<br>(11.5 J/g) |
| 138 | 135ºC<br>(103.0 J/g) | 144.4 ºC<br>(2.5 J/g) |
| 139 | 135 ºC<br>(102.8 J/g) | 145.5 ºC<br>(1.2 J/g) |
| 140 | 135 ºC<br>(102.5 J/g) | 145.5 ºC<br>(1.2 J/g) |

Annealing time15hrs. Molar mass of sample 2x$10^6$ g/mol. Heating rate 10ºC/min.
The accuracy of measured values are ± 0.5ºC.

### 5.4.3 Influence of molar mass at a constant annealing time and temperature

The continuous increase in the enthalpy of the low temperature peak with annealing time suggests kinetics in melting of the crystals which depends on the annealing temperature, where the chosen annealing temperature is below the linearly extrapolated melting temperature of 139ºC. With increasing molar mass the time required for the melting process for the same annealing temperature also increased, Table 5.3. These findings, in accordance with our earlier studies[6], suggest melting on annealing by a successive detachment of chains from the crystal surface and their reeling into the melt. A cartoon for such a melting process is depicted in Figure 5.6.

According to this concept, the disentangled crystal melts partially in the course of annealing. While, on cooling, the partially molten crystal will be embedded in the matrix of the melt crystallized sample. Where the melt crystallized sample will have the lower melting temperature compared to the part of the nascent crystals that have not melted yet. Perfectioning of the non-molten regions of the nascent crystals on annealing at these high annealing temperatures and time can be anticipated. This would cause a shift in the melting of the non-molten regions of the annealed samples to higher temperatures. This shift in the high melting peak (143.7ºC) on annealing for 15hrs at 137ºC was recorded when the sample was heated at 10ºC/min. However, on heating the same sample at 0.1ºC/min causes a decrease in the melting temperature from 143.7ºC to 139ºC. This melting temperature is in accordance with the melting temperature for the unannealed nascent sample for the same heating rate, Figure 5.7. These observations further strengthen the perfectioning of the amorphous regions on annealing and its implications on superheating of the crystals at normal heating rates. To investigate the structural changes during the annealing process X-ray studies have been performed on the samples.

**Table 5.3:** Influence of molar mass of disentangled polymer on the peak melting point after annealing experiment.

| Molar mass (Kg/mol) | Peak melting point | |
|---|---|---|
| | Lower Peak (Enthalpy) | Higher Peak (Enthalpy) |
| 2000 | 135 ºC<br>(103 J/g) | 144.4 ºC<br>(2.5 J/g) |
| 3800 | 135 ºC<br>(79.2 J/g) | 144 ºC<br>(20.1 J/g) |
| 9000 | 133 ºC<br>(52.4 J/g) | 143 ºC<br>(40.9 J/g) |

Annealing temperature and time are 138ºC and 15hrs, respectively. Heating rate 10ºC/min.
The accuracy of measured values are ± 0.5ºC.

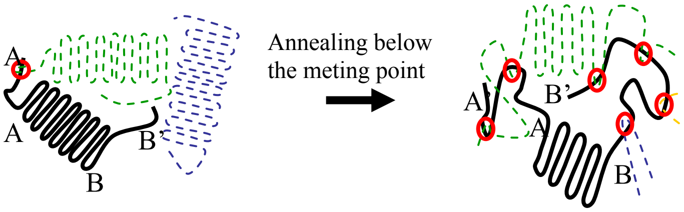

**Figure 5.6:** Illustration of partial melting during an annealing experiment. Simultaneous partial melting and perfectioning of the crystal occurs on annealing. On cooling the annealed crystal, the partially molten component crystallizes. On subsequent heating run the perfectioned crystal melts at the higher temperature, whereas the molten component that crystallized on cooling melts at the lower temperature.

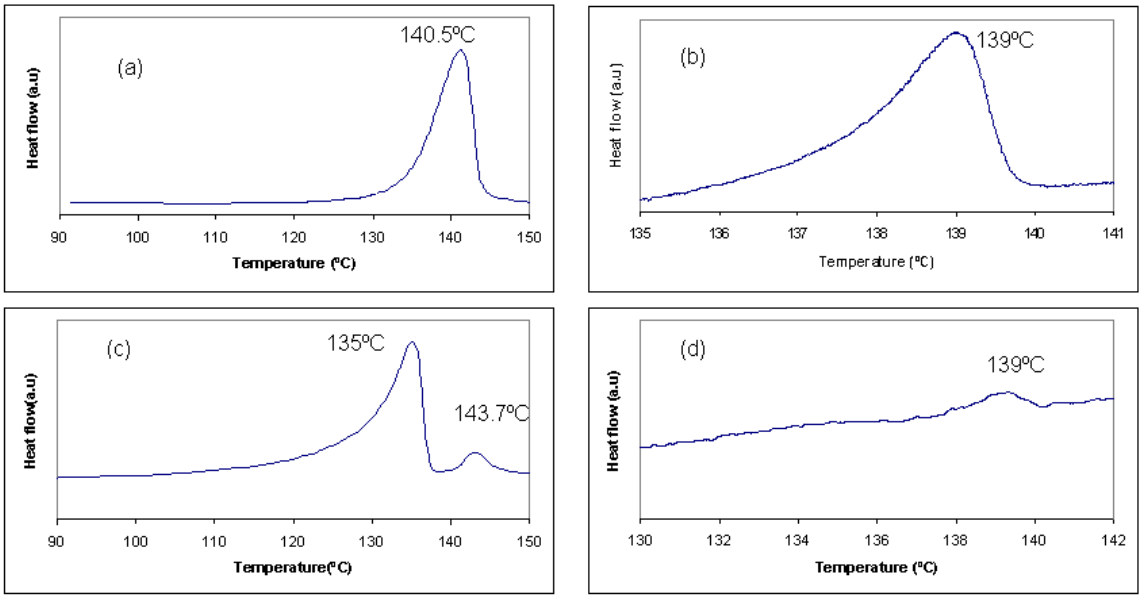

**Figure 5.7:** The sample used for DSC studies is the initially disentangled UHMWPE of molar mass 2x10$^6$ g/mol. Figures (a) and (c) show heating runs at 10ºC/min of the nascent disentangled sample and annealed sample. Prior to heating the annealed sample was annealed at 137ºC for 15hrs and then cooled to room temperature. Figures (b) and (d) show heating runs of (a) and (c) at 0.1ºC/min, respectively. From here it is apparent that while the peak for the nascent sample shifts from 140.5ºC to 139ºC, the high melting peak of the annealed sample shifts from 143.7ºC to 139ºC. The low melting peak of the annealed sample broadens and shifts at the low heating rate and is not apparent in the given temperature scale.

## 5.5 WAXS/SAXS studies on the disentangled polyethylenes

Figure 5.6 depicts two populations of crystals arising from partial melting of the nascent crystals. To have a further insight into the validity of this hypothesis, simultaneous wide and small angle X-ray scattering experiments were performed on beam line ID02 at ESRF. Figure 5.8 shows a set of WAXS patterns recorded for a series of disentangled samples annealed at 138ºC for different annealing times. The WAXS pattern for the nascent sample shows high crystallinity, where long range correlation in the highly crystalline sample results into a rich diffraction pattern. On annealing at 138ºC, the crystallinity of the sample decreases, which become apparent with the appearance of the amorphous halo next to the 110 reflection.

Unlike SAXS patterns of the nascent samples synthesized using a Ziegler-Natta catalyst[3,14] the metallocene synthesized sample showed the presence of a well defined halo, an observation in agreement with the previous findings of Sharma[15]. These results suggest that the nascent crystals obtained by metallocene synthesis have a more regular periodicity compared to the polymers synthesized by a Ziegler-Natta catalyst.

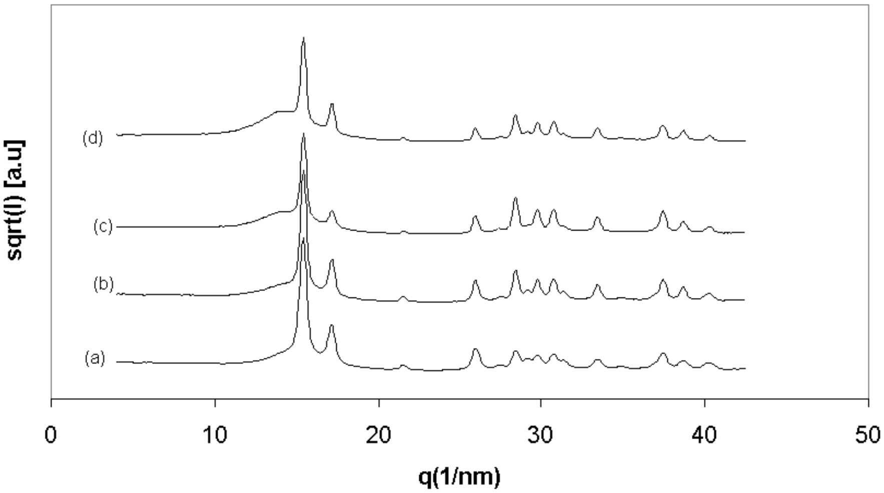

**Figure 5.8:** Comparison simultaneous WAXS pattern at room temperature on the disentangled sample having molar mass 2x10$^6$ g/mol. Nascent(a) and annealed samples at 137ºC for (b) 10, (c) 100 and (d) 300 minutes.

Figure 5.9 shows the simultaneous SAXS studies performed on the annealed samples. It is to be noted that with increasing annealing time as the crystallinity decreases (Figure 5.8), the overall SAXS intensity increases, suggesting an increase in the electron density variation of the crystalline and the amorphous components. The mean square electron density can be calculated from the experiments:

$$\langle \eta^2 \rangle = \frac{Q}{2\pi i_e} = \frac{1}{2\pi i_e} \int_0^\infty I(q) q^2 dq \qquad (5.1)$$

Q is the invariant, independent of topology or geometry of the scattering units and is the Thompson scattering constant for free electron[16].

The reason for the increase in the SAXS intensity with annealing is in accordance with the WAXS and DSC observations, where DSC shows an increase in the amount of low temperature melting peak on annealing.

On annealing, simultaneous with change in intensity it is also observed a shift in the broad hump in the SAXS pattern. The hump in the SAXS pattern arises from the average lamellae thickness i.e. the long period. On annealing (SAXS recorded on the sample b Figure 5.9), the sample shows two humps, one at a higher q (approx 0.35nm$^{-1}$, d=22 nm) and the other at a lower q (approx 0.15nm$^{-1}$, d = 42 nm). The position of the hump at the higher q (lower average long period) is same as that of the nascent sample, whereas the hump at the lower q (higher average long period) increases in intensity with increasing annealing time.

When combined with the DSC and WAXS observations the origin of the changes in the hump at lower q can be assigned to the partial melting process on annealing of the sample which tends to form smaller crystals embedded in the amorphous matrix – leading to a larger average long period. The decrease in the intensity of the hump at the higher q suggests a decrease in the number of nascent crystals.

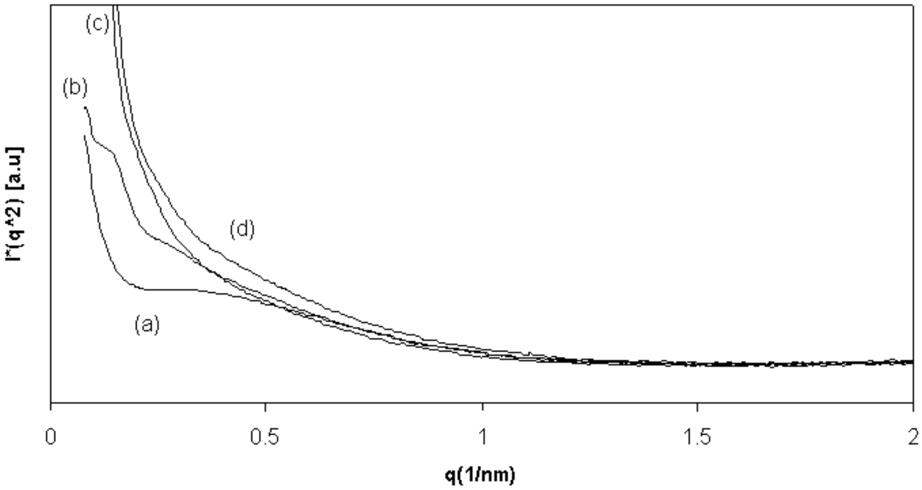

**Figure 5.9:** A comparison of the SAXS patterns at room temperature for the disentangled sample having molar mass $2x10^6$ g/mol, where the x-axis shows scattering distance $q = 2\pi/d$ in $nm^{-1}$ and the y-axis shows the Lorentz corrected scattered intensity in arbitrary units. Curve (a) represents the nascent sample, curves (b), (c) and (d) are the scattering curves obtained from the annealed samples at 137ºC for 10, 100 and 300 minutes, respectively.

## 5.6 Influence of annealing on the onset of crystallization

To investigate the influence of the annealing experiment on the onset of crystallization of the initially disentangled polymer two set of experiments have been performed, one in the vicinity of the melting point and the other well above the equilibrium melting point.

### 5.6.1 Annealing in the melt state

As discussed in chapter 4, the phase transition from the solid state to the melt state initiates entangling of chains that are initially in the disentangled state. Depending on the molar mass of the disentangled sample the required time to reach a fully entangled state varies. If the polymer is cooled before reaching the highest elastic modulus disentangled state could be retained to some extent.

The influence of entanglement on the crystallization of macromolecules has been a matter of debate. Flory and Yoon[17] argued that entanglement has no influence on crystallization from the melt since the topology of chains in melt state must be largely conserved during the time scale required for the crystallization process. Whereas Dimarzio and Hoffman[18] based on calculation and experimental observations, claimed that the disentanglement occurs during crystallization.

To investigate the influence of entanglements on the crystallization, the melt was annealed at a fixed temperature for different times. This annealing protocol was adopted to increase the number of entanglements per chain. Annealing experiments in melt state (160ºC) for different times were performed on the samples prepared in chapter 2. Figure 5.10 shows that the onset of crystallization decreases on annealing in the melt state. Table 5.4 summarizes the data obtained from DSC on the disentangled polyethylene sample. The polymer was annealed at 160ºC for different times. After the requisite annealing time, the samples were cooled to room temperature at 10ºC/min and the onset of crystallization was measured by linear integration of the exothermic peak (TA, Universal Analysis). Considering the onset of crystallization for a sample that was immediately cooled after melting as the reference temperature, ΔT is the difference between the reference temperature and the measured onset of crystallization measured in a sample left to anneal in the melt for a certain time. Table 5.4 shows that ΔT approaches a constant value after a certain annealing time in the melt. An remarkable finding is that the required annealing time in the DSC is comparable to the time needed to reach a fully entangled state in rheometry. See Figure 5.11.

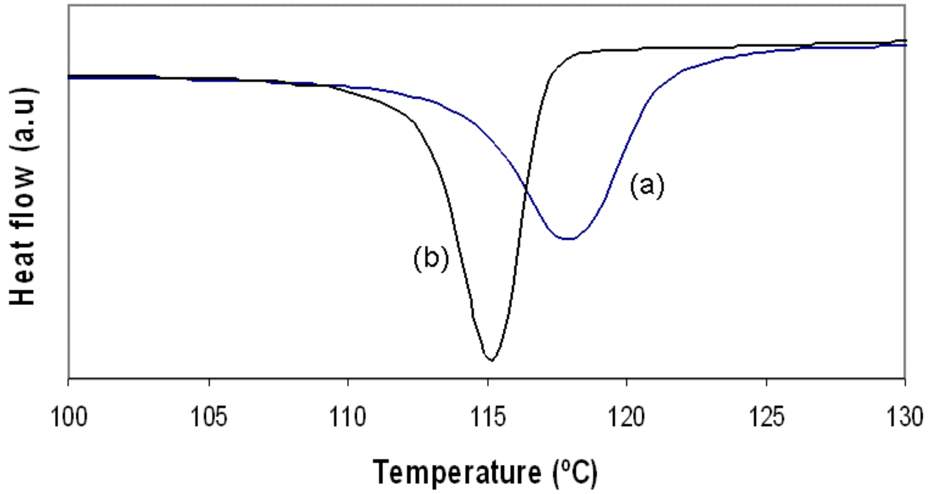

**Figure 5.10:** Cooling run at a rate of 10ºC/min on the disentangled sample having 2x10$^6$ g/mol (a) as melted at 160ºC and (b) annealed at 160ºC for 15hrs.

**Table 5.4:** Changes in the onset of crystallization versus annealing time at 160ºC Sample 2x10$^6$ g/mol, cooling rate 10ºC/min. ΔT is the difference between the onset of crystallization after 2 minutes and the given annealing time

| Annealing time(min) | Onset temperature (ºC) | ΔT (ºC) |
|---|---|---|
| 2 | 123.9 | 0 |
| 10 | 122.5 | 1.4 |
| 30 | 121.5 | 2.4 |
| 60 | 120.4 | 3.5 |
| 150 | 119.9 | 4.0 |
| 300 | 119.8 | 4.1 |
| 1000 | 119.6 | 4.3 |

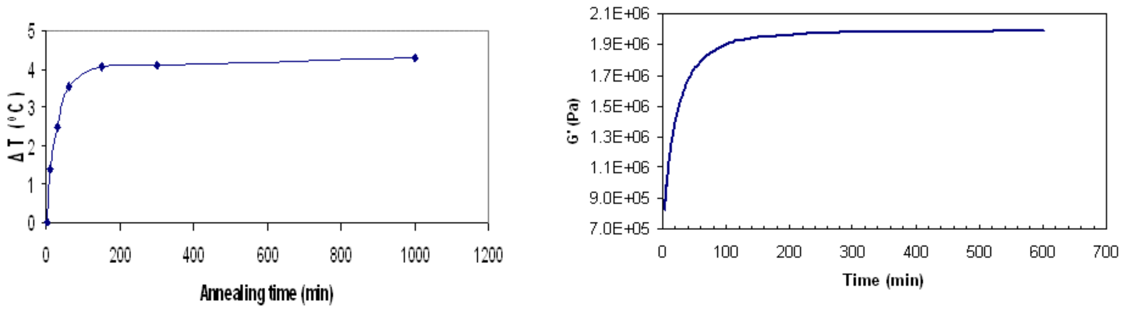

(a) (b)

**Figure 5.11:** Comparison of (a) the drop in the onset of crystallization (ΔT) versus annealing time and (b) the modulus build up versus time. Plotted data in (a) and (b) are from DSC and rheometry, respectively, at 160ºC.

A comparison of the shift in the onset of crystallization with the annealing time and the build-up of modulus with time is shown in Figure 5.11. The two curves show similar trends with time for the same annealing temperature, suggesting the influence of entanglements on the crystallization temperature. It is to be noted that the fully entangled sample does not show a similar reported shift in the crystallization temperature. The DSC observations are in agreement with the work on nucleation density reported by Yamazaki et al.[19]. Similar to the work reported in this thesis these authors observed differences in the nucleation density with increasing annealing time of the disentangled sample in the melt.

### 5.6.2 Annealing in the vicinity of the melting point

As discussed earlier, annealing below the melting point of the nascent polymer results in the partial melting of crystallites. Some part of the crystallites will melt while the others will remain intact, leading to two peaks in DSC thermogram (see Figure 5.4). The partially molten part on annealing could be anticipated due to entanglements. What follows are the observations on crystallization from the melt state of the annealed crystals. The samples were heated at 10ºC/min to the annealing temperature (below the equilibrium melting temperature) and were left to anneal for the mentioned annealing time. After the requisite annealing time, the samples were cooled to room temperature. Thus, the annealed and subsequently cooled samples were heated once again (2nd heating) at 10ºC/min to 160ºC. The samples were left in the melt at 160ºC for 1 minute and were cooled once again (2nd cooling) to room temperature. The observed onset of crystallization temperature during 2nd cooling is listed in the Table 5.5. The observations are that the onset of crystallization showed hardly any shift till the samples are left to anneal at 141ºC. The reported onset of crystallization matches with the fully disentangled melt state, suggesting the easy nucleation of the annealed samples. It is to be noted that till 140ºC, for the given annealing time the high melting peak in DSC, corresponding to the nascent morphology remains.

**Table 5.5:** Onset of crystallization for disentangled sample having a molar mass of $2x10^6$ g/mol. The chosen heating and cooling rate was 10ºC/min.

| Annealing | Onset of crystallization (ºC) | Annealing | Onset of crystallization (ºC) |
|---|---|---|---|
| 15 hrs@136ºC | 123.4 | 15 hrs@141ºC | 123.4 |
| 40 hrs@136ºC | 123.5 | 15 hrs@142ºC | 122.7 |
| 15 hrs@137ºC | 123.3 | 15 hrs@145ºC | 121.9 |
| 15 hrs@138ºC | 123.6 | 30 min@160ºC | 121.4 |
| 15 hrs@139ºC | 123.8 | 150 min@160ºC | 119.9 |
| 15 hrs@140ºC | 123.8 | 300 min@160ºC | 119.8 |

However, in the sample left to anneal above 142ºC, some decrease in the onset of crystallization temperature was observed. A remarkable feature is that a considerable shift in the onset of crystallization temperature was observed once the sample was left to anneal at or above 160ºC, though complete melting occurs at145ºC. The sample that was left to anneal at 145ºC, when compared with the sample left to anneal at 160ºC, showed a considerable difference in the onset of crystallization for the same annealing time. These findings suggest that entanglement formation in the melt state at 145ºC occurs much slower compared to the melt state at 160ºC. To explore such a possibility, rheological studies have been performed on the annealed samples. Figure 4.13 (Chapter 4) shows a comparison of the modulus build up in the fast heated and annealed samples. The sample that was annealed at 139ºC and then heated to 160ºC showed slower build up in modulus compared to the sample that was heated fast to the melt. The difference in the modulus build up can be associated with the difference in the entropy of mixing in the Region I, as stated in Chapter 4 of this thesis.

## 5.7 Conclusions

The melting points of two different molar mass UHMWPE samples having narrow polydispersity were measured by DSC. The non-linear heating rate dependence on the melting temperature of the nascent polyethylenes suggests the presence of an activation barrier in melting of the crystals.

The effect of annealing below the melting temperature was investigated for the nascent polymer by changing the time, temperature and molar mass. Subsequent heating run on the annealed samples showed two distinct melting peaks, suggesting the existence of two populations of crystallites. The lower endothermic peak (135ºC), which is independent of annealing parameters, indicates crystals obtained on partial melting. By increasing the annealing time and temperature, the higher peak shifted to higher melting temperature. The shift implies perfectioning of crystals. With increasing molar mass, the time required for the melting process at the same annealing conditions (constant time and temperature) increased. From here, it can be concluded that the melting on annealing occurs by successive detachment of chains from the crystal surface and their reeling into the melt. These findings were complemented by the simultaneous WAXS/SAXS studies.

Further annealing experiments were performed on the nascent UHMWPE well above the equilibrium melting temperature of 160ºC. It is observed that the onset of crystallization on subsequent cooling varied with the annealing time. The difference between the reference temperature and the measured onset of crystallization, ΔT, increases with increasing annealing time. A remarkable finding was that the required annealing time to reach a plateau in DSC was comparable to the time needed to reach a fully entangled state in rheometry. This suggests an influence of entanglements in the melt on the crystallization temperature.

Annealing experiments were carried out in the vicinity of the melting point and its influence on the onset of crystallization on subsequent cooling was investigated. It was observed that if the sample was left to anneal in the temperature range 142 to 145ºC, a gradual decrease in the onset of crystallization occurs. This suggests that entanglement formation in the melt state at 145ºC takes place much slower compared to the melt state at 160ºC.

## 5.8 References

[1] Wunderlich B., *Colloid Polymer Science*, **1965**, 204, 125.

[2] Chanzy H.D., Bonjour E. and Marchessault R. H., *Colloid Polymer Sci*.,**1974**, 252, 8.

[3] Engelen M. T. T. and Lemstra P. J., *Polymer Communications*,**1991**, 32, 343.

[4] Loos J., Arndt-Rosenau M., Weingarten U., Kaminsky W. and Lemstra P.J., *Polymer Bulletin*, **2002**, 48,191.

[5] Hohne G.W.H., *Polymer,* **2002**, 43, 4689.

[6] Lippits D.R., Rastogi S. and Hohne G.W.H., *Physical Review Letters*, **2006**, 96, 218303.

[7] Yao Y-F., Graf R., Spiess H. W., Lippits D. R. and Rastogi S., *Physical Review E*, **2007**, 76, 060801_R.

[8] Yao Y-F., Graf R., Spiess H. W. and Rastogi S., *Macromolecules*, **2008**, 41, 2514.

[9] Yao Y-F., Graf R., Rastogi S. and Spiess H. W., *Proceedings of IUPAC Macro*, Paris, **2008**.

[10] Rastogi S., Lippits D.R., Hohne G.W.H, Mezari B. and Magusin P.C.M.M., *J. Phys. Condens. Matter*, **2007**,19, 205122.

[11] (a) Hellmuth E. and Wunderlich B., *J. Applied Physics*, **1965**, 36, 3039,
(b) Jaffe M. and Wunderlich B., *Colloid Polymer Science*, **1967**, 216-217, 203, (c) Wunderlich B. and Czornyj G., *Macromolecules*, **1977**, 10, 906.

[12] Toda A., Hikosaka M. and Yamada K., *Polymer*, **2002**, 43, 1667.

[13] Toda A., Kojima I. and Hikosaka M., *Macromolecules*, **2008**, 41, 120.

[14] Joo Y. L., Han O. H., Lee H.-K. and Song J.K., *Polymer*, **2000**, 41, 1355.

[15] Sharma K., *Easily processable UHMWPE with narrow molecular weight distribution,* PhD thesis in Eindhoven University of Technology, **2005**.

[16] Feigin L.A. and Svergun D.I., *Structure Analysis by Small-Angle X-Ray and Neutron Scattering*, **1987**, New York: Plenum Press.

[17] Flory P.J. and Yoon D.Y., *Nature*, **1978**, 272, 226.

[18] Dimarzio E. A., Guttman C. M. and Hoffman, *J. D. Faraday Discuss. Chem. Soc.*, **1979**, 68, 210.

[19] Yamazaki S., Gu F., Watanabe K. , Okada K., Toda A. and Hikosaka M., *Polymer*, **2006**, 47, 6422.

This page is intentionally left blank

# Chapter 6

# Technology Assessment

The prospect of homogenous polymerization and the disentangled UHMWPE obtained from the provided synthesis route will be addressed in this chapter. In the first part, the capabilities of homogenous polymerization is discussed and in the next part the future of such a disentangled polymer is suggested and finally some results are reported briefly.

## 6.1 Outlook for homogenous polymerization

The homogenous dispersion of particles in a polymer matrix is one of the objectives in obtaining the desired properties of composites. If the mixing of particles and polymer occurs in melt state, the degree of mixing is determined by the melt viscosity. Due to this fact, UHMWPE can not be mixed with particles in the melt state. Homogenous polymerization could facilitate the homogenous dispersion of particles in the polymer powder directly during the synthesis of polymer. This can not be achieved during heterogeneous polymerization, such as in the slurry or the gas phase process, because the catalyst (active site to initiate polymerization) is precipitated on the surface of a porous, support where the chains start to grow and crystallize. Therefore, during heterogeneous polymerization dispersion of particles, such as calcium carbonate, inside the growing polymer chains is not feasible. On the contrary, during homogenous polymerization, the catalyst is dissolved in a solvent and dispersed in the polymerization medium, homogenously. With the catalyst, particles such as calcium carbonate, can be also dispersed very well in the polymerization medium. In the propagation step, as the polymer chains grow, they tend to crystallize in the supercooled medium. Depending on the surface of the added particles, the energy barrier for the nucleation process can be suppressed. This would facilitate nucleation for crystallization to the growing chain and will suppress nucleation on the stirrer and reactor walls, which normally lead to reactor fouling. Thus, besides providing composite properties the added particles can also act as nucleating agents for the crystallization of growing chains. Needless to say, the addition of an intractable polymer powder in the solvent will lead to a blend of two highly intractable polymers that can be obtained after polymerization. During the course of this research successful attempts were made to obtain blends of an ester-amide with UHMW-PEs. In addition, it was observed that reactor fouling, which normally occurs during homogenous polymerization, can be suppressed considerably.

## 6.2 Outlook for disentangled UHMWPE

*a. A route to strong tape*: Disentangled UHMWPE obtained directly from the reactor can be consolidated into film below the melting point and shows good drawability (above several 100%) at temperatures around 125ºC. Thus, the obtained tapes show high modulus and tenacity although due to the experimental limitation of drawing process, homogenous tapes were not obtainable and ambiguity remains in terms of comparing the modulus with fibers obtained from solution spinning. However, it is shown convincingly that drawability in the solid state could be a good indication of high modulus.[1] Therefore, due to the high drawability of films consolidated from nascent polymer powder the high modulus of drawn tapes might be comparable with the modulus of fibers obtained from solution spinning. Thus, the solid state deformation of the disentangled UHMWPE provides the benefits of the solvent free route without the need to recover huge volumes of solvent. These strong tapes have the potential to make unidirectional (UD) cross-ply laminates.

*b. Free grain boundary products*: It is well acknowledged that UHMWPE possesses outstanding physical and mechanical properties such are high wear resistance and fatigue properties that make it a good choice for highly demanding applications, i.e. artificial joints. The existing problem is the limited lifetime of implants which results in the painful and expensive revision surgery. Sliding of the implant against the counter surface (metallic or ceramic pin) results in the release of submicron size particles, so-called wear debris, which is a cause of the limited lifetime of implants. Ingham and Fisher suggested that the UHMWPE wear debris is the major reason for the implant loosening, especially in hip prosthesis, where the mechanism involved for the prosthesis failure is considered to be adhesive wear.[2] On the other hand, life time expectancy of the knee prosthesis is limited by the presence of the grain boundaries, where wearing off of the prosthesis occurs due to fatigue wear.

There have been some attempts, such as crosslinking and making composites of UHMWPE, to improve the wear resistance of polyethylene in order to overcome the failure of orthopedic implants attributed to wear debris. Whether the cross linking of polyethylene improves the wear resistance is still a matter of debate.[3,4,5,6] Dry mixing of carbon fiber as well aramid fiber and powder with the UHMWPE matrix has been tried, but have not been very successful.[7]

UHMWPE is intrinsically intractable due to high melt viscosity resulting from the high molar mass. Therefore, it is usually processed via compression molding or ram-extrusion rather than conventional polymer processing routes such as injection molding. Irrespective of the applied processing routes, all products of UHMW-PE possess fusion defects or grain boundaries. These defects are ascribed to the lingering of initial powder particle surfaces after fusion, where chains can not move from one particle to another due to the high reptation time of high molar mass chains.[8,9]

It is suggested that the fusion defects, the presence of grain boundaries, are one the reasons for delamination in the knee-prosthesis. Rastogi et al.[9] showed that the grain boundary free UHMWPE samples show higher toughness and resistance to fatigue in comparison to the sample that is not completely fused.

In this thesis, which is a continuation of the Kurelec's work[10], disentangled UHMWPE was obtained from homogenous polymerization (Chapter 2). The polymer was processed to prepare fully fused samples at 200 bars, 180ºC. Figure 6.1 shows optical micrographs of two different UHMWPE fused samples. Sintering on melting at pressures as low as 200 bar can be achieved for polymer obtained during homogenous polymerization, Fig 6.1 (b), whereas commercial grade obtained from a Ziegler Natta catalyst exhibits grain boundaries under similar compaction conditions, Fig 6.1 (a).

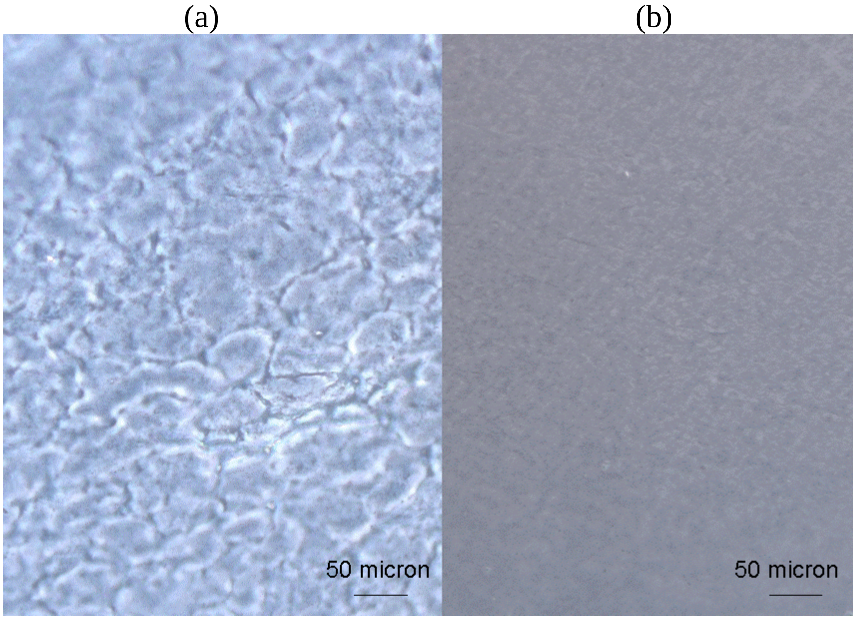

**Figure 6.1:** Phase contrast microscopy of fused UHMWPE obtained from (a) a Ziegler Natta catalyst and (b) a homogenous polymerization. Polymer powder was compacted at 200 bar and 180ºC.

To investigate the wear properties of the fully fused UHMWPE sample obtained from homogenous polymerization, a disc sample (10mm x 35mm) was prepared at 200 bar and 180ºC and was investigated in the group of Dr. Wimmer at Rush University Medical

Center, Chicago, US. The following experiments have been performed and the results have been kindly provided to our group. The original sample was machined to obtain four pin type samples. The pins are prepared according to ASTM F2025-06 and then presoaked in the serum. After 3 weeks, the required normal soaking time for the commercial grade, the specimens provided by us did not reach the desired saturated state. Therefore, the soaking process was extended further for 6 weeks. Thus, the total soaking time for the samples provided by us was 9 weeks. In spite of such a long soaking time, no fully saturated state could be reached. Furthermore, some visible non-homogeneity in the consolidated pins is observed. Wear tests were performed on the presoaked samples for a total of 1,085,000 cycles. While the sample obtained from homogenous polymerization showed lower gravimetric wear, whereas the commercial grade sample showed a lower chemical wear rate. The wear rate measured by the gravimetric method is not definite because the degree of saturation can influence the results whereas the wear rate obtained chemically would not be affected by such saturation. Though a clear explanation for these results is not found, a possible explanation is the high molar mass of the investigated polymer (around $10^7$ g/mol as determined from rheometry measurement) which needs an extremely long time to reach the fully entangled state, see Chapter 4 of this thesis. Furthermore, the difficulty in processing of this high molar mass polymer might be a reason for “visible non- homogeneities in the consolidated pins”. Indeed, observing long lasting soaking of UHMWPE samples could be indicative of the mentioned problems, long build time and difficulty in processing, which will adversely influence the mechanical properties of the material.

## 6.3 References

[1] Smith P. and Lemstra, P.J., *Journal of Material Science*, **1980**, 15, 505.
[2] Ingham E. and Fisher J., *Biomaterials,* **2005**, 26, 1271.
[3] Kurtz S.M., Muratoglu O.K., Evans M. and Edidin A.A. *Biomaterials,* **1999**, *20,* 1659.
[4] McKellop H., Shen F., Lu B., Campbell P. and Salovey R., *J. Orth. Res.* **1999**, *17,* 157.
[5] Ingram J.H., Stone M., Fisher J. and Ingham E., *Biomaterials,* **2004**, 25, 3511.
[6] Affatato S. et al, *Biomaterials,* **2005**, 26, 3259.
[7] Friedrich K., *Advances in Composite Tribology*, **1993**, Elsevier Science, Amsterdam.
[8] Jenkins, H.; Keller, A., *Macromol. Sci. Phys. B,* **1975**, *11*, 301.
[9] Rastogi S., Kurelec L., Lippits D., Cuijpers J., Wimmer M.and Lemstra P. J., *Biomacromolecules,* **2005**, 6, 942.
[10] Corbeij-Kurelec L., *Chain mobility in polymer system; on the borderline between solid and melt,* PhD thesis in Eindhoven University of Technology, **2001**.

# Appendix 1

## Reproducibility of GPC measurements for different molar masses[*]

The GPC measurements were carried out in group of Prof. Münstedt at the Institute of Polymer Materials, Erlangen University. Reproducibility of the light scattering data is shown here for four different molar masses.

Figures A1.1 and A1.2 demonstrate a good reproducibility of the signals for the batches No.1 and No.6 having molar mass[†] of approximately 2x10$^6$ g/mol, respectively. The figures also show that the concentration signals and the MALLS signals may not have the similar shape. The reproducibility of the unprocessed signal worsens with increasing molar mass of the samples. This is demonstrated in Figures A1.3 and A1.4 for the batches No.4 and No.5 having molar masses of 5.3x10$^6$ g/mol and 9.1x10$^6$ g/mol, respectively. The decrease in reproducibility of these high molar mass polymers is attributed to two reasons. Firstly, the increase in the error occurs due to decrease in polymer concentration, where the concentration is decreased with increase in the high molar mass. For an example polymer concentration is to be reduced by half with extreme increase in molar mass. The decrease in polymer concentration is also necessary because the high concentration yields peak broadening. Secondly, the high shear forces required to flow the high molar mass polymer in the columns may lead to chain scission. This effect results in tailing of the peak at higher elution volumes for the sample with the highest molar mass shown in Figure A1.4.

---

[*] From the private report kindly provided by Dr. J. Kaschta, Group of Prof. H. Münstedt in the Institute of Polymer Materials at the Erlangen University.

[†] It should be noted that the molar mass is reported here is based on melt rheometry calculation. Reader may visit Chapter 3 of this thesis for more information and GPC data.

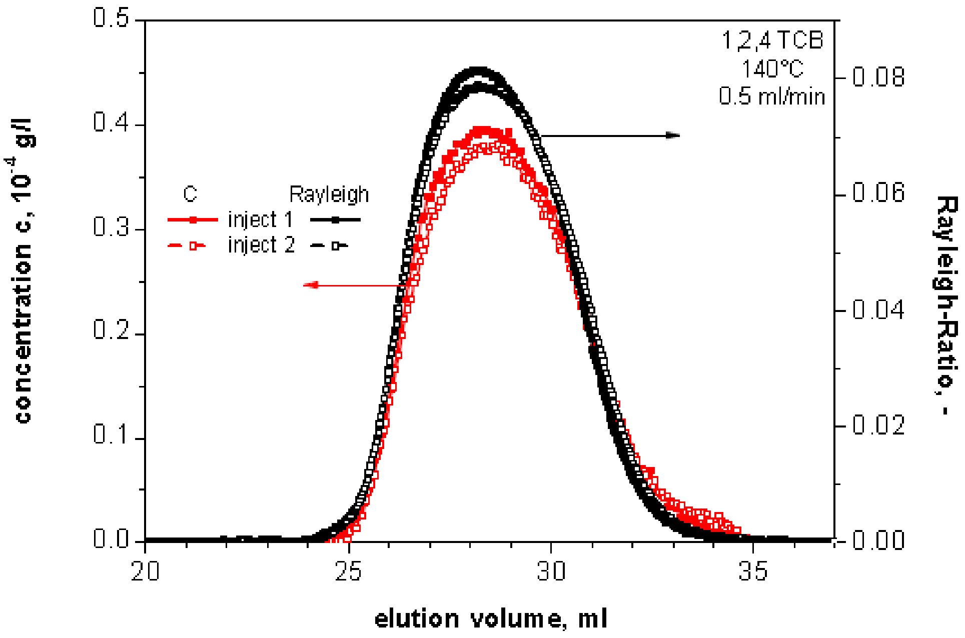

**Figure A1.1:** Reproducibility (injections 1 and 2) of the measured concentration and of the Rayleigh-ratio (90° angle) as a function of elution volume for batch No.1 having molar mass of 2x$10^6$ g/mol.

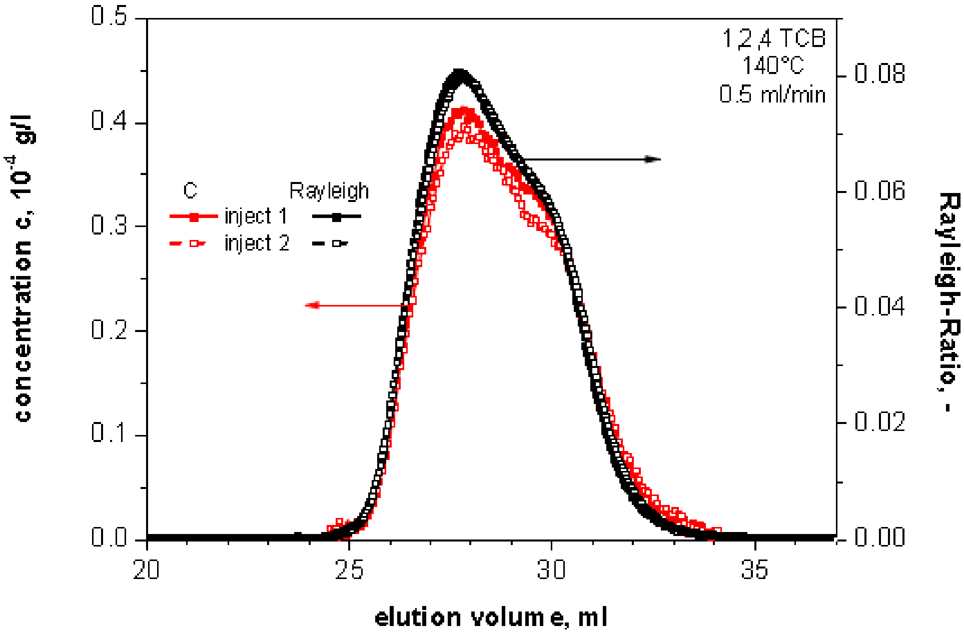

**Figure A1.2:** Reproducibility (injections 1 and 2) of the measured concentration and of the Rayleigh-ratio (90° angle) as a function of elution volume for batch No.6 having molar mass of 1.9x$10^6$ g/mol.

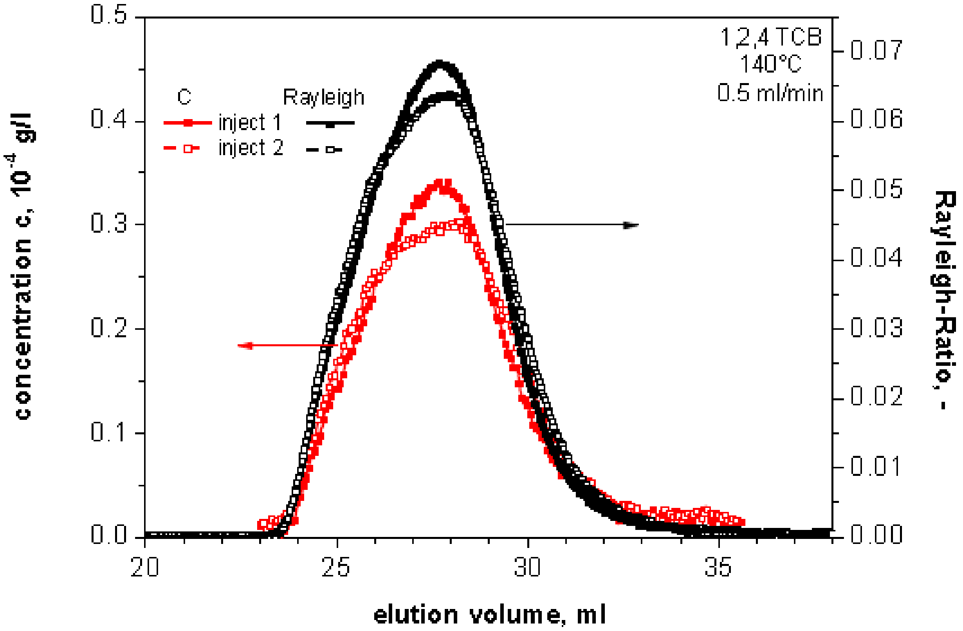

**Figure A1.3:** Reproducibility (injections 1 and 2) of the measured concentration and of the Rayleigh-ratio (90° angle) as a function of elution volume for batch No.4 having molar mass of 5.3x$10^6$ g/mol. It is to be noted that for the two injections data is not fully reproducible.

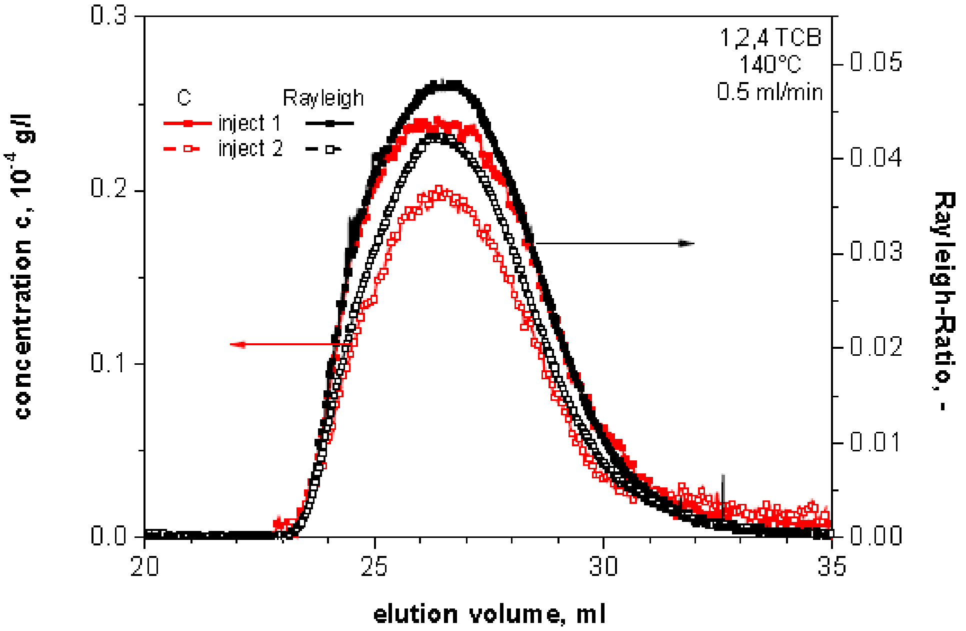

**Figure A1.4:** Reproducibility (injections 1 and 2) of the measured concentration and of the Rayleigh-ratio (90° angle) as a function of elution volume for batch No.5 having molar mass of 9.1x$10^6$ g/mol. It is to be noted that for the two injections reproducibility of the data decreases considerably.

# Appendix 2

## Following entanglement formation on the initially disentangled polymer using high resolution SAXS

Experimental data reported in this appendix is obtained during the end of this work and needs careful data analysis to obtain quantitative values. However, experimental findings on the disentangled polymer melts are clear and will strengthen the rheological aspects in Chapter 4 of this thesis.

Change in the free volume with the increasing number of entanglements suggests possible change in the scattering function of the melt with time. To explore such a possibility high resolution SAXS experiments have been performed on the beam-line ID02 at ESRF, Grenoble. To achieve the maximum signal to noise ratio and to follow changes occurring with the entanglements formation sample to detector distance was kept at approximately one meter. To follow the maximum changes in the scattering patterns during entanglement formation the chosen samples were $5.3\mathrm{x}10^6$ g/mol and $2\mathrm{x}10^6$ g/mol. After compression of the polymer powder in the solid state, below its melting temperature, the pressed powder sample (now in the form of film) was placed on the Linkam hot stage. The sample is heated from room temperature to 160ºC at 10ºC/min.

Scattering data on the disentangled UHMW-PE (5.3 x $10^6$ g/mol)

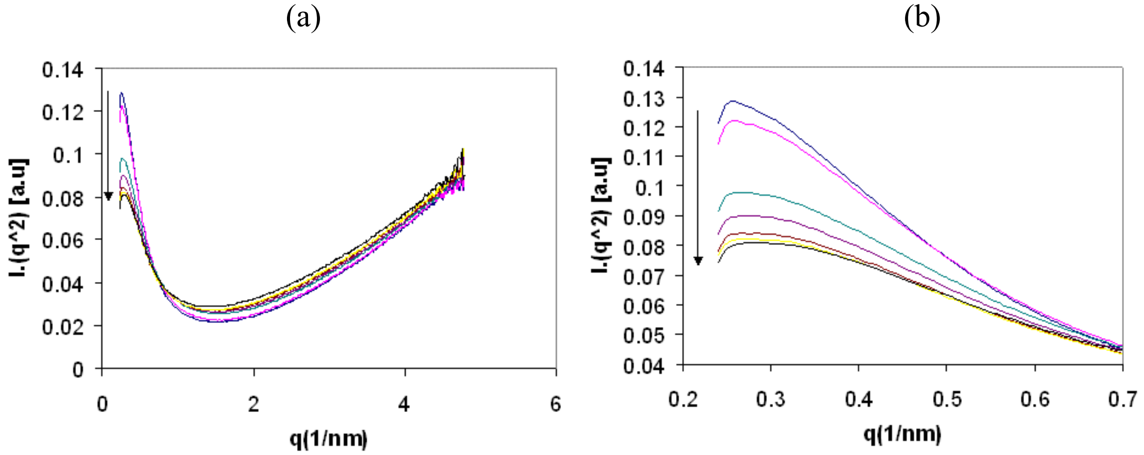

**Figure A2.1:** Lorentz corrected SAXS pattern as obtained in the initially disentangled molten polymer, having molar mass of 5.3 x $10^6$ g/mol. Arrows in the figures show the successive recorded SAXS patterns. Data shown here, from top to bottom, correspond to: immediately after melting and 1, 7, 13, 30, 60 and 180 minutes in the melt. (a) The x-ray patterns show clear changes in the scattering function of the melt with time. Each X-ray pattern was recorded for 30seconds. Time interval between each pattern was set for 15seconds. (b) The figure shows a magnified region in the figure A2.1a. From here it is evident that close to the beam stop, i.e. at lower q (= $2\sin\theta/\lambda$, where $\lambda = 0.1$ nm), the overall intensity decreases with time. This suggests that compressibility of the polymer melt is decreasing. It is to be noted that at the initial stages of the melt the overall intensity decreases fast, whereas with time the change in overall intensity decreases. Beyond one hour no substantial changes in the scattering function is observed. These findings on compressibility are in agreement with the observed changes in the normal force of the rheometer when the gap between the plates was kept constant. Our preliminary quantitative analysis suggests two different slopes beyond the compressibility regime, suggesting changes occurring in the different lengths scales of the sample – i.e. between 200 to 250 methylene units and within hundred methylene units. Changes in the scattering data beyond 0.7nm$^{-1}$ are most likely overshadowed by the changes in the WAXD of the sample.

## Scattering data on the disentangled UHMW-PE ($2x10^6$ g/mol)

To have a comparison in the scattering intensity for different molar masses, SAXS studies were performed on sample having a relatively lower molar mass of $2x10^6$ g/mol. Chemistry applied for the synthesis of this sample was the same as the one adopted for $5.3 \times 10^6$ g/mol, with the exception that this polymer was synthesized for longer time as explained in Chapter 2.

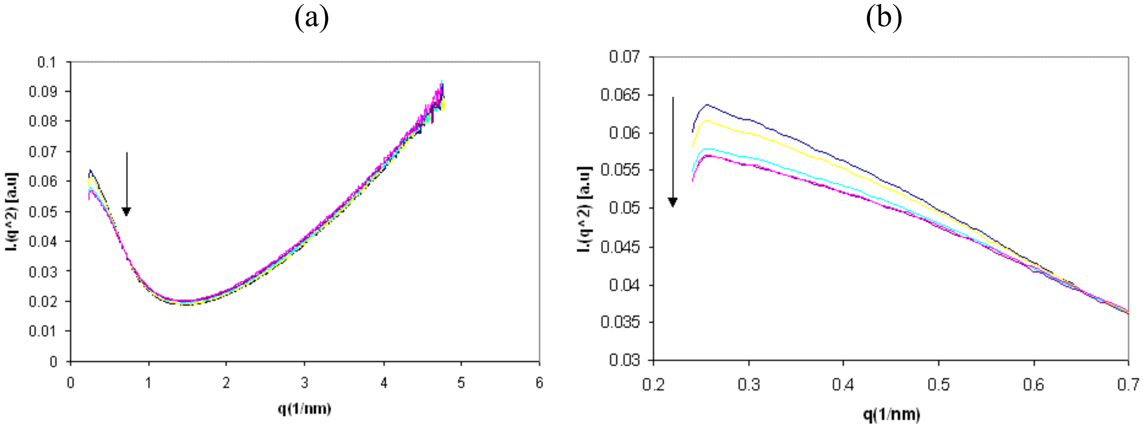
(a) (b)

**Figure A2.2:** Lorentz corrected SAXS pattern as obtained in the initially disentangled molten polymer, having molar mass of $2x10^6$ g/mol. Arrows in the figures show the successive recorded SAXS patterns. Data shown here, from top to bottom, correspond to: immediately after melting and 0.5, 5, 15 and 120 minutes in the melt. (a) The figure shows changes occurring in the SAXS pattern. When compared with Figure A2.1 the observed changes in the scattering pattern are less. This can be attributed to differences in the free volume required for the relatively low molar mass polymer. Thus changes occurring in the compressibility region of the scattering function are also small. (b) The figure shows magnified region of Figure A2.2a. Unlike Figure A2.1, the observed changes in the compressibility region are small. Similar to the Figure A2.1, changes observed in the scattering function at the very initial stages in the compressibility region of the polymer (0.25 to 0.35 $nm^{-1}$) are quiet prominent, whereas with time differences in the intensity of the scattering function decreases. Beyond fifteen minutes, no considerable changes in the scattering function are observed. When compared with Figure A2.1, the difference in the time required for the changes recorded in the scattering function are attributed to the different molar masses. The differences in the time required for the scattering functions to reach the constant value are in accordance with the differences in the required build up time for the entanglements formation. Since the two techniques, scattering and rheological, probe different length scales the measured times cannot be compared on the absolute scale though the observed trend is similar. However, the scattering functions of this molar mass also show two different slopes beyond the compressibility region. Detailed quantitative studies are in progress.

Scattering data on the fully entangled UHMW-PE (2x$10^6$ g/mol)

(a) (b)

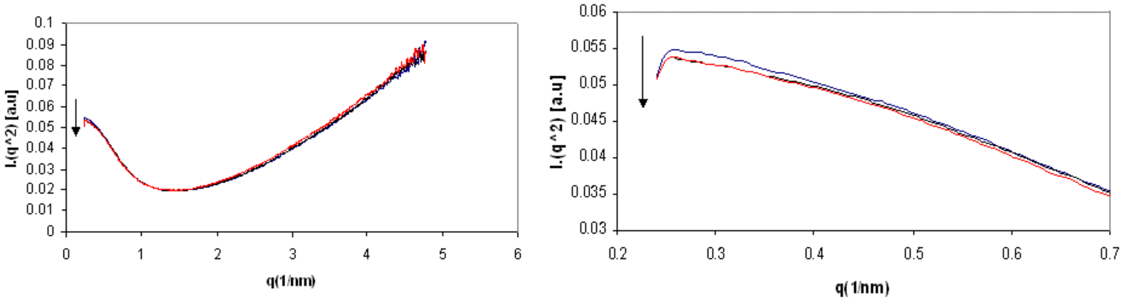

**Figure A2.3:** Lorentz corrected SAXS pattern as obtained in the fully entangled molten polymer, having molar mass of 2x$10^6$ g/mol. Arrows in the figures show the successive recorded SAXS patterns. Data shown here, from top to bottom, correspond to: immediately after melting and 1 and 120 minutes in the melt. (a) Compared to Figure A2.2 no substantial changes in the scattering function are observed. (b) The figure shows magnified region of Figure A2.3a. The x-ray patterns show no distinction between the obtained SAXS pattern after one minute and two hours in the melt.

# Appendix 3

## Reproducibility of modulus build-up for initially disentangled polymer

Most of the rheological experiments, such are time-sweep and frequency-sweep, that have been reported in this thesis were repeated several times to check the reproducibility of results. Here, experimental results obtained from time sweep experiment performed on two different molar masses are shown.

Polymer powder was compressed at 50ºC and 200 bar to obtain homogenous film having thickness of 1mm. Parallel plate geometry was used with a disk diameter of 8 mm. Oscillatory shear measurements in the linear viscoelastic (LVE) regime were carried out using a Rheometrics RMS 800. For all samples, 0.5 wt% Irganox 1010 was added and investigations were performed under a nitrogen atmosphere in order to prevent thermo-oxidative degradation.[*]

Figure A 3.1 (a) show the two set of data, experiments no.1 and no.2, obtained from time-sweep experiments performed on the sample having molar mass of 2.4x$10^6$ g/mol In the figure the data are plotted in the linear-log scale that shows a minor change between experiment no.1 and no.2. The distinction between the two experiments can be attributed to the non equilibrium state at the initial stage of the experiment. However, a good overlap between two sets of data is observed while it is plotted in linear-linear scale, Figure A 3.1 (b).

Similar trend is observed for the sample having a molar mass of 3.8x$10^6$ g/mol, Figures A 3.2 (a) and A 3.2 (b).

The reproducibility of the modulus build-up for different molar masses can be concluded from the mentioned experiments.*

---

[*] More information is provided in Chapter 4 of this thesis.

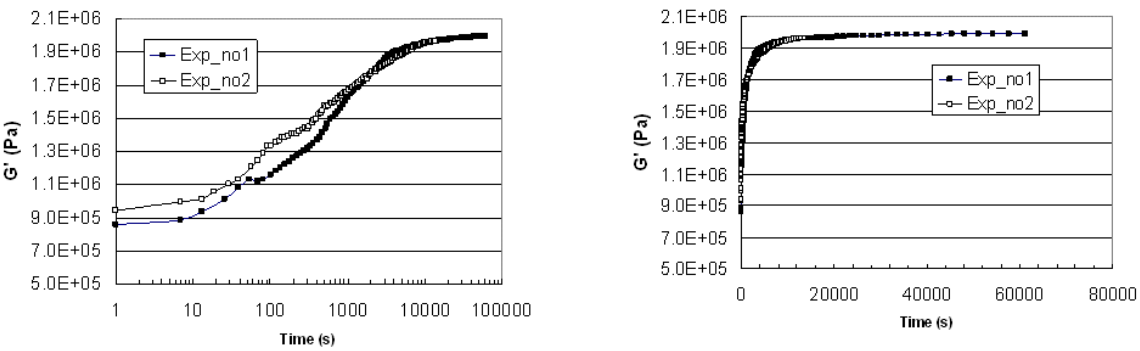
(a) (b)

**Figure A3.1:** Reproducibility of the modulus build-up performed on the sample having molar mass of 2.4x10$^6$ g/mol. Figures (a) and (b), plotted in the linear-log and linear-linear scale, respectively. Experiments were performed at constant temperature 160ºC and fixed frequency and strain of 10 rad/s and 1%, respectively.

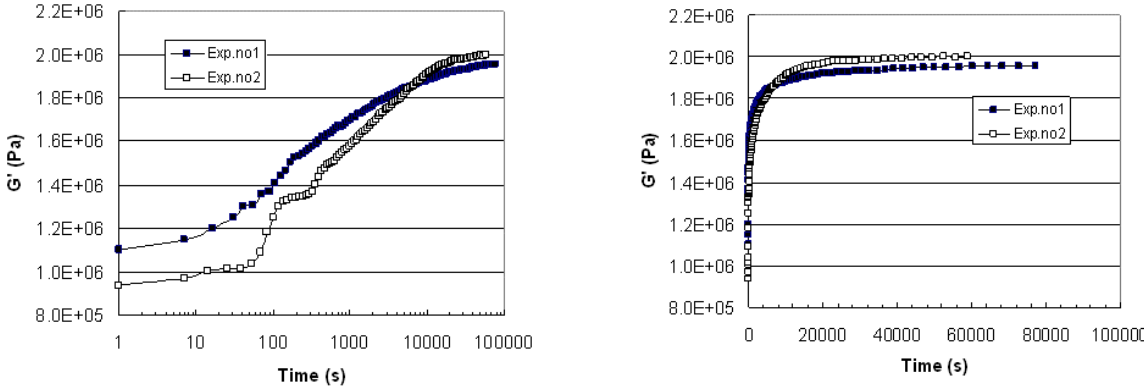
(a) (b)

**Figure A3.1:** Reproducibility of the modulus build-up performed on the sample having molar mass of 3.8x10$^6$ g/mol. Figures (a) and (b), plotted in the linear-log and linear-linear scale, respectively. Experiments were performed at constant temperature 160ºC and fixed frequency and strain of 10 rad/s and 1%, respectively.

This page is intentionally left blank

# Acknowledgments

I am deeply indebted to many people who let me commence my Ph.D. studies and helped me to complete my thesis successfully. I would like to thank:

- Prof. Piet J. Lemstra for giving me the opportunity to join his research group, Polymer Technology, SKT. His stimulating advice and all his support are gratefully acknowledged.
- Prof. Sanjay Rastogi for accepting me in his project and cooperating and discussing with me even during weekends and late in evenings. I am so grateful for his guidance in performing experiments and his assistance in the writing stage.
- Dr. Rob Duchateau and Prof. Cor Koning for the scope to perform synthesis part of this work in the Group Polymer Chemistry (SPC). Rob, thanks for the fruitful discussion.
- Dr. Gerrit Peters and Prof. Han Meijer for providing access to and help in the rheometry lab in the Group Polymer Technology (mate). Gerrit, thanks for your invaluable help.
- Prof. Doug Hourston from IPTME, Loughborough University, and Prof. Münstedt from Erlangen University for their insightful suggestions and corrections on the manuscript of this thesis.

I also would like to thank:
Professors G. Höhne, C. Bailly and E. Nies for their interest in my topic.
Dr. P. Magusin and B. Mezari from the group of Molecular Heterogeneous Catalysis, Eindhoven University and Yao Yefeng from Max Planck Institute, Mainz, for performing solid state NMR.
Dr. J. Kaschta from Erlangen University, for performing GPC measurements and very valuable report.
Dr. M. Wimmer and V. Ngai from Rush University Medical Center, Chicago for setting up six months wear test and J. Kunza for chemical analyzing.
Dr. A. Tracz from the Center of Molecular and Macromolecular Studies, Polish Academy of Science for performing AFM experiments.
Dr T. Narayan and A. Shukla from European Synchrotron Radiation Facility, Grenoble, beam-line ID02 for their help during the SAXS/WAXS experiments.
Anurag, Nilesh, Sai and IPTME's secretaries, Loughborough University, for their hospitality during my visits.

I received help and assistance from many people during my Ph.D. studies. I am thankful to Dirk, for helping me with the rheometry; Kirti, for assisting me with the polymerization reactor set up; Paulin and Anne for nice micrographs; Joost for DSC instructions; Esther, for MATLAB programming and Raf, Nilesh and other people in the Cactus Lab for sharing their experience.

Coming to our SKT group, I am so happy to have been a part of it. I had a memorable time in SKT and will miss all SKT members: Elly and Ineke “sympathetic ears”, Bob, *“he is there when you need him”*, Cees and Paulin, *“serious safety advice”*, Laurent *“with a lovely dress in the Christmas party”*, Han, Denka, Anne, Peter, Rafiq, Nilesh, Jules, Roy, Yogesh, Marjoleine, Marjolein, Luigi, Joost, Pit, Casper, Martijn, Gizela, Gosia, Chunxia, Weizhen, Lijing, Thierry, Jan, Bjorn, Elena, Maria, Primoz, Joris, Petra, Bhushan, and finally my officemate Dr. Dong.

I awarded a scholarship from Sahand University of Technology that supported financially by Ministry of Science, Research and Technology of I.R. Iran. I would like to express my gratitude to both organizations especially to the board of Sahand University of Technology.

In the company of my Iranian friends and their families I always felt at home. My thanks go to Mohammads (all four of them), Ali, Reza, Hamids (both of them), Madjid, Afshin, Kambiz, Arash, Amir, Siamak, Parisa and Parinaz.

I am indebted to my mother who has encouraged me all through my life. I express my best thanks to my mother and father in law for their supports. My brothers and sisters and my brothers and sisters in law, I have been very fortunate to have your constant love and support.

Lastly, I would like to extend my deepest thanks and best gratitude to my lovely family, Shabnam and Aysan, for their tremendous patience, support and kindness throughout all these years especially in the writing stage of the thesis.

# Curriculum Vitae

Saeid Talebi was born on the 3rd of June 1969 in Ardebil, Iran. He gained a bachelor's degree in Chemical Engineering and a Master's degree in Polymer Engineering from the Amirkabir University of Technology in Tehran, Iran.

Saeid started his professional career at the Sahand University of Technology in 1994. In 2004, he was granted a Ph.D. scholarship from the Ministry of Science, Research and Technology of I. R. Iran then he joined the Polymer Technology Group (Chair: Prof. P. J. Lemstra) at the Eindhoven University of Technology (TU/e) as a Ph.D. student. During his Ph.D. study, he completed two modulus of the course "Registered Polymer Technologist" (RPK, Register Polymeerkundige), organized by the "National Dutch Graduate School of Polymer Science and Technology" (PTN, Polymeertechnologie Nederlands).